

**STABILITY AUGMENTATION OF A SEMI-AUTONOMOUS
WHEELCHAIR**

**A MASTER THESIS SUBMITTED TO
THE GRADUATE SCHOOL OF NATURAL AND APPLIED SCIENCES
OF
MIDDLE EAST TECHNICAL UNIVERSITY**

BY

H. MÜJDE AYIK

**IN PARTIAL FULFILLMENT OF THE REQUIREMENTS
FOR
THE DEGREE OF MASTER OF SCIENCE
IN
MECHANICAL ENGINEERING**

SEPTEMBER 2004

Approval of the Graduate School of Natural and Applied Sciences

Prof. Dr. Canan ÖZGEN
Director

I certify that this thesis satisfies all the requirements as a thesis for the degree of Master of Science.

Prof. Dr. Kemal İDER
Head of Department

This is to certify that we have read this thesis and that in our opinion it is fully adequate, in scope and quality, as a thesis for the degree of Master of Science.

Prof. Dr. Kemal ÖZGÖREN
Supervisor

Examining Committee Members

Prof. Dr. Samim UNLUSOY (METU, ME) _____
Prof. Dr. Kemal ÖZGÖREN (METU, ME) _____
Prof. Dr. Reşit SOYLU (METU, ME) _____
Prof. Dr. Kemal İDER (METU, ME) _____
Yar. Dç. Metin SALAMCI (GAZI U., ME) _____

I hereby declare that all information in this document has been obtained and presented in accordance with academic rules and ethical conduct. I also declare that, as required by these rules and conduct, I have fully cited and referenced all material and results that are not original to this work.

Name, Last Name : H. Mjde AYIK

Signature:

ABSTRACT

**STABILITY AUGMENTATION OF A SEMI-AUTONOMOUS
WHEELCHAIR**

Ayık, H.Müjde

M.S., Department of Mechanical Engineering

Supervisor : Prof. Dr. Kemal Özgören

September 2004, 148 pages

In this thesis, the dynamic modeling of a wheelchair-human system is performed, and the effects of steering action and sudden slope changes along the path on the system stability are analyzed for different road and driving conditions. For the cases where the wheelchair system is unstable three methods are proposed for stability augmentation. This study is performed to improve the stability of the wheelchair system under varying road conditions so as to increase the limit of independency for wheelchair users and enhance their life quality.

Two separate mathematical models are obtained for the wheelchair driven on constant sloped and changing sloped roads. Matlab Simulink models are constructed with the obtained mathematical models and control structure. The stability of the system is analyzed by case studies and it is seen that the system is unstable in some of these cases. Three methods are used for enhancement of the stability. One is the speed reduction via joystick module during steep turns, by which the speed of the wheelchair is reduced automatically for a safe steering, but the wheelchair follows the desired course. The second method is the use of a shape filter in order to obtain a less jerky response for the speed. As a final method, the center of mass of the wheelchair-human system is shifted gently in a controlled manner to the side where the reaction force on the wheels decreases.

Keywords: Semi-autonomous wheelchair, stability augmentation, active shifting of center of mass, motion on sloped surfaces, toppling analysis.

ÖZ

YARI OTONOM BİR TEKERLEKLİ SANDALYE İÇİN KARARLILIK ARTTIRIMI

Ayık, H.Müjde

Yüksek Lisans, Makina Mühendisliği Bölümü

Tez Yöneticisi : Prof. Dr. Kemal Özgören

Eylül 2004, 148 sayfa

Bu tez çalışması kapsamında, bir tekerlekli sandalye-insan sistemi modellenmiş, ve farklı yol ve sürüş koşullarında, yol üzerindeki ani eğim değişikliklerinin ve manevranın sistem kararlılığı üzerindeki etkileri incelenmiştir. Tekerlekli sandalye sisteminin kararsız olduğu durumlar için kararlılığı artırmak amacıyla üç yöntem önerilmiştir. Bu çalışma, tekerlekli sandalye sisteminin değişen yol koşullarındaki kararlılığını iyileştirerek kullanıcıların hareket özgürlüğünün ve yaşam kalitelerinin artırılması amacıyla yapılmıştır.

Sabit ve değişken eğimli yollarda sürülen bir tekerlekli sandalye için iki ayrı matematiksel model elde edilmiştir. Elde edilen matematiksel modeller ve denetim yapısıyla Matlab Simulink modelleri oluşturulmuştur. Sistemin kararlılığı farklı durum çalışmalarıyla incelenerek, bazı durumlarda sistemin kararsız olduğu gözlenmiştir. Kararlılığı artırmak amacıyla üç yöntem kullanılmıştır. Bunlardan birisi, keskin dönüşlerde hızın otomatik olarak düşürülmesidir, bu sayede tekerlekli sandalyenin hızı güvenli bir dönüş için düşürülür ancak tekerlekli sandalye istenen yolu takip eder. İkinci yöntem, hızdaki ani iniş ve çıkışları engellemek amacıyla düşük geçişli bir filtrenin kullanılmasıdır. Son yöntem olarak da, tekerlekli sandalye-insan sisteminin ağırlık merkezi denetimli olarak tekerlekler üzerindeki tepki kuvvetinin azaldığı tarafa doğru yavaşça kaydırılmıştır.

Anahtar Sözcükler: Yarı-otonom tekerlekli sandelye, kararlılık iyileştirilmesi, ağırlık merkezinin aktif kaydırılması, eğimli yüzeylerde hareket, devrilme analizi

ACKNOWLEDGEMENTS

I would, first of all, like to thank to Prof. Dr. Kemal Özgören for his guidance, suggestions and great support throughout the study.

I am grateful to my colleagues Asst. Ali E. Turgut, Asst. Kutluk Bilge Arıkan, and Asst. Serkan Gürođlu for their useful discussions. Special thanks are due to Asst. İbrahim Sarı and Asst. Gökhan Özyurt.

I would, sincerely, like to thank to my family for their patience, support and love.

TABLE OF CONTENTS

PLAGIARISM.....	iii
ABSTRACT.....	iv
ÖZ.....	vi
ACKNOWLEDGEMENTS.....	viii
TABLE OF CONTENTS.....	ix
LIST OF FIGURES.....	xii
LIST OF TABLES.....	xiv
CHAPTER	
1. INTRODUCTION.....	1
1.1 Definition of the Problem.....	1
1.2 History of the Study and Previous Research.....	3
1.3 The Objective of the Thesis.....	9
1.4 The Scope of the Thesis.....	10
2. SYSTEM DYNAMICS.....	12
2.1 Definition of the System.....	12
2.2 Mathematical Analysis of the System.....	13
2.2.1 Equations of Motion for Constant Slope Road.....	14
2.2.2 Equations of Motion for Changing Slope Road.....	34
2.3 System Components and Control Structure.....	43
2.3.1 DC Motor.....	49
2.3.2 Joystick.....	51
2.3.3 Velocity Control of the Wheelchair.....	55
2.3.4 Yaw Angle Control of the Wheelchair.....	56
2.3.5 Methods of Stability Augmentation.....	59
3. CASE STUDIES.....	74
3.1 System Analysis for Reliable Situations.....	74

3.1.1	Reliable Cases for Roads with Constant Slopes.....	74
3.1.1.1	Case 1: Wheelchair Traveling on a Level Road.....	74
3.1.1.2	Case 2: Wheelchair Steering on a Level Road.....	76
3.1.1.3	Case 3: Wheelchair Braking on a Downhill Slope.....	78
3.1.1.4	Case 4: Wheelchair Braking on an Uphill Slope.....	80
3.1.1.5	Case 5: Wheelchair Steering on a Downhill Slope.....	82
3.1.1.6	Case 6: Wheelchair Steering on a Side Slope	84
3.1.1.7	Case 7: Wheelchair Steering on an Uphill Slope.....	86
3.1.1.8	Case 8: Wheelchair Steering on a Road With Both Uphill and Side Slope.....	88
3.1.2	Reliable Cases for Roads with Changing Slopes	90
3.1.2.1	Case 9: Wheelchair on a Road With a Changing Downhill Slope	90
3.1.2.2	Case 10: Wheelchair on a Road With a Changing Uphill Slope.....	92
3.1.2.3	Case 11: Wheelchair on a Road With Changing Uphill and Downhill Slopes	94
3.2	System Analysis for Unreliable Situations	96
3.2.1	Unreliable Cases for Roads with Constant Slopes.....	96
3.2.1.1	Case 12: Wheelchair Toppling to the Right on a Downhill Slope.....	96
3.2.1.2	Case 13: Wheelchair Toppling to the Back on a Side Slope.....	98
3.2.1.3	Case 14: Wheelchair Toppling to the Back on a Road with a Constant Uphill and Side Slope	100
3.2.2	Unreliable Cases for Roads with Changing Slopes.....	102
3.2.2.1	Case 15: Wheelchair Toppling to the Back on a Road With a Changing Uphill Slope.....	102
3.2.2.2	Case 16: Wheelchair Toppling to the Front on a Road With a Changing Downhill Slope	104
3.2.2.3	Case 17: Wheelchair Toppling to the Back on a Road With Both Changing Downhill and Uphill Slopes.....	106

3.3	Reduction of Unreliable Cases by the Methods of Stability Augmentation.....	108
3.3.1	Enhancement of Stability for Case 12.....	108
3.3.2	Enhancement of Stability for Case 13.....	111
3.3.3	Enhancement of Stability for Case 14.....	114
3.3.4	Enhancement of Stability for Case 15.....	117
3.3.5	Enhancement of Stability for Case 16.....	119
3.3.6	Enhancement of Stability for Case 17.....	121
4.	CONCLUSIONS	123
4.1	Discussion	123
4.2	Conclusions and Recommendations for Future Work	126
	REFERENCES.....	128
APPENDICES		
A.	CALCULATION OF CENTER OF MASS FOR THE WHEELCHAIR-HUMAN SYSTEM	131
B.	CALCULATION OF MASS MOMENT OF INERTIA FOR THE WHEELCHAIR-HUMAN SYSTEM	137
C.	ANTHROPOMETRIC DATA AND DIMENSIONS OF HUMAN BODY SEGMENTS.....	147

LIST OF FIGURES

FIGURES

1.1. Simulation of a Person on a Wheelchair with Active Leveling	8
2.1. Road Profiles With Constant and Changing Slopes.....	13
2.2. Wheelchair Driven On a Double-Sided Slope	14
2.3. Top and Side View of the Wheelchair	16
2.4. Side View of the Wheelchair on a Level Planar Surface	25
2.5. Wheelchair on a Changing Slope Road	35
2.6. Simulink Model of the Wheelchair System on a Constant Slope Road	44
2.7. Simulink Model of the Wheelchair System on a Changing Slope Road	46
2.8. Downhill and Uphill Road Profiles.....	47
2.9. A Changing Sloped Road Profile.....	48
2.10. The Subsystem 'ROAD PROFILE'	48
2.11. Mechanical Portion of the Motor	49
2.12. Joystick Inputs.....	51
2.13. Simulation of the Joystick.....	52
2.14. Reference Angular Velocities for a Ramp Input of V_x	52
2.15. Reference Angular Velocities for a Step Input of V_x	53
2.16. Reference Angular Velocities for Positive V_x and V_y	54
2.17. Reference Yaw Angle Block.....	57
2.18. Actual and Reference Yaw Angle for a Specific Case	58
2.19. xy Position of the Wheelchair for a Specific Case.....	59
2.20. 'Voltage y' for the Specific Case	59
2.21. Sharp Turns of the Wheelchair at Maximum Speed	60
2.22. The Angular Velocities of the Right and Left Rear Wheels	60
2.23. The Total Reaction Force on the Right Wheels	61
2.24. Bode Diagram for $a/(s+a)$	62
2.25. xy Position and Yaw Angle of the Wheelchair.....	63
2.26. Angular Velocities, Torques and Motor Voltages	63
2.27. Reaction Forces	64
2.28. Angular Velocities, Torques and Motor Voltages When a Shape Filter is Used	65
2.29. Reaction Forces When a Shape Filter is Used	65

2.30. Top View of the Wheelchair	66
2.31. Simulink Model of the Wheelchair System on a Constant Slope Road, Including the Center of Mass Shifting.....	67
2.32. Simulink Model of the Wheelchair System on a Changing Slope Road, Including the Center of Mass Shifting.....	68
2.33. Position and Yaw Angle of the Wheelchair Steering on an Uphill Slope.....	70
2.34. Angular Velocities of the Rear Wheels, Motor Torques and Motor Voltages for the Wheelchair Steering on an Uphill Slope	71
2.35. Reaction Forces for the Wheelchair Steering on an Uphill Slope	72
2.36. Position of the Shifted Center of Mass	73
2.37. Reaction Forces After the Center of Mass is Shifted	73
3.1. Response of the Wheelchair System for Case 1.....	75
3.2. Response of the Wheelchair System for Case 2.....	77
3.3. Response of the Wheelchair System for Case 3.....	79
3.4. Response of the Wheelchair System for Case 4.....	81
3.5. Response of the Wheelchair System for Case 5.....	83
3.6. Response of the Wheelchair System for Case 6.....	85
3.7. Response of the Wheelchair System for Case 7.....	87
3.8. Response of the Wheelchair System for Case 8.....	89
3.9. Response of the Wheelchair System for Case 9.....	91
3.10. Response of the Wheelchair System for Case 10.....	93
3.11. Response of the Wheelchair System for Case 11.....	95
3.12. Response of the Wheelchair System for Case 12.....	97
3.13. Response of the Wheelchair System for Case 13.....	99
3.14. Response of the Wheelchair System for Case 14.....	101
3.15. Response of the Wheelchair System for Case 15.....	103
3.16. Response of the Wheelchair System for Case 16.....	105
3.17. Response of the Wheelchair System for Case 17.....	107
3.18. System Response With Enhanced Stability for Case 12.....	110
3.19. System Response With Enhanced Stability for Case 13.....	113
3.20. System Response With Enhanced Stability for Case 14.....	116
3.21. System Response With Enhanced Stability for Case 15.....	118
3.22. System Response With Enhanced Stability for Case 16.....	120
3.23. System Response With Enhanced Stability for Case 17.....	122
A.1. Top and Side View of the Wheelchair-Human System	131
B.1. Right Rear Wheel	145
C.1. Relative Dimensions of the Average Human Body	148

LIST OF TABLES

TABLE

A.1. Center of Mass Calculation of the System Components.....	133
B.1. Inertia Calculation of the System Components	138
C.1. Anthropometric Data.....	148

CHAPTER 1

INTRODUCTION

1.1. Definition of the Problem

Large numbers of powered wheelchairs are based on a construction that has two independently driven rear wheels and two front casters. Two DC motors drive the wheelchair. A user's commands are transformed by a joystick into electrical signals that set the wheel speed and direction. Wheelchair design has two main priorities one of which is to increase the independent movement of wheelchair users, and the other is to improve the wheelchair safety. Therefore, improving the stability of the whole human-wheelchair system is an important aspect for the wheelchair safety.

The stability of the wheelchair has a strong subjective character. User's control strategies are based on his internal sense concerning the speed of the wheelchair, his perception of the riding surface, the dynamic parameters of the human-wheelchair system, and the position of the human body according to the wheelchair seat. Wheelchair incidents may be caused by improper user's commands due to changes in the user's emotional condition, inadequate user experience in wheelchair operation, and wrong determination of the characteristics of the riding surface. Moreover, the wheelchair system may lose its stability due to the sudden slope changes along the path, and high speeds during steering. The wheelchair may tend to turn downhill when driven across a sloping surface, speed up excessively when going on a downhill-sloped road or slow down and even slide back in reverse direction when going on an uphill-sloped road. These problems may be serious for handicapped people who may be paralyzed, or who may be incapable of giving correct decisions in their mind concerning the speed of the wheelchair such that he may speed up the wheelchair on a sloping surface while steering.

As mentioned previously, the riding surface of the wheelchair may have downhill-uphill slopes, side slopes, or both. The riding surface may also have abruptly changing slopes along the path of the wheelchair. Such roads may have to be crossed for any journey. Therefore, it is important to clarify the dynamic characteristics and stability of the wheelchairs for different driving conditions on different roads from the point of users and providers.

The semi- autonomous wheelchair system handled within the scope of this thesis has two casters on the front and two rear wheels driven by two independent actuators. The speed and direction angle of the wheelchair is determined by the patient in terms of movements of the joystick. If the joystick is moved forward only then the wheelchair speeds up without any steering, whereas the wheelchair turns right or left as the patient moves the joystick to the right or left. In other words, the user's commands are transformed to voltages in the joystick, which determine the reference angular velocities of the rear wheels and the reference heading angle of the wheelchair. The angular velocities of the rear wheels are compared with the actual angular velocities measured by encoders, and the errors are to be minimized by the speed controllers; as a result, motor voltages are produced. Speed control of the wheelchair can be considered as a low level control and it prevents the wheelchair from excessive speeding on a downhill slope so that the desired speed is maintained. As a high level control, the direction angle of the wheelchair is controlled by the patient such that if the heading angle of the wheelchair is not proper for the user he moves the joystick more to the left or right to maintain the desired direction of the wheelchair.

The mathematical model of the wheelchair-human system is obtained using Newton-Euler formulation and the simulation of this system is performed by using Matlab Simulink. While obtaining the mathematical model of the system it is assumed that the human body is fixed to the wheelchair seat, which may be the case when the patient is paralyzed or when a seat belt is used. The stability of the wheelchair system is analyzed by means of the results of the several simulations carried out for different driving conditions and road profiles.

The reaction forces on the wheels of the wheelchair are analyzed in order to determine the wheelchair stability. As an example, if the total reaction force on the rear wheels takes a value of zero or below during motion, it means that the rear wheels lose contact with the ground so that the wheelchair will topple to the front. In order to improve the stability of the wheelchair system in such cases, three methods are proposed for stability augmentation. These methods are speed reduction during steering by means of modification of the user's commands, shape filter to prevent a sudden change in the wheelchair speed, and center of mass shifting.

1.2. History of the Study and Previous Research

Powered wheelchairs take an important role in the research area of mechanical and control engineering. Most of the research about this topic is either done as to improve the performance of the wheelchair-human system by improving the stability or by designing the system itself in terms of mechanical design, mathematical modeling, and controller design.

The analysis of wheelchair motion on a sloping surface is performed in University of California [1]. In this study of Shung, a mathematical model of the wheelchair system driven on a double-sided sloping surface is obtained using Newton's 2nd Law. The wheelchair has two rear wheels driven independently and two casters at the front. While driving the equations of motion for the system it is assumed that only vertical forces act on the front casters; the two front wheels carry equal weight; the position of the center of mass is fixed relative to the wheelchair, the wheels do not skid; and the changes of slopes along the path are close to zero. The mathematical model presented in the work of Shung does not include the effects of suspension dynamics. The goal of the modeling effort is not a complete description of the wheelchair dynamics, but rather a design tool for a design of a feedback controller. Within the scope of thesis study, Newton-Euler formulation is used to model the system mathematically and the effects of sudden

slope changes along the path are also included on system dynamics such that the wheelchair motion is analyzed for different road profiles. Because, sudden slope changes along the path of the wheelchair affect the tipping stability when the wheelchair is driven on an uphill or downhill slope. Unlike the study of Shung, two front casters do not carry equal weight since the reaction forces on each of the front casters determine the stability of the wheelchair against toppling to the sides. Moreover, off-diagonal inertia terms are not included in the study of Shung whereas it is included in the mathematical model obtained in the thesis. Since the wheelchair has only one plane of symmetry, off-diagonal inertia terms are important for tipping stability analysis.

A wheelchair velocity feedback controller is presented in another work [2]. Such a controller is designed to reduce the control demands on a wheelchair driver in outdoor driving and in low speed maneuvering. A dynamic model of the wheelchair obtained in [1] is used in the controller design. A computer simulation study is conducted for the controller. The effects of P and PI control on the system performance are compared for selected hypothetical situations like wheelchair traveling on a level ground, downhill slope, side slope, or on a double sided slope. Since the dynamic equations of the system are nonlinear control gains for both P and PI systems are chosen by trial and error as a compromise between speed of response, precision, smoothness, and system stability in selected situations. According to the study, both P and PI controllers dramatically reduce the effect of slope disturbances on the wheelchair speed and heading, and hence should make the wheelchair's handling easier on unevenly sloping road. PI control is considered to be clearly superior in such a way that it provides a significantly less jerky response to sudden joystick motions. According to the results obtained in [2], the velocity feedback controller should make the wheelchair easier to drive under varying road conditions. Velocity feedback control is also used within the scope of this thesis study such that the angular velocities of the rear wheels are controlled as a low-level speed control of the wheelchair system. Results of the simulations carried out show that control of the angular velocities prevents an excessive speeding on a downhill slope, also helps

maintaining the desired speed on an uphill slope. In the study [2], the user is removed from inside the control loop such that he does not adjust the joystick to keep the speed and direction close to the desired values. However, the patient controls the direction angle of the wheelchair within the scope of this thesis such that he moves it more or less to the sides to get the desired direction. Human mental control behavior for the wheelchair heading is modeled as a proportional controller in the thesis study. Moreover, case studies are performed to analyze the wheelchair motion and stability for different driving conditions on roads with both constant and changing slopes.

A mathematical model of the wheelchair system is obtained; and then stability conditions of the system for a violent fall, and direction hold stability of the wheelchair on a downhill slope are analyzed in the work of H. Ohnabe and F. Mizuguchi [3]. Mathematical expressions are obtained for the stability of the wheelchair on a downhill slope and the stability against falling over due to the centrifugal force at the turn. Furthermore, the directional stability of the wheelchair on a downhill slope is analyzed since it is difficult for the wheelchair to travel in a straight line where there is a slope affecting the heading angle of the wheelchair. In the thesis study, the stability of the wheelchair system is analyzed by means of analysis of reaction forces of the wheels. Instead of deriving mathematical expressions, the wheelchair system stability is examined by several simulations carried out for different driving and road conditions. Moreover, the effect of sudden slope changes on the system stability is also considered within the scope of the thesis study. The stability analysis is performed not only for roads with a downhill slope; but the roads that have uphill slopes; side slopes, double-sided slopes or changing slopes are also considered in the thesis.

Another study concerns powered wheelchair control based on the dynamical criteria of stability [4]. The stability of powered four-wheeled wheelchairs with two driving wheels and two small sized front wheels is analyzed in this work. The proposed controller includes a special module that analyses user's commands before their execution. This module automatically modifies the commands that could jeopardize wheelchair equilibrium stability. The wheelchair steering

process could become safer by the rejection or modification of the commands of the patient. The user's mental burden is decreased by this way. The commands of the user are transformed into relevant commands for the wheelchair speed and direction by means of joystick movements. Stability conditions for the wheelchair steering on a level ground, and traveling on an inclined plane are derived. When the patient gives speed commands that violate the criteria of stability, these commands that lead to stability loss are transmitted to the speed controller in a modified form. In these cases the wheelchair follows the desired routine, but its movement speed is reduced. A specific algorithm is used to process the information coming from joystick inputs of the user and the sensors that deliver information about the dynamic parameters of the system. If the user's commands violate the stability condition derived analytically, these commands are converted to proper commands. A modification in user's command via joystick is also used within the scope of this thesis. However, neither an analytical expression is derived for stability nor the joystick inputs are checked for any stability condition, and no sensor is used in the process of modification of user's commands. Instead, the speed of the wheelchair is reduced automatically during steep turns by the joystick module that converts the voltages into the reference angular velocities, as mentioned in Section 2.3.2 of Chapter 2. In other words, as the patient increases the voltage in y direction of the joystick more, the speed of the wheelchair is reduced more for a safe steering. The steeper the wheelchair turns the lower the wheelchair speed is.

Static and dynamic stability analyses for racing wheelchairs, and the simple case of roll stability while turning are investigated in another study [5]. The degree of roll stability is highly related with the area of the footprint which is the area constructed by connecting the adjacent contact points of the wheels with lines. For a wheelchair to be statically stable the center of gravity of the whole wheelchair-human system must remain within the footprint. As the wheelchair system is tilted the footprint becomes smaller and the system becomes more apt to fall. Furthermore, analysis of roll stability during steering is conducted and critical roll stability velocity is determined for the wheelchair on a flat roadway

and downhill slope. The result of this study [5] shows that while turning, racing wheelchairs with three wheels may be less stable than those with four, and both three and four wheeled chairs are more apt to fall over while turning on a downhill slope than on a level surface. This result is also validated within the scope of this thesis such that after carrying several simulations it is seen that the wheelchair has a more tendency to become unstable while steering on a downhill, uphill, or side slope rather than on a level ground.

Another important issue in the research area of the wheelchair is the loss of upright postural stability of the patients, which may result in a discomfort of the patient or even a loss of control over the wheelchair. Because, the patient who does not have the requisite upper body strength and endurance may not be able to bring his body back to an upright position. As a research in this topic, a system capable of examining postural stability of the users to perturbations within a laboratory environment is developed in another study [6]. The system provides a means of highly reproducible perturbations to a subject seated in a wheelchair. Design of the device is guided by the desire to produce dynamic disturbances similar to what might be experienced by the patient during their travels along the path. The longitudinal acceleration is usually specified for tests involving braking, while for turning maneuvers, the lateral acceleration is normally measured. The platform where the wheelchair and the subject placed on the seat is pitched forward to simulate a brake and it is rolled to the right to simulate a left turn. Stability of the subject placed on the seat of the wheelchair is analyzed with several movements of the platform to simulate dynamic disturbances. However, postural movements of the wheelchair user are neglected within the scope of this thesis, which may be the case when the patient is paralyzed or a seat belt is used. While obtaining the mathematical model of the wheelchair-human system in the thesis, it is assumed that the patient is fixed relative to the wheelchair seat.

In the work of William W.Li and Shahram Payandeh [7], the effects of a human driver on the tipping stability of a powered wheelchair is concerned. The tipping stability is measured by the angle of tilt required to induce a loss of contact between any of the wheels of the wheelchair and the ground. Expressions are

derived relating the static and dynamic tipping criteria to the position and relative mass of the human. A simple simulation which can accomplish the goals of improving tipping stability and limiting shear forces on the driver is shown in Figure 1.1. The single mass model at the left has two masses rigidly joined together. The model at the right has the second mass under active control. In this second model, the first mass consists of wheelchair wheels, batteries and motors while the seat and the driver are included in the movable second mass.

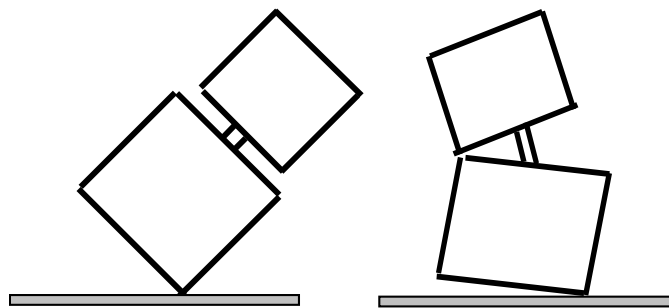


Figure 1.1. Simulation of a Person on a Wheelchair With Active Leveling

The active mechanism proposed in [7] consists of a powered rotational joint, similar to those found in manually controlled tiltable wheelchair seats, which pitches the driver and the seat back and forth. The resulting change in the attitude of the driver-seat system can be used to prevent the wheelchair from toppling to the front or backside such that the tipping stability of the whole wheelchair human system is improved. Active shifting of the center of mass in a controlled manner as concerned in the study [7] is also used within the scope of this thesis. However, the second mass that includes the driver and the seat is not tilted but shifted not only in back and forth direction, but to the sides also. Therefore, not only the pitch stability but also the rolling stability of the wheelchair is improved within the scope of this thesis. Moreover, the results of improved stability are validated with the case studies performed by means of several simulations carried out in Matlab Simulink environment for different driving and road conditions.

Other methods like speed reduction via joystick module for a safe steering, and a shape filter are also used for the purpose of stability augmentation.

The dynamic stability test [8] is performed for the wheelchairs such that the wheelchair is accelerated and braked going up and down on a tilted surface. As a result of this study, the stability limit is defined by the tilt angle at which the wheels are observed to lose contact with the ground.

In the static stability test [9], a wheelchair including a test dummy as the patient is placed upon a tiltable platform. Then, the wheelchair is gently tilted in several different directions and the stability limit is recorded for each.

A recent work [10] considers the development of a wheelchair for people with special needs, which is capable of navigating semi-autonomously within its workspace. This system is expected to prove useful to people with impaired mobility and limited fine motor control of the upper extremities. Among the implemented behaviors of this robotic system are the avoidance of obstacles, the motion in the middle of the free space and the following of a moving target specified by the user (e.g., a person walking in front of the wheelchair). The wheelchair is equipped with sonars, which are used for distance measurement in preselected critical directions, and with a panoramic camera with a 360 degree field of view, which is used for following a moving target.

There are many different electronic systems used recently in powered wheelchairs depending on the disabilities of the user. The joystick is the cheapest and the most efficient type of command generator. However for those who cannot control joystick because of limited control of upper extremities or some other disabilities, wheelchairs controlled by voice commands [11] or robotic wheelchairs equipped with sonars [12], ultrasonic sensors [13] are also available.

1.3. The Objective of the Thesis

Mobility is one of the key factors that contribute to quality of life. The degree of mobility is directly related to one's level of independence. Powered wheelchairs

are the primary means by which many physically disabled people extend the limits of their mobility. These limits, though, are circumscribed by the user's commands and reflexes, and the range of places the wheelchair can safely take the user. Extending the limits of independence of the patients by improving the stability of the wheelchairs is the main point in this thesis. The user may give improper commands in terms of speed due to his mental restrictions, reduced reflexes or inexperience, which may result in instability while steering on a sloped road. For such a case, the user's commands are modified via joystick such that the wheelchair follows the desired course but its movement speed is reduced. Knowing when both of the wheels on one side of the wheelchair lose contact with the ground is important because this will cause instability such that the wheelchair will topple to the other side. For such a case, the wheelchair seat with the driver is tilted gently to the side where the reaction force reduces to a value of zero. Therefore, shifting of the center of mass is an important method for augmentation of stability. Shape filter and modification of user's commands for speed reduction during steering are the other methods used for stability augmentation within the scope of this thesis.

1.4. The Scope of the Thesis

At the beginning of the study, a literature survey regarding the topic is carried out so that a general opinion about the previous research is obtained. As a result, control algorithms used for the speed control of the wheelchair, mathematical modeling of the system dynamics, and several methods for improvement of the wheelchair stability are underlined, which is presented in Section 1.2.

In chapter 2, detailed nonlinear mathematical models of the system are obtained using Newton-Euler formulation for two different road profiles, which are roads with double-sided slopes, and roads with changing slopes along the path. The mathematical models obtained are used to construct the Matlab Simulink models. Then, the system components like the joystick and DC motors, and control

structure of the wheelchair system are discussed. Finally, the methods for the augmentation of wheelchair stability are proposed.

In the second part of the study that is presented in Chapter 3, the results of several simulations carried out for different driving conditions and road profiles are analyzed. Initially, several case studies are performed for the wheelchair system that is stable while driven on different constant sloped and changing sloped roads. Then, cases where the wheelchair system is unstable are examined. Finally, reduction of unstable cases by means of stability augmentation methods is accomplished.

In Chapter 4 of the thesis study, the results obtained are discussed and future recommendations are stated.

CHAPTER 2

SYSTEM DYNAMICS

2.1. Definition of the System

The system is composed of a semi-autonomous wheelchair, and a human body, which is assumed to be fixed relative to the wheelchair seat. The wheelchair is composed of two independently driven rear wheels and two casters at the front. The speed and direction of the wheelchair are determined by the patient in terms of joystick movements. In other words, the reference angular velocities and the reference yaw angle are determined by means of joystick voltages. The actual angular velocities are compared with the reference angular velocities and the errors are to be minimized by two independent controllers. Right and left motor voltages are produced as outputs of these controllers. The control of angular velocities can be considered as a low level control. The direction angle of the wheelchair is controlled by the patient, which can be considered as a high level control. If the wheelchair direction is not proper for the user he or she moves the joystick to the left or right until the wheelchair reaches the desired heading angle. The motion of the system is analyzed in two different types of roads as described below.

- i) The road is a double-sided sloping road where the changes of slopes along the path are zero. There exists both an uphill-downhill slope and a side slope of the road. Such a road can be seen in Plot (1) of Figure 2.1 on the next page, where OXYZ is defined as the inertial frame fixed on the earth in such a way that the plane OXY is horizontal.

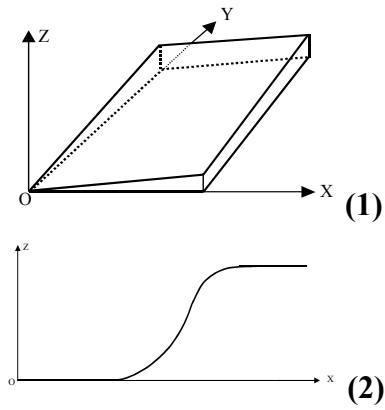


Figure 2.1. Road Profiles With Constant and Changing Slopes

ii) The sloping road where the slope is changing can be seen in Plot (2) of Figure 2.1, where Oxz is the inertial frame fixed on the earth.

2.2. Mathematical Analysis of the System

Including the effects of both slope changes and maneuverability complicates the mathematical model dramatically. Because of that; they are analyzed by two different road profiles as explained in the previous section so that two distinct mathematical models of the system are obtained. In the first model, the wheelchair system has two degrees of freedom while moving on a double-sided sloping road. The effects of maneuverability on the system stability are analyzed by using this mathematical model. However; the wheelchair has only one degree of freedom while traveling on a changing slope road. How the slope changes affect the system stability is studied in this second model obtained for a road profile with a changing slope.

The analysis of the system dynamics in both of the models is based on some simplifying assumptions:

- Only vertical forces act on the front castors, i.e., friction forces are neglected on the front casters,
- The effects of human postural movements are neglected,

- The rear wheels do not skid;
- Suspension dynamics is neglected.

2.2.1. Equations of Motion for Constant Slope Road

The wheelchair driven on a double-sided slope is shown in Figure 2.2. $F_e \{O; \vec{u}_1^{(e)}, \vec{u}_2^{(e)}, \vec{u}_3^{(e)}\}$ is defined as the inertial frame fixed on the earth, and $F_w \{G; \vec{u}_1^{(w)}, \vec{u}_2^{(w)}, \vec{u}_3^{(w)}\}$ as the wheelchair fixed frame where $\vec{u}_3^{(w)}$ is perpendicular to the slope surface, $G\vec{u}_1^{(w)}$ is in-line with the direction of longitudinal axis of the wheelchair, also defining the direction in which the wheelchair travels along the way. Frame $F_s \{O; \vec{u}_1^{(s)}, \vec{u}_2^{(s)}, \vec{u}_3^{(s)}\}$ is the intermediate frame on the earth and it is parallel to the wheelchair fixed frame when the wheelchair moves forward with zero heading angle. The rotation of frame $F_w \{G; \vec{u}_1^{(w)}, \vec{u}_2^{(w)}, \vec{u}_3^{(w)}\}$ with respect to frame $F_s \{O; \vec{u}_1^{(s)}, \vec{u}_2^{(s)}, \vec{u}_3^{(s)}\}$ is designated by the heading angle φ .

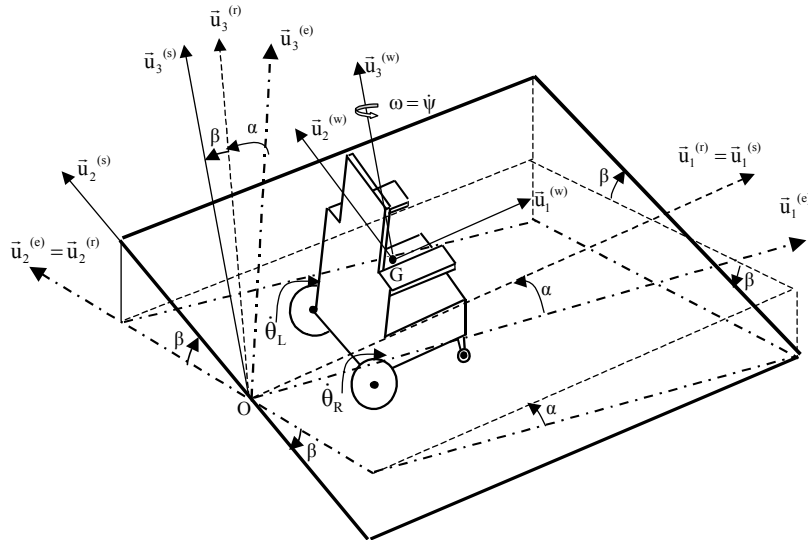


Figure 2.2. Wheelchair Driven on a Double-Sided Slope

In Figure 2.2; the parameters are defined as

- α : up/downhill slope of the road
- β : side slope of the road
- ψ : heading angle of the wheelchair
- $\dot{\theta}_R, \dot{\theta}_L$: angular velocities of the right and left rear wheels

Successive rotations observed in the earth fixed reference frame $F_e \{O; \bar{u}_1^{(e)}, \bar{u}_2^{(e)}, \bar{u}_3^{(e)}\}$ can be designated by the following definition.

$$F_e \xrightarrow{\bar{u}_2^{(e)}, -\alpha} F_r \xrightarrow{\bar{u}_1^{(r)}, \beta} F_s \xrightarrow{\bar{u}_3^{(s)}, \psi} F_w \quad (2.1)$$

In the rotating frame based sequence (RFB) shown above; F_e is the initial frame, F_w is the final frame and F_r, F_s are the intermediate frames [14]. Moreover, α, β , and ψ are Euler angles whereas $\bar{u}_2^{(e)}, \bar{u}_1^{(r)}, \bar{u}_3^{(s)}$ are unit vectors to define the axis of rotation.

The transformation matrices between the frames are as follows:

$$\hat{C}^{(e, s)} = e^{-\bar{u}_2 \alpha} e^{\bar{u}_1 \beta} \quad (2.2)$$

$$\hat{C}^{(e, w)} = e^{-\bar{u}_2 \alpha} e^{\bar{u}_1 \beta} e^{\bar{u}_3 \psi} \quad (2.3)$$

The angular velocity of the wheelchair can be written as

$$\bar{\omega}_{w/e} = \bar{\omega}_w = \bar{\omega}_{w/s} + \bar{\omega}_{s/r} + \bar{\omega}_{r/e} \quad (2.4)$$

where $\bar{\omega}_{w/e}$ is the angular velocity of wheelchair frame F_w with respect to earth fixed frame F_e .

Since slopes α and β are constant ;

$$\bar{\omega}_{s/r} = 0 \quad (2.5)$$

and

$$\bar{\omega}_{r/e} = 0 \quad (2.6)$$

Then, Equation 2.4 becomes

$$\vec{\omega}_w = \vec{\omega}_{w/s} = \dot{\psi} \vec{u}_3^{(s)} \quad (2.7)$$

Differentiating the above expression in the earth frame F_e , one can get the expression for the angular acceleration of the wheelchair.

$$\vec{\alpha}_w = D_e \omega_{w/e} = \ddot{\psi} \vec{u}_3^{(s)} \quad (2.8)$$

Top and side views of the wheelchair can be seen in Figure 2.3.

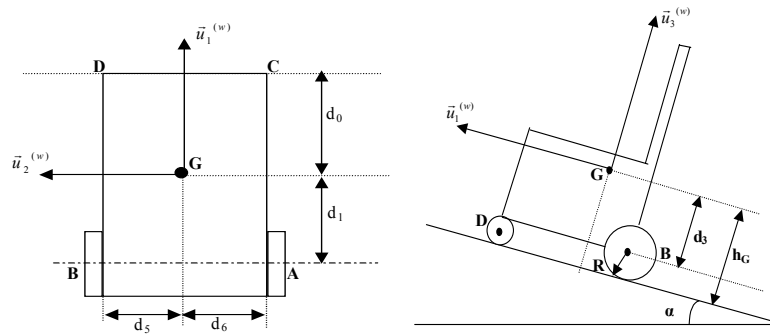


Figure 2.3. Top and Side View of the Wheelchair.

In this Figure;

- A, B : center of mass of the right and left rear wheels
- C, D : center of mass of the right and left front casters
- G : center of mass of the wheelchair
- R : radius of the right and left rear wheels
- d_0 : the distance that locates G with respect to the front axle, in $\vec{u}_1^{(w)}$ direction
- d_1 : the distance that locates G with respect to the rear axle, in $\vec{u}_1^{(w)}$ direction
- d_3 : the distance that locates G above the axle of the rear wheels, in $\vec{u}_3^{(w)}$ direction

- d_5 : the distance between the left rear wheel and the forward axis passing through G, in $\bar{u}_2^{(w)}$ direction
- d_6 : the distance between the right rear wheel and the forward axis passing through G, in $\bar{u}_2^{(w)}$ direction
- h_G : height of the center of mass of the wheelchair from the ground

The position vectors of points G, A and B with respect to the origin O of the earth fixed frame $F_e \{O; \bar{u}_1^{(e)}, \bar{u}_2^{(e)}, \bar{u}_3^{(e)}\}$ can be written by Equations 2.9, 2.10 and 2.11, respectively, where x and y are the displacements of the wheelchair in $\bar{u}_1^{(s)}$ and $\bar{u}_2^{(s)}$ direction.

$$\bar{r}_{G/O} = \bar{r}_G = x\bar{u}_1^{(s)} + y\bar{u}_2^{(s)} + h_G\bar{u}_3^{(s)} \quad (2.9)$$

$$\bar{r}_{A/O} = \bar{r}_A = x\bar{u}_1^{(s)} + y\bar{u}_2^{(s)} + R\bar{u}_3^{(s)} - d_1\bar{u}_1^{(w)} - d_6\bar{u}_2^{(w)} \quad (2.10)$$

$$\bar{r}_{B/O} = \bar{r}_B = x\bar{u}_1^{(s)} + y\bar{u}_2^{(s)} + R\bar{u}_3^{(s)} - d_1\bar{u}_1^{(w)} + d_5\bar{u}_2^{(w)} \quad (2.11)$$

By differentiating the position vector \bar{r}_G in the earth frame, the velocity of point G can be obtained as follows:

$$\bar{V}_G = D_e \bar{r}_{G/O} = D_s \bar{r}_{G/O} = \dot{x}\bar{u}_1^{(s)} + \dot{y}\bar{u}_2^{(s)} \quad (2.12)$$

Note that differentiation in frame F_s and F_e does not make any difference since angular velocity of frame F_s with respect to frame F_e is zero.

Velocity of the point A is

$$\bar{V}_A = D_e \bar{r}_{A/O} = D_s \bar{r}_{A/O} = \dot{x}\bar{u}_1^{(s)} + \dot{y}\bar{u}_2^{(s)} - d_1 D_s \bar{u}_1^{(w)} - d_6 D_s \bar{u}_2^{(w)} \quad (2.13)$$

where $D_s \bar{u}_1^{(w)}$ and $D_s \bar{u}_2^{(w)}$ are the differentiation of unit vectors $\bar{u}_1^{(w)}$ and $\bar{u}_2^{(w)}$ in the frame $F_s \{O; \bar{u}_1^{(s)}, \bar{u}_2^{(s)}, \bar{u}_3^{(s)}\}$. They can be derived as follows:

$$D_s \bar{u}_1^{(w)} = D_w \bar{u}_1^{(w)} + \bar{\omega}_{w/s} \times \bar{u}_1^{(w)} \quad (2.14)$$

and

$$D_s \vec{u}_2^{(w)} = D_w \vec{u}_2^{(w)} + \vec{\omega}_{w/s} \times \vec{u}_2^{(w)} \quad (2.15)$$

Differentiation of a unit vector in its own frame gives zero. Therefore;

$$D_w \vec{u}_1^{(w)} = D_w \vec{u}_2^{(w)} = 0 \quad (2.16)$$

Equation 2.17 gives an expression for the angular velocity of frame $F_s \{O; \vec{u}_1^{(s)}, \vec{u}_2^{(s)}, \vec{u}_3^{(s)}\}$ with respect to frame $F_w \{G; \vec{u}_1^{(w)}, \vec{u}_2^{(w)}, \vec{u}_3^{(w)}\}$.

$$\vec{\omega}_{w/s} = \dot{\psi} \vec{u}_3^{(s)} = \dot{\psi} \vec{u}_3^{(w)} \quad (2.17)$$

Velocity of Point A can be obtained by substituting Equations 2.16 and 2.17 into Equations 2.14 and 2.15, and rearranging the terms in Equation 2.13.

$$\vec{V}_A = \dot{x} \vec{u}_1^{(s)} + \dot{y} \vec{u}_2^{(s)} - d_1 \dot{\psi} \vec{u}_2^{(w)} + d_6 \dot{\psi} \vec{u}_1^{(w)} \quad (2.18)$$

Velocity of point B can be written as

$$\vec{V}_B = D_e \vec{r}_{B/O} = D_s \vec{r}_{B/O} = \dot{x} \vec{u}_1^{(s)} + \dot{y} \vec{u}_2^{(s)} - d_1 D_s \vec{u}_1^{(w)} + d_5 D_s \vec{u}_2^{(w)} \quad (2.19)$$

Inserting Equations 2.14 and 2.15 into Equation 2.19, the following equation is obtained.

$$\vec{V}_B = \dot{x} \vec{u}_1^{(s)} + \dot{y} \vec{u}_2^{(s)} - d_1 \dot{\psi} \vec{u}_2^{(w)} - d_5 \dot{\psi} \vec{u}_1^{(w)} \quad (2.20)$$

Accelerations of points G, A and B can be derived by differentiating the velocity terms in frame $F_s \{O; \vec{u}_1^{(s)}, \vec{u}_2^{(s)}, \vec{u}_3^{(s)}\}$. The following equations represent these accelerations.

$$\vec{a}_G = \ddot{x} \vec{u}_1^{(s)} + \ddot{y} \vec{u}_2^{(s)} \quad (2.21)$$

$$\vec{a}_A = \ddot{x} \vec{u}_1^{(s)} + \ddot{y} \vec{u}_2^{(s)} + \ddot{\psi} (d_6 \vec{u}_1^{(w)} - d_1 \vec{u}_2^{(w)}) + \dot{\psi}^2 (d_1 \vec{u}_1^{(w)} + d_6 \vec{u}_2^{(w)}) \quad (2.22)$$

$$\vec{a}_B = \ddot{x} \vec{u}_1^{(s)} + \ddot{y} \vec{u}_2^{(s)} - \ddot{\psi} (d_5 \vec{u}_1^{(w)} + d_1 \vec{u}_2^{(w)}) + \dot{\psi}^2 (d_1 \vec{u}_1^{(w)} - d_5 \vec{u}_2^{(w)}) \quad (2.23)$$

Angular velocities of the right and left rear wheels with respect to earth fixed frame can be written by Equations 2.24 and 2.25. In these equations, the letters R and L denotes right and left rear wheels respectively.

$$\vec{\omega}_{R/e} = \vec{\omega}_{R/w} + \vec{\omega}_{w/e} \quad (2.24)$$

and

$$\vec{\omega}_{L/e} = \vec{\omega}_{L/w} + \vec{\omega}_{w/e} \quad (2.25)$$

where

$$\vec{\omega}_{R/w} = \dot{\theta}_R \vec{u}_2^{(w)} \quad (2.26)$$

and

$$\vec{\omega}_{L/w} = \dot{\theta}_L \vec{u}_2^{(w)} \quad (2.27)$$

The terms θ_R and θ_L denotes the angular displacements of right and left rear wheels.

If Equations 2.24 and 2.25 are differentiated in frame $F_s \{O; \vec{u}_1^{(s)}, \vec{u}_2^{(s)}, \vec{u}_3^{(s)}\}$, one can get the following two equations for the angular accelerations of the right and left rear wheels.

$$\vec{\alpha}_{R/e} = \vec{\alpha}_R = D_s \vec{\omega}_{R/w} + D_s \vec{\omega}_w \quad (2.28)$$

$$\vec{\alpha}_{L/e} = \vec{\alpha}_L = D_s \vec{\omega}_{L/w} + D_s \vec{\omega}_w \quad (2.29)$$

Equation 2.28 can be rewritten as

$$\vec{\alpha}_R = \vec{\alpha}_w + D_s \left(\dot{\theta}_R \vec{u}_2^{(w)} \right) \quad (2.30)$$

where

$$D_s \left(\dot{\theta}_R \vec{u}_2^{(w)} \right) = D_w \left(\dot{\theta}_R \vec{u}_2^{(w)} \right) + \vec{\omega}_{w/s} \times \dot{\theta}_R \vec{u}_2^{(w)} \quad (2.31)$$

Rearranging the terms in Equation 2.31 gives

$$D_s \left(\dot{\theta}_R \vec{u}_2^{(w)} \right) = \ddot{\theta}_R \vec{u}_2^{(w)} + \left(\dot{\psi} \vec{u}_3^{(s)} \right) \times \dot{\theta}_R \vec{u}_2^{(w)} \quad (2.32)$$

Substituting Equation 2.8 and 2.32 into Equation 2.30, the angular acceleration of the right rear wheel with respect to the earth frame can be derived as in the following equation.

$$\vec{\alpha}_R = \ddot{\psi}\vec{u}_3^{(w)} + \ddot{\theta}_R\vec{u}_2^{(w)} - \dot{\psi}\dot{\theta}_R\vec{u}_1^{(w)} \quad (2.33)$$

Similarly the angular acceleration of the left rear wheel is obtained as

$$\vec{\alpha}_L = \ddot{\psi}\vec{u}_3^{(w)} + \ddot{\theta}_L\vec{u}_2^{(w)} - \dot{\psi}\dot{\theta}_L\vec{u}_1^{(w)} \quad (2.34)$$

Wheels are assumed to roll without slipping. One can rewrite the velocities of center of mass of right and left rear wheels, V_A and V_B as follows.

$$\vec{V}_A = (\dot{\theta}_R\vec{u}_2^{(w)}) \times (\mathbf{R}\vec{u}_3^{(w)}) = \mathbf{R}\dot{\theta}_R\vec{u}_1^{(w)} \quad (2.35)$$

Similarly;

$$\vec{V}_B = (\dot{\theta}_L\vec{u}_2^{(w)}) \times (\mathbf{R}\vec{u}_3^{(w)}) = \mathbf{R}\dot{\theta}_L\vec{u}_1^{(w)} \quad (2.36)$$

Note that

$$\vec{V}_A \cdot \vec{u}_1^{(w)} = \mathbf{R}\dot{\theta}_R \quad (2.37)$$

$$\vec{V}_B \cdot \vec{u}_1^{(w)} = \mathbf{R}\dot{\theta}_L \quad (2.38)$$

and

$$\vec{V}_A \cdot \vec{u}_2^{(w)} = 0 \quad (2.39)$$

$$\vec{V}_B \cdot \vec{u}_2^{(w)} = 0 \quad (2.40)$$

In order to use the above equations one should resolve the velocities of right and left rear wheels derived previously in Equations 2.18 and 2.20 in Frame $F_w \{G; \vec{u}_1^{(w)}, \vec{u}_2^{(w)}, \vec{u}_3^{(w)}\}$. In matrix notation velocities of the right and left rear wheels resolved in frame F_w can be rewritten as follows.

$$\vec{V}_A^{(w)} = \dot{x}\vec{u}_1^{(s/w)} + \dot{y}\vec{u}_2^{(s/w)} - d_1\dot{\psi}\vec{u}_2^{(w/w)} + d_6\dot{\psi}\vec{u}_1^{(w/w)} \quad (2.41)$$

and

$$\vec{V}_B^{(w)} = \dot{x}\vec{u}_1^{(s/w)} + \dot{y}\vec{u}_2^{(s/w)} - d_1\dot{\psi}\vec{u}_2^{(w/w)} - d_5\dot{\psi}\vec{u}_1^{(w/w)} \quad (2.42)$$

Equation 2.41 can be rewritten as,

$$\bar{V}_A^{(w)} = \dot{x}e^{-\bar{u}_3\psi}\bar{u}_1 + \dot{y}e^{-\bar{u}_3\psi}\bar{u}_2 - d_1\dot{\psi}\bar{u}_2 + d_6\dot{\psi}\bar{u}_1 \quad (2.43)$$

Rearranging the terms, one can get the following equation.

$$\bar{V}_A^{(w)} = \dot{x}(\bar{u}_1 \cos(\psi) - \bar{u}_2 \sin(\psi)) + \dot{y}(\bar{u}_2 \cos(\psi) + \bar{u}_1 \sin(\psi)) - d_1\dot{\psi}\bar{u}_2 + d_6\dot{\psi}\bar{u}_1 \quad (2.44)$$

After some manipulations, velocity of point A resolved in wheelchair fixed frame can be rewritten in vector notation as follows.

$$\vec{V}_A = (\dot{x}\cos(\psi) + \dot{y}\sin(\psi) + d_6\dot{\psi})\bar{u}_1^{(w)} + (\dot{y}\cos(\psi) - \dot{x}\sin(\psi) - d_1\dot{\psi})\bar{u}_2^{(w)} \quad (2.45)$$

Similarly, the velocity of the left rear wheel can be obtained after similar manipulations are performed for Equation 2.42.

$$\vec{V}_B = (\dot{x}\cos(\psi) + \dot{y}\sin(\psi) - d_5\dot{\psi})\bar{u}_1^{(w)} + (\dot{y}\cos(\psi) - \dot{x}\sin(\psi) - d_1\dot{\psi})\bar{u}_2^{(w)} \quad (2.46)$$

If Equation 2.45 and 2.46 are substituted into Equations 2.37 and 2.38, respectively, the following two equations are obtained for the independent variables $\dot{\theta}_R$ and $\dot{\theta}_L$.

$$\dot{\theta}_R = \frac{\dot{x}\cos(\psi) + \dot{y}\sin(\psi) + d_6\dot{\psi}}{R} \quad (2.47)$$

and

$$\dot{\theta}_L = \frac{\dot{x}\cos(\psi) + \dot{y}\sin(\psi) - d_5\dot{\psi}}{R} \quad (2.48)$$

Substitution of Equation 2.45 and 2.46 into Equation 2.39 and 2.40 gives Equation 2.49.

$$\dot{\psi} = \frac{\dot{y}\cos(\psi) - \dot{x}\sin(\psi)}{d_1} \quad (2.49)$$

Multiplying Equation 2.47 and 2.48 by the term 'R', and then adding the obtained equations, Equation 2.50 can be obtained. Subtraction of these equations gives Equation 2.51.

$$R(\dot{\theta}_R + \dot{\theta}_L) = 2(\dot{x}\cos(\psi) + \dot{y}\sin(\psi)) + (d_6 - d_5)\dot{\psi} \quad (2.50)$$

$$R(\dot{\theta}_R - \dot{\theta}_L) = 2d_2\dot{\psi} \quad (2.51)$$

where

$$d_2 = \frac{d_5 + d_6}{2} \quad (2.52)$$

Inserting Equation 2.49 into Equation 2.50 and 2.51, the obtained equations can be written in the following matrix representation form.

$$\begin{bmatrix} 2\cos(\psi) - \frac{(d_6 - d_5)}{d_1}\sin(\psi) & 2\sin(\psi) + \frac{(d_6 - d_5)}{d_1}\cos(\psi) \\ -\sin(\psi) & \cos(\psi) \end{bmatrix} \begin{bmatrix} \dot{x} \\ \dot{y} \end{bmatrix} = \begin{bmatrix} R(\dot{\theta}_R + \dot{\theta}_L) \\ \frac{Rd_1}{2d_2}(\dot{\theta}_R - \dot{\theta}_L) \end{bmatrix} \quad (2.53)$$

If $\dot{\theta}_R$ and $\dot{\theta}_L$ are to be used as independent variables, one can obtain the following equation by taking inverse of the above matrix.

$$\begin{bmatrix} \dot{x} \\ \dot{y} \end{bmatrix} = \begin{bmatrix} \frac{\cos(\psi)}{2} & \frac{-2\sin(\psi) + \frac{(d_5 - d_6)}{d_1}\cos(\psi)}{2} \\ \frac{\sin(\psi)}{2} & \frac{2\cos(\psi) + \frac{(d_5 - d_6)}{d_1}\sin(\psi)}{2} \end{bmatrix} \begin{bmatrix} R(\dot{\theta}_R + \dot{\theta}_L) \\ \frac{Rd_1}{2d_2}(\dot{\theta}_R - \dot{\theta}_L) \end{bmatrix} \quad (2.54)$$

After some manipulations, the expressions for \dot{x} and \dot{y} are obtained in terms of $\dot{\theta}_R$ and $\dot{\theta}_L$ as in the following equation.

$$\dot{x} = \frac{R}{2}(\dot{\theta}_R + \dot{\theta}_L)\cos(\psi) + \frac{Rd_1}{4d_2}\left(-2\sin(\psi) + \frac{d_5 - d_6}{d_1}\cos(\psi)\right)(\dot{\theta}_R - \dot{\theta}_L) \quad (2.55)$$

$$\dot{y} = \frac{R}{2}(\dot{\theta}_R + \dot{\theta}_L)\sin(\psi) + \frac{Rd_1}{4d_2}\left(2\cos(\psi) + \frac{d_5 - d_6}{d_1}\sin(\psi)\right)(\dot{\theta}_R - \dot{\theta}_L) \quad (2.56)$$

Equation 2.51 can be rewritten in the following form in terms of $\dot{\theta}_R$ and $\dot{\theta}_L$.

$$\dot{\psi} = R\frac{(\dot{\theta}_R - \dot{\theta}_L)}{2d_2} \quad (2.57)$$

Equation 2.58, 2.59 and 2.60 are obtained by direct differentiation of the Equations 2.55, 2.56 and 2.57.

$$\begin{aligned} \ddot{x} = & \frac{R}{2}(\ddot{\theta}_R + \ddot{\theta}_L)\cos(\psi) - \frac{R}{2}(\dot{\theta}_R + \dot{\theta}_L)\dot{\psi}\sin(\psi) + \frac{Rd_1}{4d_2}\left(-2\sin(\psi) + \frac{d_5 - d_6}{d_1}\cos(\psi)\right) \\ & (\ddot{\theta}_R - \ddot{\theta}_L) + \frac{Rd_1}{4d_2}\left(-2\dot{\psi}\cos(\psi) - \dot{\psi}\frac{d_5 - d_6}{d_1}\sin(\psi)\right)(\dot{\theta}_R - \dot{\theta}_L) \end{aligned} \quad (2.58)$$

$$\begin{aligned} \ddot{y} = & \frac{R}{2}(\ddot{\theta}_R + \ddot{\theta}_L)\sin(\psi) + \frac{R}{2}(\dot{\theta}_R + \dot{\theta}_L)\dot{\psi}\cos(\psi) + \frac{Rd_1}{4d_2}\left(2\cos(\psi) + \frac{d_5 - d_6}{d_1}\sin(\psi)\right) \\ & (\ddot{\theta}_R - \ddot{\theta}_L) + \frac{Rd_1}{4d_2}\left(-2\dot{\psi}\sin(\psi) + \dot{\psi}\frac{d_5 - d_6}{d_1}\cos(\psi)\right)(\dot{\theta}_R - \dot{\theta}_L) \end{aligned} \quad (2.59)$$

$$\ddot{\psi} = R\frac{(\ddot{\theta}_R - \ddot{\theta}_L)}{2d_2} \quad (2.60)$$

The velocity of the center of mass of the wheelchair can be written in matrix notation as follows.

$$\bar{V}_G^{(w)} = \bar{V}_A^{(w)} - (-d_1\dot{\psi}\bar{u}_2 + d_6\dot{\psi}\bar{u}_1) \quad (2.61)$$

Inserting Equation 2.43 into the above equation, one can get

$$\bar{V}_G^{(w)} = \dot{x}(\bar{u}_1\cos(\psi) - \bar{u}_2\sin(\psi)) + \dot{y}(\bar{u}_2\cos(\psi) + \bar{u}_1\sin(\psi)) \quad (2.62)$$

In vector notation, velocity of point G is

$$\vec{V}_G = (\dot{x}\cos(\psi) + \dot{y}\sin(\psi))\bar{u}_1^{(w)} + (\dot{y}\cos(\psi) - \dot{x}\sin(\psi))\bar{u}_2^{(w)} \quad (2.63)$$

Accelerations of the center of mass of the wheelchair, right and left rear wheels can be derived by differentiation of Equations 2.63, 2.45 and 2.46.

$$\vec{a}_G = D_w \vec{V}_G^{(w)} + \vec{\omega}_{w/e} \times \vec{V}_G^{(w)} \quad (2.64)$$

$$\vec{a}_A = D_w \vec{V}_A^{(w)} + \vec{\omega}_{w/e} \times \vec{V}_A^{(w)} \quad (2.65)$$

$$\vec{a}_B = D_w \vec{V}_B^{(w)} + \vec{\omega}_{w/e} \times \vec{V}_B^{(w)} \quad (2.66)$$

Substitution of Equation 2.4, 2.63, 2.45 and 2.46 into the Equations 2.64, 2.65 and 2.66 gives the following three equations after some manipulations.

$$\vec{a}_G = (\ddot{x}\cos(\psi) + \ddot{y}\sin(\psi))\vec{u}_1^{(w)} + (\ddot{y}\cos(\psi) - \ddot{x}\sin(\psi))\vec{u}_2^{(w)} \quad (2.67)$$

$$\begin{aligned} \vec{a}_A = & (\ddot{x}\cos(\psi) + \ddot{y}\sin(\psi) + d_6\ddot{\psi} + d_1\dot{\psi}^2)\vec{u}_1^{(w)} \\ & + (\ddot{y}\cos(\psi) - \ddot{x}\sin(\psi) - d_1\ddot{\psi} + d_6\dot{\psi}^2)\vec{u}_2^{(w)} \end{aligned} \quad (2.68)$$

$$\begin{aligned} \vec{a}_B = & (\ddot{x}\cos(\psi) + \ddot{y}\sin(\psi) - d_5\ddot{\psi} + d_1\dot{\psi}^2)\vec{u}_1^{(w)} \\ & + (\ddot{y}\cos(\psi) - \ddot{x}\sin(\psi) - d_1\ddot{\psi} - d_5\dot{\psi}^2)\vec{u}_2^{(w)} \end{aligned} \quad (2.69)$$

The gravitational acceleration can be written as

$$\vec{g} = -g\vec{u}_3^{(e)} \quad (2.70)$$

If gravitational acceleration vector is resolved in wheelchair fixed frame, the following expression can be obtained.

$$\vec{g}^{(w)} = -g\vec{u}_3^{(e/w)} \quad (2.71)$$

Equation 2.71 can be rewritten in the following form.

$$\vec{g}^{(w)} = -g\hat{C}^{(w,e)}\vec{u}_3^{(e/e)} \quad (2.72)$$

where $\hat{C}^{(w,e)}$ is the transformation matrix from earth frame to the wheelchair frame.

$$\hat{C}^{(w,e)} = [\hat{C}^{(e,w)}]^T \quad (2.73)$$

Substitution of Equation 2.3 into Equation 2.73 and then into Equation 2.72 gives

$$\vec{g}^{(w)} = -g\mathbf{e}^{-\tilde{u}_3\psi}\mathbf{e}^{-\tilde{u}_1\beta}\mathbf{e}^{\tilde{u}_2\alpha}\vec{u}_3^{(e/e)} \quad (2.74)$$

where, if $i \neq j$,

$$\mathbf{e}^{\tilde{u}_i\alpha}\vec{u}_j = u_i\cos(\alpha) + (\vec{u}_i \times \vec{u}_j)\sin(\beta) \quad (2.75)$$

The rule shown in Equation (2.75) can be used to rewrite Equation 2.74.

$$\vec{g}^{(w)} = -ge^{-\tilde{u}_3\psi} e^{-\tilde{u}_1\beta} (\tilde{u}_3\cos(\alpha) + \tilde{u}_1\sin(\alpha)) \quad (2.76)$$

After some manipulations Equation 2.76 can be rewritten as follows.

$$\vec{g} = -gc_1\vec{u}_1^{(w)} - gc_2\vec{u}_2^{(w)} - gc_3\vec{u}_3^{(w)} \quad (2.77)$$

where

$$c_1 = \cos(\alpha)\sin(\beta)\sin(\psi) + \sin(\alpha)\cos(\psi) \quad (2.78)$$

$$c_2 = \cos(\alpha)\sin(\beta)\cos(\psi) - \sin(\alpha)\sin(\psi) \quad (2.79)$$

and

$$c_3 = \cos(\alpha)\cos(\beta) \quad (2.80)$$

Figure 2.4 shows the side view of the wheelchair on a level planar surface.

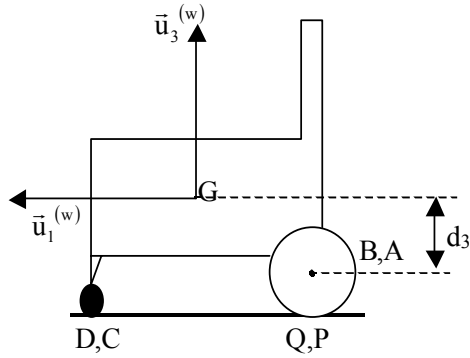


Figure 2.4. Side View of the Wheelchair on a Level Planar Surface.

In Figure 2.4;

- B, A : the center of mass of the left, right rear wheels
- Q, P : the contact point of left, right rear wheels with the ground
- D, C : the contact point of left, right front casters with the ground

The wheelchair system is composed of three connected rigid bodies, which are the right rear wheel, the left rear wheel and the wheelchair body to which the human body is fixed. Front casters are assumed to have negligible mass and friction. Equations 2.81, 2.82 and 2.83 show Newton Equations for the wheelchair body, right rear wheel and left rear wheel, respectively.

$$m_w \vec{a}_G = \vec{F}_A + \vec{F}_B + \vec{F}_C + \vec{F}_D + m_w \vec{g} \quad (2.81)$$

$$m_R \vec{a}_A = -\vec{F}_A + \vec{F}_P + m_R \vec{g} \quad (2.82)$$

$$m_L \vec{a}_B = -\vec{F}_B + \vec{F}_Q + m_L \vec{g} \quad (2.83)$$

where m_w , m_R , and m_L are the mass of the wheelchair, right rear wheel and left rear wheel; \vec{F}_A is the internal force between the right rear wheel and the wheelchair body, and \vec{F}_B is the internal force between the left rear wheel and the wheelchair body. \vec{F}_C , \vec{F}_D and \vec{F}_P , \vec{F}_Q are the external forces applied from the ground to the right, left front casters; and right, left rear wheels.

Equations 2.84, 2.85 and 2.86 show Euler Equations for the wheelchair body, right rear wheel and left rear wheel, respectively.

$$\begin{aligned} D_o(\check{J}_{WG} \cdot \vec{\omega}_w) &= \check{J}_{WG} \cdot \vec{\alpha}_w + \vec{\omega}_w \times \check{J}_{WG} \cdot \vec{\omega}_w \\ &= \vec{r}_{GA} \times \vec{F}_A + \vec{r}_{GB} \times \vec{F}_B + \vec{r}_{GC} \times \vec{F}_C + \vec{r}_{GD} \times \vec{F}_D - \vec{M}_R - \vec{M}_L \end{aligned} \quad (2.84)$$

$$D_o(\check{J}_{RA} \cdot \vec{\omega}_R) = \check{J}_{RA} \cdot \vec{\alpha}_R + \vec{\omega}_R \times \check{J}_{RA} \cdot \vec{\omega}_R = \vec{M}_R + \vec{r}_{AP} \times \vec{F}_P \quad (2.85)$$

$$D_o(\check{J}_{LB} \cdot \vec{\omega}_L) = \check{J}_{LB} \cdot \vec{\alpha}_L + \vec{\omega}_L \times \check{J}_{LB} \cdot \vec{\omega}_L = \vec{M}_L + \vec{r}_{BQ} \times \vec{F}_Q \quad (2.86)$$

The position vectors \vec{r}_{GA} , \vec{r}_{GB} , \vec{r}_{GC} , \vec{r}_{GD} , \vec{r}_{AP} and \vec{r}_{BQ} can be written using Figure 2.3 and Figure 2.4.

$$\vec{r}_{GA} = -d_1 \vec{u}_1^{(w)} - d_6 \vec{u}_2^{(w)} - d_3 \vec{u}_3^{(w)} \quad (2.87)$$

$$\vec{r}_{GB} = -d_1 \vec{u}_1^{(w)} + d_5 \vec{u}_2^{(w)} - d_3 \vec{u}_3^{(w)} \quad (2.88)$$

$$\vec{r}_{GC} = d_0 \vec{u}_1^{(w)} - d_6 \vec{u}_2^{(w)} - h_G \vec{u}_3^{(w)} \quad (2.89)$$

$$\vec{r}_{GD} = d_0 \vec{u}_1^{(w)} + d_5 \vec{u}_2^{(w)} - h_G \vec{u}_3^{(w)} \quad (2.90)$$

$$\vec{r}_{AP} = -R \vec{u}_3^{(w)} \quad (2.91)$$

$$\vec{r}_{BQ} = -R \vec{u}_3^{(w)} \quad (2.92)$$

The inertia dyadics of the wheelchair and right-left rear wheels can be defined by Equations 2.93 and 2.94. The location of the center of mass of the wheelchair is calculated in Appendix A. The calculations of components of inertia dyadic of the wheelchair which has a plane of symmetry about plane $\{\vec{u}_1^{(w)}, \vec{u}_3^{(w)}\}$, and the rear wheels can be found in Appendix B.

$$\begin{aligned} \check{J}_{WG} &= J_{11} \vec{u}_1^{(w)} \vec{u}_1^{(w)} + J_{22} \vec{u}_2^{(w)} \vec{u}_2^{(w)} + J_{33} \vec{u}_3^{(w)} \vec{u}_3^{(w)} \\ &+ J_{31} [\vec{u}_3^{(w)} \vec{u}_1^{(w)} + \vec{u}_1^{(w)} \vec{u}_3^{(w)}] \end{aligned} \quad (2.93)$$

$$\check{J}_{RA} = \check{J}_{LB} = J_s \vec{u}_2^{(w)} \vec{u}_2^{(w)} + J_n [\vec{u}_3^{(w)} \vec{u}_3^{(w)} + \vec{u}_1^{(w)} \vec{u}_1^{(w)}] \quad (2.94)$$

where J_n and J_s are the lateral and polar inertia components of the rear wheels which have inertial symmetry about their axis through A and B .

The force and moment terms in Euler Equations can be written in an expanded form as follows. Remember that front casters have negligible mass and friction.

$$\vec{F}_A = F_{A1} \vec{u}_1^{(w)} + F_{A2} \vec{u}_2^{(w)} + F_{A3} \vec{u}_3^{(w)} \quad (2.95)$$

$$\vec{F}_B = F_{B1} \vec{u}_1^{(w)} + F_{B2} \vec{u}_2^{(w)} + F_{B3} \vec{u}_3^{(w)} \quad (2.96)$$

$$\vec{F}_P = F_{P1} \vec{u}_1^{(w)} + F_{P2} \vec{u}_2^{(w)} + F_{P3} \vec{u}_3^{(w)} \quad (2.97)$$

$$\vec{F}_Q = F_{Q1} \vec{u}_1^{(w)} + F_{Q2} \vec{u}_2^{(w)} + F_{Q3} \vec{u}_3^{(w)} \quad (2.98)$$

$$\vec{F}_C = F_{C3} \vec{u}_3^{(w)} \quad (2.99)$$

$$\vec{F}_D = F_{D3} \vec{u}_3^{(w)} \quad (2.100)$$

$$\vec{M}_R = M_{R1} \vec{u}_1^{(w)} + T_R \vec{u}_2^{(w)} + M_{R3} \vec{u}_3^{(w)} \quad (2.101)$$

$$\vec{M}_L = M_{L1} \vec{u}_1^{(w)} + T_L \vec{u}_2^{(w)} + M_{L3} \vec{u}_3^{(w)} \quad (2.102)$$

In Equations 2.101 and 2.102, the motor torques supplied from the right and left motors are denoted by T_R and T_L .

There are twenty unknowns which are:

$$\ddot{x}, \ddot{y}, F_{A1}, F_{A2}, F_{A3}, F_{B1}, F_{B2}, F_{B3}, F_{P1}, F_{P2}, F_{P3}, F_{Q1}, F_{Q2}, \\ F_{Q3}, F_{C3}, F_{D3}, M_{R1}, M_{R3}, M_{L1}, M_{L3}$$

T_R and T_L are the inputs of the wheelchair system. Although there exists twenty unknowns, there are only eighteen (3x6) system equations formed by scalar components of Equations 2.81, 2.82, 2.83, 2.84, 2.85, and 2.86 in the wheelchair fixed frame. Therefore a solvability assumption can be made without loss of generality such that

$$F_{A2} = F_{B2} \quad (2.103)$$

From Equations 2.82 and 2.83, one can obtain six scalar (2x3) equations for \vec{F}_P and \vec{F}_Q .

$$\vec{F}_P = m_R (\vec{a}_A - \vec{g}) + \vec{F}_A \quad (2.104)$$

$$\vec{F}_Q = m_L (\vec{a}_B - \vec{g}) + \vec{F}_B \quad (2.105)$$

The remaining twelve (4x3) equations are for the other unknowns. Now; if the total front reaction force which is $F_{C3} + F_{D3}$ is assigned to be one unknown, for remaining twelve unknowns, there exists twelve equations. These equations are obtained by substituting Equations 2.104 and 2.105 into the Equations 2.81, 2.84, 2.85 and 2.86, and rearranging them.

$$\vec{F}_A + \vec{F}_B + \vec{F}_C + \vec{F}_D = m_w (\vec{a}_G - \vec{g}) \quad (2.106)$$

$$\vec{r}_{GA} \times \vec{F}_A + \vec{r}_{GB} \times \vec{F}_B + \vec{r}_{GC} \times \vec{F}_C + \vec{r}_{GD} \times \vec{F}_D \\ - \vec{M}_R - \vec{M}_L = \check{J}_{WG} \cdot \vec{\alpha}_w + \vec{\omega}_w \times \check{J}_{WG} \cdot \vec{\omega}_w \quad (2.107)$$

$$\vec{M}_R + \vec{r}_{AP} \times [m_R (\vec{a}_A - \vec{g}) + \vec{F}_A] = \check{J}_{RA} \cdot \vec{\alpha}_R + \vec{\omega}_R \times \check{J}_{RA} \cdot \vec{\omega}_R \quad (2.108)$$

$$\vec{M}_L + \vec{r}_{BQ} \times [m_L (\vec{a}_B - \vec{g}) + \vec{F}_B] = \check{J}_{LB} \cdot \vec{\alpha}_L + \vec{\omega}_L \times \check{J}_{LB} \cdot \vec{\omega}_L \quad (2.109)$$

Now, the unknowns are:

$$\ddot{x}, \ddot{y}, F_{A1}, F_{A2}, F_{A3}, F_{B1}, F_{B3}, (F_{C3} + F_{D3}), M_{R1}, M_{R3}, M_{L1}, M_{L3}$$

Three scalar equations can be obtained by expanding the Equation 2.106 in wheelchair fixed frame components. These equations are as follows.

$$F_{A1} + F_{B1} = m_w (a_{G1} + gc_1) \quad (2.110)$$

$$2F_{A2} = m_w (a_{G2} + gc_2) \quad (2.111)$$

$$F_{A3} + F_{B3} + F_{C3} + F_{D3} = m_w gc_3 \quad (2.112)$$

Substituting Equations 2.87, 2.88, 2.89, 2.90, 2.93, 2.7 and 2.8 into Equation 2.107; and then expanding the vector equation in frame F_w components, three scalar equations can be obtained.

$$-d_6 F_{A3} + 2d_3 F_{A2} + d_5 F_{B3} - d_6 F_{C3} + d_5 F_{D3} - M_{R1} - M_{L1} = J_{31} \ddot{\psi} \quad (2.113)$$

$$d_1 F_{A3} - d_3 F_{A1} + d_1 F_{B3} - d_3 F_{B1} - d_0 F_{C3} - d_0 F_{D3} - T_R - T_L = J_{31} \dot{\psi}^2 \quad (2.114)$$

$$-2d_1 F_{A2} + d_6 F_{A1} - d_5 F_{B1} - M_{R3} - M_{L3} = J_{33} \ddot{\psi} \quad (2.115)$$

If Equations 2.91, 2.94, 2.7 and 2.8 are inserted into Equation 2.108, the following scalar equations are obtained after some manipulations.

$$M_{R1} + Rm_R (a_{A2} + gc_2) + RF_{A2} = -J_s \dot{\theta}_R \dot{\psi} \quad (2.116)$$

$$T_R - Rm_R (a_{A1} + gc_1) - RF_{A1} = J_s \ddot{\theta}_R \quad (2.117)$$

$$M_{R3} = J_n \ddot{\psi} \quad (2.118)$$

The following equations are obtained by substitution of Equation 2.92, 2.94, 2.7 and 2.8 into the Equation 2.109.

$$M_{L1} + Rm_L (a_{B2} + gc_2) + RF_{B2} = -J_s \dot{\theta}_L \dot{\psi} \quad (2.119)$$

$$T_L - Rm_L (a_{B1} + gc_1) - RF_{B1} = J_s \ddot{\theta}_L \quad (2.120)$$

$$M_{L3} = J_n \ddot{\psi} \quad (2.121)$$

Equation 2.111 can be rewritten in the following form.

$$F_{A2} = \frac{1}{2} m_w (a_{G2} + gc_2) \quad (2.122)$$

Inserting Equation 2.122 into Equation 2.116, and rearranging the terms, one can get Equation 2.123.

$$M_{R1} = -J_s \dot{\theta}_R \dot{\psi} - R m_R (a_{A2} + gc_2) - \frac{1}{2} m_w R (a_{G2} + gc_2) \quad (2.123)$$

Similarly, substituting Equation 2.122 into Equation 2.119, the following equation can be obtained.

$$M_{L1} = -J_s \dot{\theta}_L \dot{\psi} - R m_L (a_{B2} + gc_2) - R F_{B2} \quad (2.124)$$

Rearranging Equations 2.117 and 2.120, the expressions for F_{A1} and F_{B1} can be obtained.

$$F_{A1} = \frac{T_R}{R} - m_R (a_{A1} + gc_1) - \frac{J_s}{R} \ddot{\theta}_R \quad (2.125)$$

$$F_{B1} = \frac{T_L}{R} - m_L (a_{B1} + gc_1) - \frac{J_s}{R} \ddot{\theta}_L \quad (2.126)$$

Substitution of Equations 2.125 and 2.126 into the Equation 2.110, one can get the following.

$$\frac{T_R + T_L}{R} - \frac{J_s}{R} (\ddot{\theta}_R + \ddot{\theta}_L) - m_R (a_{A1} + a_{B1} + 2gc_1) = m_w (a_{G1} + gc_1) \quad (2.127)$$

If Equations 2.122, 2.125, 2.126, 2.118, and 2.121 are substituted into the Equation 2.115, Equation 2.128 is obtained.

$$\begin{aligned} & -m_w d_1 (a_{G2} + gc_2) + d_6 \left[-\frac{J_s}{R} \ddot{\theta}_R - m_R (a_{A1} + gc_1) + \frac{T_R}{R} \right] \\ & - d_5 \left[-\frac{J_s}{R} \ddot{\theta}_L - m_L (a_{B1} + gc_1) + \frac{T_L}{R} \right] - 2J_n \ddot{\psi} = J_{33} \ddot{\psi} \end{aligned} \quad (2.128)$$

Note that the masses of right and left rear wheels are equal, which means

$$m_L = m_R \quad (2.129)$$

In Equations 2.127 and 2.128; a_{A1} , a_{B1} and a_{G1} are the accelerations of point A, point B and point G respectively, in $\bar{u}_1^{(w)}$ direction; a_{G2} is the acceleration of the center of mass of the wheelchair in $\bar{u}_2^{(w)}$ direction. Equation 2.127 and 2.128 can be rewritten by the substitution of Equations 2.57, 2.60, 2.67, 2.68, 2.69 and 2.78. Then the obtained equations can be rearranged as follows.

$$\ddot{\theta}_L = \frac{\frac{C + Ad_6}{R} T_R - \frac{C - Ad_5}{R} T_L - [C(m_w + 2m_R) + Am_R(d_6 - d_5)]g}{BC - AD} \frac{(\cos(\alpha)\sin(\beta)\sin(\psi) + \sin(\alpha)\cos(\psi)) - Am_w d_1 g (\cos(\alpha)\sin(\beta)\cos(\psi) - \sin(\alpha)\sin(\psi)) + (EC - AG)(\dot{\theta}_R - \dot{\theta}_L)^2 - AF(\dot{\theta}_R^2 - \dot{\theta}_L^2)}{(2.130)}$$

and

$$\ddot{\theta}_R = \frac{\frac{T_R + T_L}{R} - (m_w + 2m_R)g(\cos(\alpha)\sin(\beta)\sin(\psi) + \sin(\alpha)\cos(\psi)) + E(\dot{\theta}_R - \dot{\theta}_L)^2 - B\ddot{\theta}_L}{A} \quad (2.131)$$

where

$$A = \frac{J_s}{R} + m_R R + m_w \frac{R}{2} + \frac{m_w R}{4d_2} (d_5 - d_6) \quad (2.132)$$

$$B = \frac{J_s}{R} + m_R R + m_w \frac{R}{2} - \frac{m_w R}{4d_2} (d_5 - d_6) \quad (2.133)$$

$$C = \frac{m_L R (d_5 - d_6)}{2} + \frac{m_L R (d_5 - d_6)^2}{4d_2} - \frac{m_w R d_1^2}{2d_2} - \frac{m_R R (d_5^2 + d_6^2)}{2d_2} - \frac{(J_{33} + 2J_n)R}{2d_2} - \frac{J_s}{R} d_6 \quad (2.134)$$

$$D = \frac{m_L R (d_5 - d_6)}{2} - \frac{m_L R (d_5 - d_6)^2}{4d_2} + \frac{m_w R d_1^2}{2d_2} + \frac{m_R R (d_5^2 + d_6^2)}{2d_2} + \frac{(J_{33} + 2J_n)R}{2d_2} + \frac{J_s}{R} d_6 \quad (2.135)$$

$$E = m_w \frac{R^2 d_1}{4d_2^2} \quad (2.136)$$

$$F = m_w \frac{R^2 d_1}{4d_2} \quad (2.137)$$

$$G = \frac{m_w R^2 d_1 (d_5 - d_6)}{8d_2^2} \quad (2.138)$$

Equations 2.130 and 2.131 are the equations of motion that are two coupled nonlinear differential equations for the wheelchair system, which has two degrees of freedom.

The other equations are used to obtain the reaction forces applied from the ground. In fact, after the total front reaction force is found, each of the reaction forces on the right and left rear wheels can be derived separately. However, the total reaction force on one side of the wheelchair approaches zero if the wheelchair tends to topple about the other side. For example, when the wheelchair tends to topple to the right, the total reaction force on the left hand side of the wheelchair will approach to zero. Because of that, it is thought that considering the total reaction force at the left hand side of the wheelchair is sufficient for such a case. Therefore, in order to analyze the reaction forces; the equations for the total reaction force on the front casters, total reaction force on the rear wheels, total reaction force on the right caster and right rear wheel, and total reaction force on the left caster and the left rear wheel, will be derived.

Equations 2.112 and 2.114 can be rewritten in the following forms.

$$F_{C3} + F_{D3} = m_w g c_3 - (F_{A3} + F_{B3}) \quad (2.139)$$

$$d_1 (F_{A3} + F_{B3}) - d_3 (F_{A1} + F_{B1}) - d_0 (F_{C3} + F_{D3}) = T_R + T_L + J_{31} \dot{\psi}^2 \quad (2.140)$$

Inserting Equation 2.125, 2.126 and 2.139 into Equation 2.140, one can get the following equation after some manipulations.

$$\begin{aligned} (d_1 + d_0)(F_{A3} + F_{B3}) &= T_R + T_L + J_{31} \dot{\psi}^2 \\ &+ d_3 m_w (\ddot{x} \cos(\psi) + \ddot{y} \sin(\psi) + g c_1) + d_0 m_w g \cos(\alpha) \cos(\beta) \end{aligned} \quad (2.141)$$

Substituting Equation 2.57, 2.58, 2.59 and 2.78 into Equation 2.141, Equation 2.142 is obtained.

$$(F_{A3} + F_{B3}) = \frac{1}{(d_1 + d_0)} \left[\begin{aligned} & T_R + T_L + d_3 m_w \frac{R}{2} (\ddot{\theta}_R + \ddot{\theta}_L) + d_3 m_w \frac{R}{4d_2} (d_5 - d_6) (\ddot{\theta}_R - \ddot{\theta}_L) \\ & + \left(\frac{J_{31} R^2}{4d_2^2} - \frac{d_3 m_w R^2 d_1}{4d_2^2} \right) (\dot{\theta}_R - \dot{\theta}_L)^2 + d_0 m_w g \cos(\alpha) \cos(\beta) \\ & + d_3 m_w g (\cos(\alpha) \sin(\beta) \sin(\psi) + \sin(\alpha) \cos(\psi)) \end{aligned} \right] \quad (2.142)$$

Adding the Equations 2.104 and 2.105 , the following scalar equation can be obtained.

$$F_{P3} + F_{Q3} = 2m_R g \cos(\alpha) \cos(\beta) + (F_{A3} + F_{B3}) \quad (2.143)$$

Inserting Equation 2.142 into Equation 2.143, the *total reaction force on the rear wheels* of the wheelchair can be obtained, whereas the *total reaction force on the front casters* can be derived from Equation 2.122.

$$F_{C3} + F_{D3} = m_w g \cos(\alpha) \cos(\beta) - (F_{A3} + F_{B3}) \quad (2.144)$$

Rearranging Equation 2.113,

$$\begin{aligned} -d_6 (m_w g c_3 - (F_{B3} + F_{D3})) + d_5 (F_{B3} + F_{D3}) &= M_{R1} + M_{L1} \\ -2d_3 F_{A2} + L_{31} \ddot{\psi} & \end{aligned} \quad (2.145)$$

If Equations 2.80, 2.116, 2.119, 2.122 and 2.60 are inserted into Equation 2.145, one can obtain,

$$\begin{aligned} (F_{B3} + F_{D3}) &= \left(\frac{J_{31} R}{4d_2^2} - \frac{(R + d_3) m_w R d_1}{4d_2^2} \right) (\ddot{\theta}_R - \ddot{\theta}_L) - \frac{(R + d_3) m_w R^2}{16d_2^3} (d_5 - d_6) (\dot{\theta}_R - \dot{\theta}_L)^2 \\ &- \left(\frac{J_s R}{4d_2^2} + (2m_L R + m_w (R + d_3)) \frac{R^2}{8d_2^2} \right) (\dot{\theta}_R^2 - \dot{\theta}_L^2) + \frac{d_6}{2d_2} m_w g \cos(\alpha) \cos(\beta) \\ &- \frac{(m_L R + m_w (R + d_3))}{2d_2} g (\cos(\alpha) \sin(\beta) \cos(\psi) - \sin(\alpha) \sin(\psi)) \end{aligned} \quad (2.145)$$

Remember that

$$F_{B3} = F_{Q3} - m_L g \cos(\alpha) \cos(\beta) \quad (2.146)$$

$$F_{A3} = F_{P3} - m_R g \cos(\alpha) \cos(\beta) \quad (2.147)$$

Substitution of Equation 2.146 into Equation 2.145 gives the *total reaction force on the left wheels* of the wheelchair, which is denoted by ‘ $F_{Q3} + F_{D3}$ ’.

In order to obtain the total reaction force on the right wheels, one should perform the following manipulations.

$$F_{P3} + F_{C3} = m_R g \cos(\alpha) \cos(\beta) + (F_{A3} + F_{C3}) \quad (2.147)$$

where from Equation 2.112,

$$F_{A3} + F_{C3} = m_w g \cos(\alpha) \cos(\beta) - (F_{B3} + F_{D3}) \quad (2.148)$$

Then Equation 2.147 becomes,

$$F_{P3} + F_{C3} = (m_w + m_R) g \cos(\alpha) \cos(\beta) - (F_{B3} + F_{D3}) \quad (2.149)$$

The *total reaction force on the left wheels* can be obtained by substituting Equation 2.145 into Equation 2.149.

2.2.2. Equations of Motion for Changing Slope Road

This second mathematical model is derived to analyze the effects of sudden slope changes on the system stability. The turning effect is not included in this model. The wheelchair driven on a changing slope road is shown in Figure 2.5 on the next page. $F_e \{O; \vec{u}_1^{(e)}, \vec{u}_2^{(e)}, \vec{u}_3^{(e)}\}$ is defined as the inertial frame fixed on the earth, and $F_w \{G; \vec{u}_1^{(w)}, \vec{u}_2^{(w)}, \vec{u}_3^{(w)}\}$ as the wheelchair fixed frame. The wheelchair system has only one degree of freedom in this case.

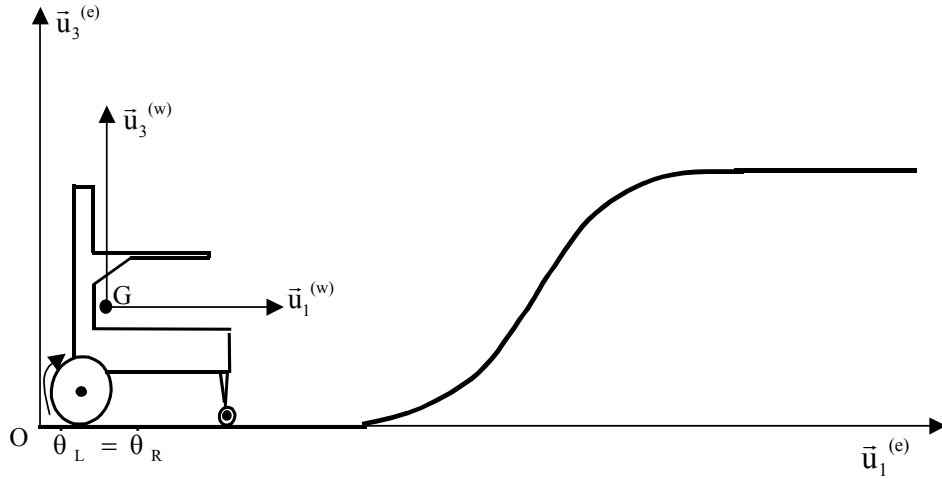


Figure 2.5. Wheelchair on a Changing Slope Road

Successive rotations observed in the earth fixed reference frame $F_e \{O; \bar{u}_1^{(e)}, \bar{u}_2^{(e)}, \bar{u}_3^{(e)}\}$ can be designated by the following definition.

$$F_e \xrightarrow{\bar{u}_2^{(e)}, -\alpha} F_w \quad (2.150)$$

In Equation 2.150, α is the changing up-downhill slope of the road. The transformation matrix between the frames is:

$$\hat{C}^{(e, w)} = e^{-\bar{u}_2 \alpha} \quad (2.151)$$

The angular velocity of the wheelchair can be written as

$$\vec{\omega}_{w/e} = \vec{\omega}_w = -\dot{\alpha} \bar{u}_2^{(e)} = -\dot{\alpha} \bar{u}_2^{(w)} \quad (2.152)$$

where $\vec{\omega}_{w/e}$ is the angular velocity of wheelchair frame F_w with respect to earth fixed frame F_e .

Differentiating the above expression in the earth frame F_e , one can get the expression for the angular acceleration of the wheelchair.

$$\vec{\alpha}_w = D_e \vec{\omega}_{w/e} = -\ddot{\alpha} \bar{u}_2^{(w)} \quad (2.153)$$

From Figure 2.3; the position vector of points G, A and B with respect to the origin O of the earth fixed frame $F_e\{O; \bar{u}_1^{(e)}, \bar{u}_2^{(e)}, \bar{u}_3^{(e)}\}$ can be written by Equations 2.154, 2.155 and 2.156, respectively.

$$\bar{r}_{G/O} = \bar{r}_G = x\bar{u}_1^{(w)} + h_G\bar{u}_3^{(w)} \quad (2.154)$$

$$\bar{r}_{A/O} = \bar{r}_A = (x - d_1)\bar{u}_1^{(w)} - d_2\bar{u}_2^{(w)} + R\bar{u}_3^{(w)} \quad (2.155)$$

$$\bar{r}_{B/O} = \bar{r}_B = (x - d_1)\bar{u}_1^{(w)} + d_2\bar{u}_2^{(w)} + R\bar{u}_3^{(w)} \quad (2.156)$$

Note that,

$$d_5 = d_6 = d_2 \quad (2.157)$$

By differentiating the position vectors in the earth frame, the velocity of points G, A and B can be obtained as follows after some manipulations.

$$\bar{V}_G = D_e \bar{r}_{G/O} = \dot{x}\bar{u}_1^{(w)} + xD_e \bar{u}_1^{(w)} + h_G D_e \bar{u}_3^{(w)} \quad (2.158)$$

$$\bar{V}_A = D_e \bar{r}_{A/O} = \dot{x}\bar{u}_1^{(w)} + (x - d_1)D_e \bar{u}_1^{(w)} - d_2 D_e \bar{u}_2^{(w)} + R D_e \bar{u}_3^{(w)} \quad (2.159)$$

$$\bar{V}_B = D_e \bar{r}_{B/O} = \dot{x}\bar{u}_1^{(w)} + (x - d_1)D_e \bar{u}_1^{(w)} + d_2 D_e \bar{u}_2^{(w)} + R D_e \bar{u}_3^{(w)} \quad (2.160)$$

where $D_e \bar{u}_1^{(w)}$, $D_e \bar{u}_2^{(w)}$ and $D_e \bar{u}_3^{(w)}$ are the differentiation of unit vectors $\bar{u}_1^{(w)}$, $\bar{u}_2^{(w)}$, and $\bar{u}_3^{(w)}$ in the frame $F_e\{O; \bar{u}_1^{(e)}, \bar{u}_2^{(e)}, \bar{u}_3^{(e)}\}$. They can be derived as follows:

$$D_e \bar{u}_1^{(w)} = D_w \bar{u}_1^{(w)} + \bar{\omega}_{w/e} \times \bar{u}_1^{(w)} \quad (2.161)$$

$$D_e \bar{u}_2^{(w)} = D_w \bar{u}_2^{(w)} + \bar{\omega}_{w/e} \times \bar{u}_2^{(w)} \quad (2.162)$$

and

$$D_e \bar{u}_3^{(w)} = D_w \bar{u}_3^{(w)} + \bar{\omega}_{w/e} \times \bar{u}_3^{(w)} \quad (2.163)$$

Differentiation of a unit vector in its own frame gives zero. Therefore;

$$D_w \bar{u}_1^{(w)} = D_w \bar{u}_2^{(w)} = D_w \bar{u}_3^{(w)} = 0 \quad (2.164)$$

Substituting Equation 2.152 and 2.164 into Equations 2.161, 2.162 and 2.163, and rearranging the terms in Equations 2.158, 2.159 and 2.160, the following equations are obtained for the velocities of points G, A and B

$$\vec{V}_G = (\dot{x} - h_G \dot{\alpha}) \bar{u}_1^{(w)} + x \dot{\alpha} \bar{u}_3^{(w)} \quad (2.165)$$

$$\vec{V}_A = (\dot{x} - R \dot{\alpha}) \bar{u}_1^{(w)} + (x - d_1) \dot{\alpha} \bar{u}_3^{(w)} \quad (2.166)$$

$$\vec{V}_B = \vec{V}_A \quad (2.167)$$

Accelerations of points G, A and B can be derived by differentiating the velocity terms in frame $F_e \{O; \bar{u}_1^{(e)}, \bar{u}_2^{(e)}, \bar{u}_3^{(e)}\}$. The following equations represent these accelerations.

$$\bar{a}_G = (\ddot{x} - h_G \ddot{\alpha} - x \dot{\alpha}^2) \bar{u}_1^{(w)} + (x \ddot{\alpha} + 2\dot{x}\dot{\alpha} - h_G \dot{\alpha}^2) \bar{u}_3^{(w)} \quad (2.168)$$

$$\bar{a}_A = (\ddot{x} - R \ddot{\alpha} - (x - d_1) \dot{\alpha}^2) \bar{u}_1^{(w)} + ((x - d_1) \ddot{\alpha} + 2\dot{x}\dot{\alpha} - R \dot{\alpha}^2) \bar{u}_3^{(w)} \quad (2.169)$$

$$\bar{a}_B = \bar{a}_A \quad (2.170)$$

Angular velocities of the right and left rear wheels with respect to earth fixed frame can be written by Equations 2.171 and 2.172. In these equations, the letters R and L denotes right and left rear wheels respectively.

$$\vec{\omega}_{R/e} = \vec{\omega}_{R/w} + \vec{\omega}_{w/e} \quad (2.171)$$

and

$$\vec{\omega}_{L/e} = \vec{\omega}_{L/w} + \vec{\omega}_{w/e} \quad (2.172)$$

where

$$\vec{\omega}_{R/w} = \dot{\theta}_R \bar{u}_2^{(w)} \quad (2.173)$$

and

$$\vec{\omega}_{L/w} = \dot{\theta}_L \bar{u}_2^{(w)} \quad (2.174)$$

The terms θ_R and θ_L denotes the angular displacements of right and left rear wheels.

If Equations 2.171 and 2.172 are differentiated in frame $F_e \{O; \vec{u}_1^{(e)}, \vec{u}_2^{(e)}, \vec{u}_3^{(e)}\}$, one can get the following two equations for the angular accelerations of the right and left rear wheels.

$$\vec{\alpha}_{R/e} = \vec{\alpha}_R = D_e \vec{\omega}_{R/w} + D_e \vec{\omega}_w \quad (2.175)$$

$$\vec{\alpha}_{L/e} = \vec{\alpha}_L = D_e \vec{\omega}_{L/w} + D_e \vec{\omega}_w \quad (2.176)$$

Equation 2.175 can be rewritten as

$$\vec{\alpha}_R = \vec{\alpha}_w + D_e (\dot{\theta}_R \vec{u}_2^{(w)}) \quad (2.177)$$

where

$$D_e (\dot{\theta}_R \vec{u}_2^{(w)}) = D_w (\dot{\theta}_R \vec{u}_2^{(w)}) + \vec{\omega}_{w/e} \times \dot{\theta}_R \vec{u}_2^{(w)} \quad (2.178)$$

Rearranging the terms in Equation 2.178 gives

$$D_e (\dot{\theta}_R \vec{u}_2^{(w)}) = \ddot{\theta}_R \vec{u}_2^{(w)} + (-\dot{\alpha} \vec{u}_2^{(w)}) \times \dot{\theta}_R \vec{u}_2^{(w)} \quad (2.179)$$

Then Equation 2.179 becomes

$$\vec{\alpha}_R = (\ddot{\theta}_R - \dot{\alpha}) \vec{u}_2^{(w)} \quad (2.180)$$

Similarly the angular acceleration of the left rear wheel is obtained as

$$\vec{\alpha}_L = (\ddot{\theta}_L - \dot{\alpha}) \vec{u}_2^{(w)} \quad (2.181)$$

Wheels are assumed to roll without slipping. One can rewrite the velocities of center of mass of the right and left rear wheels, V_A and V_B .

$$\vec{V}_A = (\dot{\theta}_R \vec{u}_2^{(w)}) \times (R \vec{u}_3^{(w)}) = R \dot{\theta}_R \vec{u}_1^{(w)} \quad (2.182)$$

Similarly;

$$\vec{V}_B = (\dot{\theta}_L \vec{u}_2^{(w)}) \times (R \vec{u}_3^{(w)}) = R \dot{\theta}_L \vec{u}_1^{(w)} \quad (2.183)$$

Note that

$$\vec{V}_A \cdot \vec{u}_1^{(w)} = R \dot{\theta}_R \quad (2.184)$$

$$\vec{V}_B \cdot \vec{u}_1^{(w)} = R \dot{\theta}_L \quad (2.185)$$

If Equation 2.166 and 2.167 are substituted into Equations 2.184 and 2.185, respectively, the following two equations are obtained for independent variables $\dot{\theta}_R$ and $\dot{\theta}_L$.

$$\dot{\theta}_R = \frac{\dot{x} - R\dot{\alpha}}{R} \quad (2.186)$$

and

$$\dot{\theta}_L = \dot{\theta}_R \quad (2.187)$$

From equation 2.186 an expression for \dot{x} is obtained in terms of $\dot{\theta}_R$.

$$\dot{x} = R(\dot{\theta}_R + \dot{\alpha}) \quad (2.188)$$

By differentiating the above equation, one can get the following.

$$\ddot{x} = R(\ddot{\theta}_R + \ddot{\alpha}) \quad (2.189)$$

The gravitational acceleration can be written as

$$\vec{g} = -g\vec{u}_3^{(e)} \quad (2.190)$$

If gravitational acceleration vector is resolved in wheelchair fixed frame, the following expression can be obtained.

$$\vec{g}^{(w)} = -g\vec{u}_3^{(e/w)} \quad (2.191)$$

Equation 2.191 can be rewritten in the following form.

$$\vec{g}^{(w)} = -g\hat{C}^{(w,e)}\vec{u}_3^{(e/e)} \quad (2.192)$$

where $\hat{C}^{(w,e)}$ is the transformation matrix from earth frame to the wheelchair frame.

$$\hat{C}^{(w,e)} = [\hat{C}^{(e,w)}]^T \quad (2.193)$$

Then Equation 2.192 can be rewritten as

$$\vec{g}^{(w)} = -g\mathbf{e}^{\tilde{u}_2\alpha}\vec{u}_3^{(e/e)} \quad (2.194)$$

where

$$e^{\bar{u}_i \alpha} \bar{u}_j = u_i \cos(\alpha) + (\bar{u}_i \times \bar{u}_j) \sin(\beta) \quad (2.195)$$

The rule shown in Equation (2.195) can be used to rewrite Equation 2.194.

$$\bar{\mathbf{g}}^{(w)} = -\mathbf{g}(\bar{u}_3 \cos(\alpha) + \bar{u}_1 \sin(\alpha)) \quad (2.196)$$

After some manipulations an expression for the gravitational acceleration is derived as follows.

$$\bar{\mathbf{g}} = -\mathbf{g}c_1 \bar{u}_1^{(w)} - \mathbf{g}c_3 \bar{u}_3^{(w)} \quad (2.197)$$

where

$$c_1 = \sin(\alpha) \quad (2.198)$$

$$c_3 = \cos(\alpha) \quad (2.199)$$

The same Newton-Euler equations in the previous section hold also for this case. These equations are rewritten in this section as follows.

$$\bar{\mathbf{F}}_A + \bar{\mathbf{F}}_B + \bar{\mathbf{F}}_C + \bar{\mathbf{F}}_D = m_w (\bar{\mathbf{a}}_G - \bar{\mathbf{g}}) \quad (2.200)$$

$$\begin{aligned} \bar{\mathbf{r}}_{GA} \times \bar{\mathbf{F}}_A + \bar{\mathbf{r}}_{GB} \times \bar{\mathbf{F}}_B + \bar{\mathbf{r}}_{GC} \times \bar{\mathbf{F}}_C + \bar{\mathbf{r}}_{GD} \times \bar{\mathbf{F}}_D \\ - \bar{\mathbf{M}}_R - \bar{\mathbf{M}}_L = \check{\mathbf{J}}_{wG} \cdot \check{\bar{\boldsymbol{\alpha}}}_w + \bar{\boldsymbol{\omega}}_w \times \check{\mathbf{J}}_{wG} \cdot \bar{\boldsymbol{\omega}}_w \end{aligned} \quad (2.201)$$

$$\bar{\mathbf{M}}_R + \bar{\mathbf{r}}_{AP} \times [m_R (\bar{\mathbf{a}}_A - \bar{\mathbf{g}}) + \bar{\mathbf{F}}_A] = \check{\mathbf{J}}_{RA} \cdot \check{\bar{\boldsymbol{\alpha}}}_R + \bar{\boldsymbol{\omega}}_R \times \check{\mathbf{J}}_{RA} \cdot \bar{\boldsymbol{\omega}}_R \quad (2.202)$$

$$\bar{\mathbf{M}}_L + \bar{\mathbf{r}}_{BQ} \times [m_L (\bar{\mathbf{a}}_B - \bar{\mathbf{g}}) + \bar{\mathbf{F}}_B] = \check{\mathbf{J}}_{LB} \cdot \check{\bar{\boldsymbol{\alpha}}}_L + \bar{\boldsymbol{\omega}}_L \times \check{\mathbf{J}}_{LB} \cdot \bar{\boldsymbol{\omega}}_L \quad (2.203)$$

where

$$\bar{\mathbf{r}}_{GA} = -\mathbf{d}_1 \bar{u}_1^{(w)} - \mathbf{d}_2 \bar{u}_2^{(w)} - \mathbf{d}_3 \bar{u}_3^{(w)} \quad (2.204)$$

$$\bar{\mathbf{r}}_{GB} = -\mathbf{d}_1 \bar{u}_1^{(w)} + \mathbf{d}_2 \bar{u}_2^{(w)} - \mathbf{d}_3 \bar{u}_3^{(w)} \quad (2.205)$$

$$\bar{\mathbf{r}}_{GC} = \mathbf{d}_0 \bar{u}_1^{(w)} - \mathbf{d}_2 \bar{u}_2^{(w)} - \mathbf{h}_G \bar{u}_3^{(w)} \quad (2.206)$$

$$\bar{\mathbf{r}}_{GD} = \mathbf{d}_0 \bar{u}_1^{(w)} + \mathbf{d}_2 \bar{u}_2^{(w)} - \mathbf{h}_G \bar{u}_3^{(w)} \quad (2.207)$$

$$\bar{\mathbf{r}}_{AP} = -\mathbf{R} \bar{u}_3^{(w)} \quad (2.208)$$

$$\vec{r}_{BQ} = -R\vec{u}_3^{(w)} \quad (2.209)$$

Since the wheelchair does not turn while moving, right and left front casters carry equal weight. Then the following equation can be written as a constraint.

$$F_{C3} = F_{D3} \quad (2.210)$$

There exist twelve equations, and twelve unknowns now.

$$\ddot{x}, F_{A1}, F_{A2}, F_{A3}, F_{B1}, F_{B2}, F_{B3}, F_{C3}, M_{R1}, M_{R3}, M_{L1}, M_{L3}$$

Three scalar equations can be obtained by expanding the Equation 2.200 in wheelchair fixed frame components. These equations are as follows.

$$F_{A1} + F_{B1} = m_w (a_{G1} + gc_1) \quad (2.211)$$

$$F_{A2} + F_{B2} = 0 \quad (2.212)$$

$$F_{A3} + F_{B3} + 2F_{C3} = m_w (a_{G3} + gc_3) \quad (2.213)$$

Note that the heading angle of the wheelchair is zero since there is no turn effect.

$$\psi = \dot{\psi} = \ddot{\psi} = 0 \quad (2.214)$$

Substituting Equations 2.204, 2.205, 2.206, 2.207, 2.93, 2.152 and 2.153 into Equation 2.201; three scalar equations can be obtained after some manipulations.

$$d_2(F_{B3} - F_{A3}) + d_3(F_{A2} + F_{B2}) - M_{R1} - M_{L1} = 0 \quad (2.215)$$

$$d_1(F_{A3} + F_{B3}) - d_3(F_{A1} + F_{B1}) - 2d_0F_{C3} - T_R - T_L = -J_{22}\ddot{\alpha} \quad (2.216)$$

$$d_2(F_{A1} - F_{B1}) - d_1(F_{A2} + F_{B2}) - M_{R3} - M_{L3} = 0 \quad (2.217)$$

If Equations 2.208, 2.180 and 2.171 are inserted into Equation 2.202, the following scalar equations are obtained.

$$M_{R1} + RF_{A2} = 0 \quad (2.218)$$

$$T_R - Rm_R(a_{A1} + gc_1) - RF_{A1} = J_s(\ddot{\theta}_R - \ddot{\alpha}) \quad (2.219)$$

$$M_{R3} + 0 = 0 \quad (2.220)$$

The following equations are obtained by substitution of Equation 2.209, 2.181 and 2.172 into the Equation 2.203.

$$M_{R1} + RF_{A2} = M_{L1} + RF_{B2} \quad (2.221)$$

$$T_R - RF_{A1} = T_L - RF_{B1} \quad (2.222)$$

$$M_{R3} + 0 = M_{L3} + 0 \quad (2.223)$$

After some manipulations are performed on the equations 2.111-2.223, the equation of motion and the reaction forces are obtained.

The equation of motion of single dof system is obtained as in the following expression.

$$\begin{aligned} T_R - \left(Rm_R + \frac{Rm_w}{2} + \frac{J_s}{R} \right) \ddot{x} + R \left(m_R + \frac{Rm_w}{2} \right) \dot{\alpha}^2 x - Rm_R d_1 \dot{\alpha}^2 \\ + \left(R^2 m_R + \frac{Rh_G m_w}{2} + 2J_s \right) \ddot{\alpha} = \left(m_R + \frac{Rm_w}{2} \right) g \sin(\alpha) \end{aligned} \quad (2.224)$$

where

$$\ddot{\theta}_R = \ddot{\theta}_L = \frac{\ddot{x} - R\ddot{\alpha}}{R} \quad (2.225)$$

Since the wheelchair does not turn, same amount of torques are supplied by the motors.

The *total front casters' reaction force* is derived after some manipulations.

$$F_{C3} + F_{D3} = 2 \left(\frac{m_w}{2} (x\ddot{\alpha} + 2\dot{x}\dot{\alpha} - h_G \dot{\alpha}^2 + g \cos(\alpha)) - F_{A3} \right) \quad (2.226)$$

where

$$F_{A3} = \frac{1}{d_0 + d_1} \left[\frac{m_w d_0}{2} (x\ddot{\alpha} + 2\dot{x}\dot{\alpha} - h_G \dot{\alpha}^2 + g \cos(\alpha)) + \frac{m_w d_3}{2} (\ddot{x} - x\dot{\alpha}^2 - h_G \ddot{\alpha} + g \sin(\alpha)) - \frac{J_{22} \ddot{\alpha}}{2} + T_R \right] \quad (2.227)$$

The total reaction force applied on the rear wheels is shown in Equation 2.228.

$$F_{P3} + F_{Q3} = 2(m_R((x - d_1)\ddot{\alpha} + 2\dot{x}\dot{\alpha} - R\dot{\alpha}^2 + g\cos(\alpha)) + F_{A3}) \quad (2.228)$$

Equations 2.229 and 2.230 show the *total reaction forces applied on the right, and left wheels* respectively.

$$F_{C3} + F_{P3} = \frac{m_w}{2}(x\ddot{\alpha} + 2\dot{x}\dot{\alpha} - h_G\dot{\alpha}^2 + g\cos(\alpha)) + m_R((x - d_1)\ddot{\alpha} + 2\dot{x}\dot{\alpha} - R\dot{\alpha}^2 + g\cos(\alpha)) \quad (2.229)$$

and

$$F_{D3} + F_{Q3} = F_{C3} + F_{P3} \quad (2.230)$$

Note that the total reaction forces applied on the left and right wheels are same. Because the wheelchair does not turn; it has only a forward movement.

2.3. System Components and Control Structure

Two Simulink models are formed for the two mathematical models obtained for constant and changing sloped roads. Simulink model for the constant slope road is shown in Figure 2.6 on the next page. As can be seen from this figure, there are two inputs to the joystick, which are ‘Voltage x’ and ‘Voltage y’. These two inputs are determined by the user. ‘Voltage x’ is related with the velocity of the wheelchair whereas ‘Voltage y’ is related with the heading angle. The higher the ‘Voltage x’ the faster the wheelchair is, and the higher the ‘Voltage y’ the more sharp the wheelchair turns. The joystick produces suitable reference angular velocities according to these voltages. Then, the actual angular velocities of the right and left rear wheels are compared with these reference values, and the errors are to be minimized by the PI controllers, and the proper motor voltages are produced. These motor voltages go to the right and left motor dynamics, and the motor torques are produced. The equation of motion of the wheelchair system is modeled in the subsystem denoted by ‘WHEELCHAIR DYNAMICS’.

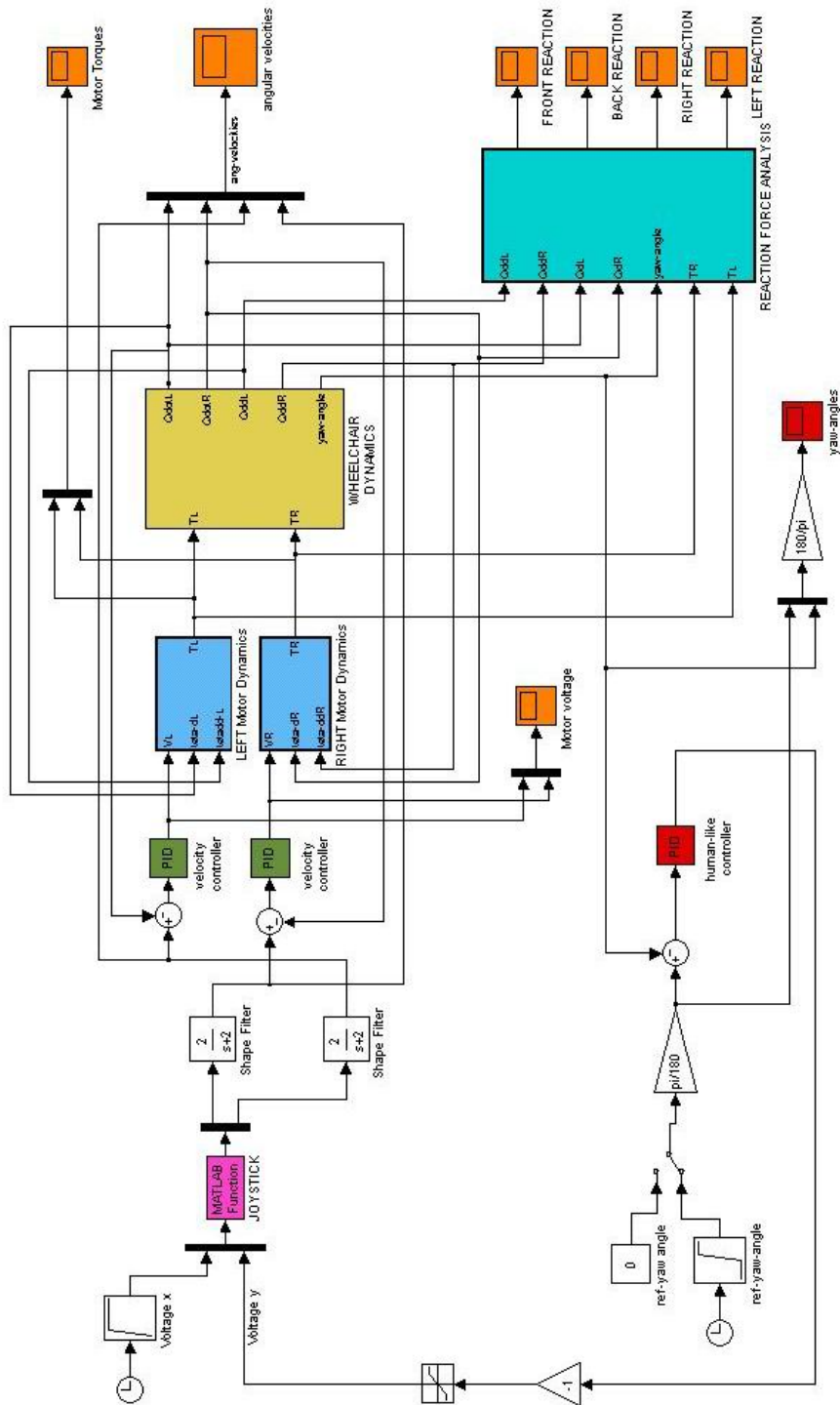


Figure 2.6. Simulink Model of the Wheelchair System on a Constant Slope Road

The proportional controller denoted by 'human-like controller' in Figure 2.6 is used to control the heading angle of the wheelchair by means of an approximated mental control behaviour of the driver. If the heading angle of the wheelchair is not the same as the reference input defined by the user, he will change the direction of the wheelchair in a desired manner by means of joystick movements. Therefore, the output of this controller is the 'Voltage y ' which determines the steepness of the wheelchair turns.

Angular velocities, and accelerations of the right and left rear wheels, the yaw angle and torque inputs go into the subsystem 'REACTION FORCE ANALYSIS' in Figure 2.6, and the total reaction forces on the front casters, rear wheels, the wheels on the left and right side of the wheelchair are obtained.

The Simulink model of the wheelchair system driven on a changing slope road can be seen in Figure 2.7 on the next page. Note that there is a manual switch after the reference yaw angle blocks. This switch is used either to give a reference yaw angle of zero or changing values. Since the turning effect of the wheelchair is not considered in this model, the heading angle of the wheelchair remains always zero. Therefore, a constant value of zero is used as a reference yaw angle value here. The other block which gives changing values for reference yaw angle is used in the previous model instead. Because, different heading angles desired by the driver can be defined by this block as a function of time. Here, the system has only one degree of freedom unlike the other model. The difference in this model is that there exists a subsystem to model the road, and the outputs of this subsystem are the changing slope of the road and its time derivatives, which are fed to the subsystem 'WHEELCHAIR DYNAMICS'.

The road is modeled as a function of position ' x '. Four different mathematical functions are used to model the road. The important thing to consider while choosing these functions is that the function should be continuous. There should not be any discontinuity that will cause a sudden jump on the slope of the road. Because such a jump on the slope of the road, and the time rate of change of this slope will cause a problem in the solution of dynamic equations of the system.

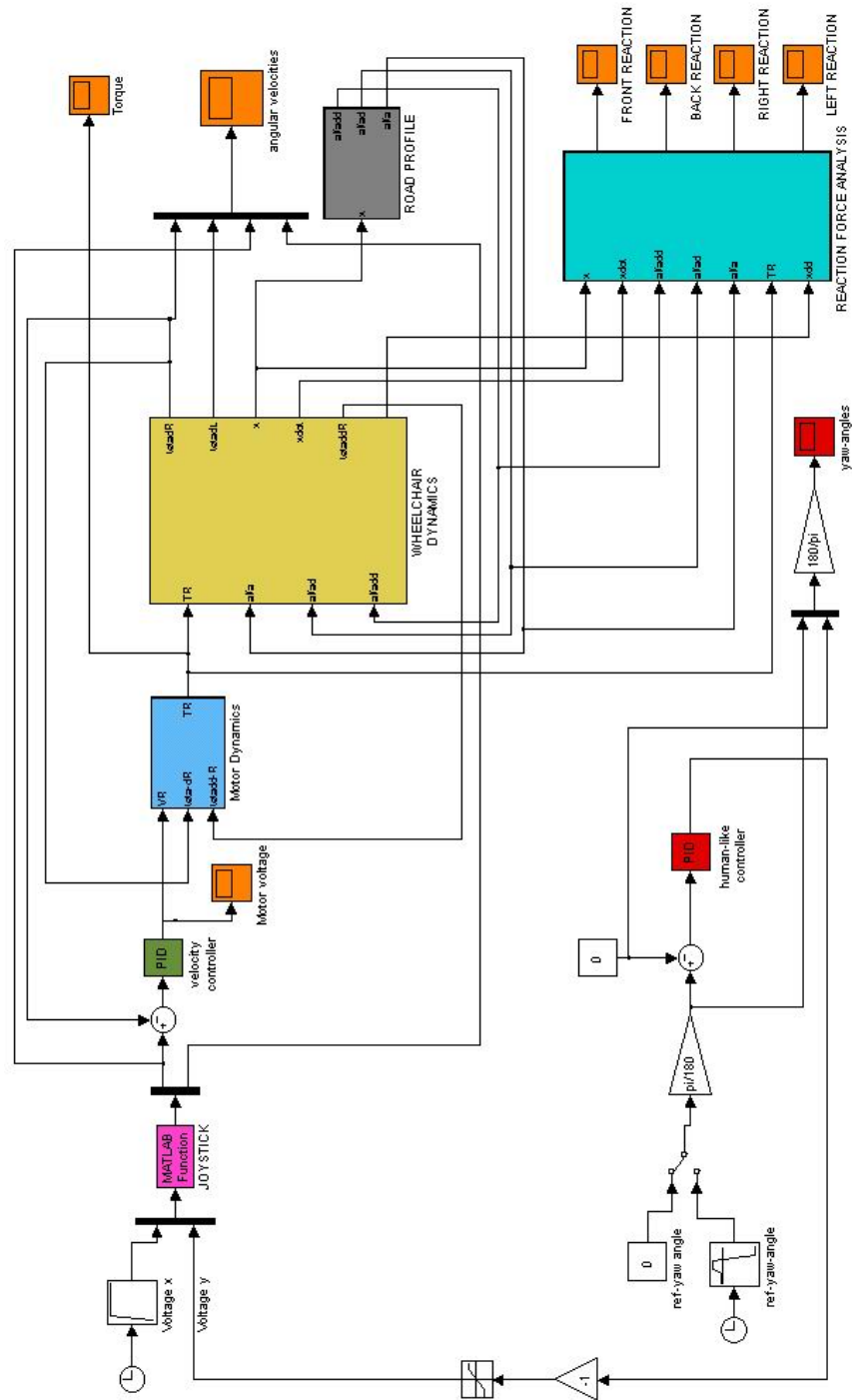


Figure 2.7. Simulink Model of the Wheelchair System on a Changing Slope Road

The road functions used in the simulation are approximations of real roads. For a smooth downhill and uphill slope, the hyperbolic tangent function [15] is modified as follows.

$$z = h \left(\frac{e^{-a(x-b)} - 1}{e^{-a(x-b)} + 1} \right) + h \quad (2.231)$$

$$z = h \left(\frac{e^{a(x-b)} - 1}{e^{a(x-b)} + 1} \right) + h \quad (2.232)$$

Equations 2.231 and 2.232 represent a smooth downhill slope and uphill slope respectively. 'h' denotes the altitude of the road. As the value of 'b' decreases and 'a' increases, the slope of the road becomes steeper as shown in Figure 2.8.

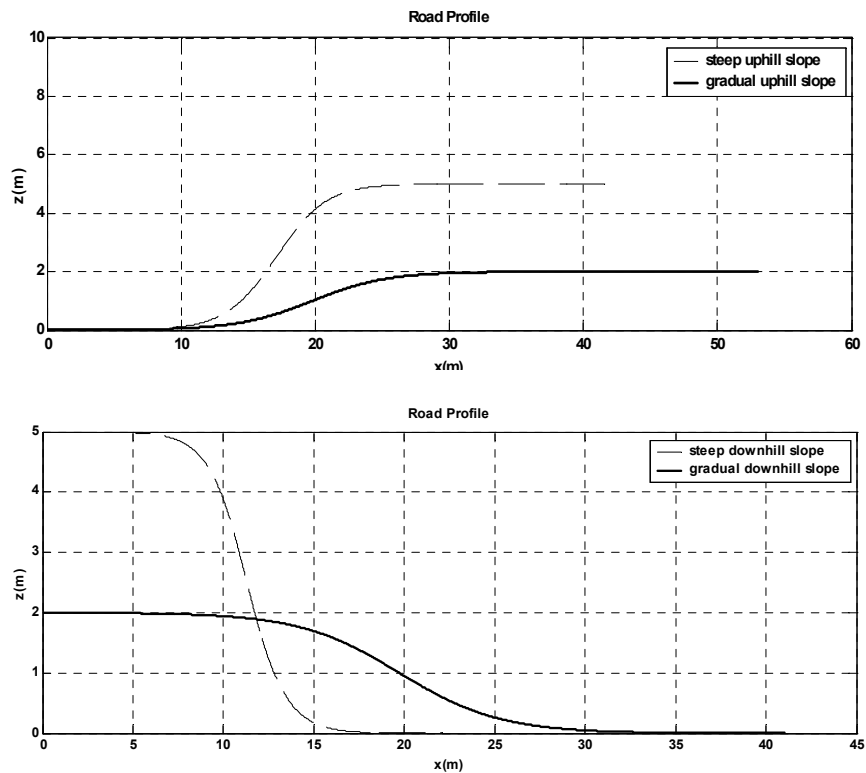


Figure 2.8. Downhill and Uphill Road Profiles.

The road profile shown in Figure 2.9 is obtained by the following mathematical function [16].

$$z = h \left(\frac{1}{1 + a(x - b)^4} \right) \quad (2.233)$$

where ‘h’ denotes the altitude of the road. As the value of ‘b’ increases and ‘a’ decreases, the slope of the road becomes steeper.

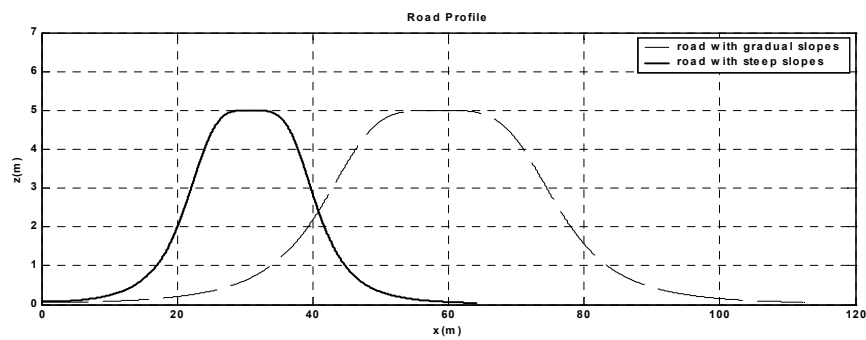


Figure 2.9. A Changing Sloped Road Profile

Figure 2.10 shows the detailed view of the subsystem ‘ROAD PROFILE’.

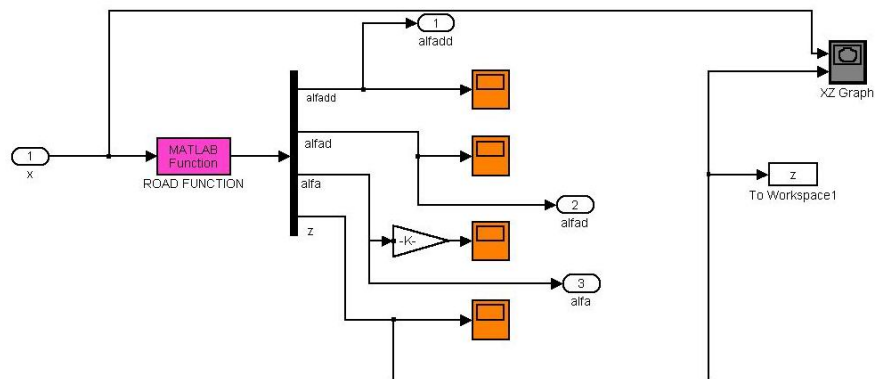


Figure 2.10. The Subsystem ‘ROAD PROFILE’

The position of the wheelchair in $\bar{u}_1^{(w)}$ direction, 'x', goes into the road function where the road profile is obtained as a function of 'x' by means of Equations 2.231, 2.232 or 2.233. Then the terms z , α , $\dot{\alpha}$ and $\ddot{\alpha}$ are obtained.

2.3.1. DC Motor

The next step in determining the equations of motion of the system is the derivation of motor dynamic equations since the motor itself also shows a dynamic behavior.

Figure 2.11 shows the armature mechanical loading diagram of the motor.

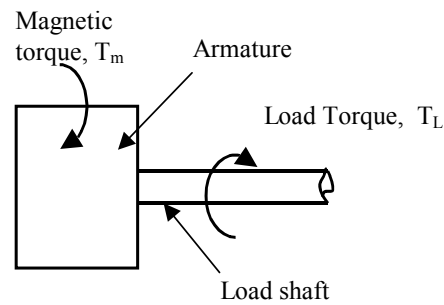


Figure 2.11. Mechanical Portion of the Motor

If the stator is made of a permanent magnet, then one can take the field current constant [17]. Thus, the magnetic torque of the motor can be expressed as

$$T_m = i_m K_t \quad (2.234)$$

There exist two motors, which supply torques to the left and right rear wheels separately in the wheelchair system. These motors are permanent magnet DC motors and can be defined by the following dynamic equations [17].

$$V_m = i_m R_m + K_e \omega_m + L_m \left(\frac{di_m}{dt} \right) \quad (2.235)$$

$$i_m K_t - T_L = J_m \left(\frac{d\omega_m}{dt} \right) \quad (2.236)$$

The parameters in Equations 2.235 and 2.236 can be defined as follows.

R_m	:	resistance of the armature windings of the motor
i_m	:	armature current
V_m	:	supply voltage to the armature
K_e	:	motor voltage constant
ω_m	:	angular speed of the motor
L_m	:	motor inductance
K_t	:	motor torque constant
T_L	:	load torque
J_m	:	polar moment of inertia of the motor

The transient response of motor voltage to changes in motor current is assumed to be negligible, i.e., $L_m \left(\frac{di_m}{dt} \right)$ is taken as zero [17].

Coulomb friction and associated dead band effects, magnetic hysteresis, magnetic saturation and eddy current effects are neglected in obtaining the dynamic model of the motors [17].

The maximum torque requirement and the wheelchair maximum velocity are important parameters in the selection of suitable actuators. In order to choose a proper actuator for the wheelchair system, the commercial wheelchair motors have been investigated. As a result, it has been seen that the maximum velocity of a standard wheelchair used in commercial applications is about 1,8-3,2 m/s and the maximum torque requirement is about 55 N.m [18]. These values have also

been verified by the simulations carried out. Finally, a DC-motor, which satisfies the above criteria, is selected from one of the available manufacturers [19].

2.3.2. Joystick

The two-axis joystick as shown in Figure 2.12 translates two degrees of freedom hand motion in two voltages V_x and V_y . The speed of the wheelchair, and the sharpness of the turns are determined by V_x and V_y , respectively. In other words, the user's commands are transformed by means of a joystick into electrical signals that set the wheel speed and the wheel direction.

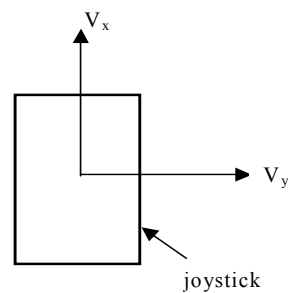


Figure 2.12. Joystick Inputs

Referring to Figure 2.6, it is seen that the 'JOYSTICK FUNCTION' in the simulations converts two input voltages to reference angular velocities that are compared with the actual angular velocities. The outputs of the PI controllers are suitable motor voltages that are inputs to the motor dynamics.

The joystick produces voltages in the range of -5 V and $+5$ V. For full speed forward the joystick output is about $+5$ V

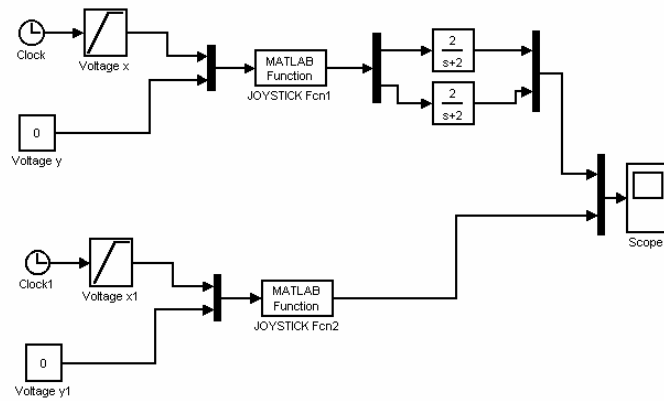


Figure 2.13. Simulation of the Joystick

In Figure 2.13, the voltage inputs are converted to reference angular velocities. If a shape filter is used sudden jumps of the angular velocities are prevented.

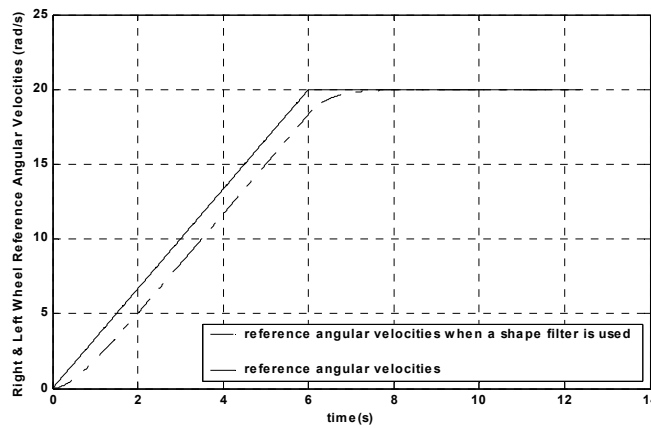


Figure 2.14. Reference Angular Velocities for a Ramp Input of V_x

Figure 2.14 shows the case when V_x is increased from 0 V to a maximum voltage of +5 V in six seconds and then remained constant, and V_y is given zero by the

user. The angular velocities of the right and left rear wheels are the same since no voltage is given in y direction, and they reach to their maximum value due to the reference maximum voltage in x direction. When a shape filter is used the sudden increase of the reference angular velocities of the right and left rear wheels become gradual although the user input was a ramp function.

When a sudden jump of the V_x from 0 V to 5 V occurs as a step function, the reference angular velocities are obtained as shown in Figure 2.15. Since there is no voltage in y direction the angular velocities of the right and left rear wheels are equal. When a shape filter is used, the sudden jump in the reference angular velocities is prevented by a gradual increase. The only disadvantage of such a filter is that it causes a time lag.

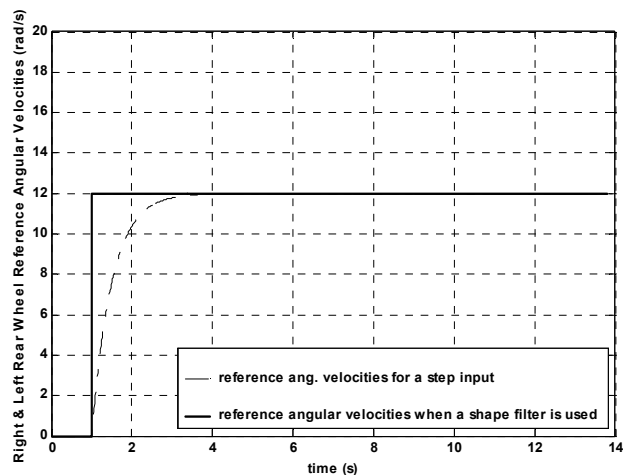


Figure 2.15. Reference Angular Velocities for a Step Input of V_x

The higher the voltage in x direction the higher the speed of the wheelchair is. If the patient wants to have a sharp turn at high speeds this can disturb him. The user's commands of high speeds during steep turns should be modified automatically such that the wheelchair follows the desired course, but its movement speed is reduced. This modification is carried out during the interpretation of voltage values by means of the joystick.

The following equations are used in the joystick function during simulations.

$$\ddot{\theta}_L = (K_3 - K_1|V_y|)V_x + K_2V_y \quad (2.237)$$

$$\ddot{\theta}_R = (K_3 - K_1|V_y|)V_x - K_2V_y \quad (2.238)$$

Joystick converts the voltage inputs to the reference angular velocities for right and left rear wheels by Equations 2.237 and 2.238, where V_x and V_y are the voltages in x and y direction, K_1 , K_2 and K_3 are specified constants. The values of these constants are determined according to the results of several simulations carried out. If desired, they can be changed according to the system performance. Referring to these equations it can be seen that as the voltage in y direction is increased, the speed of the wheelchair is decreased and the difference between the angular velocities of the right and left wheels are increased.

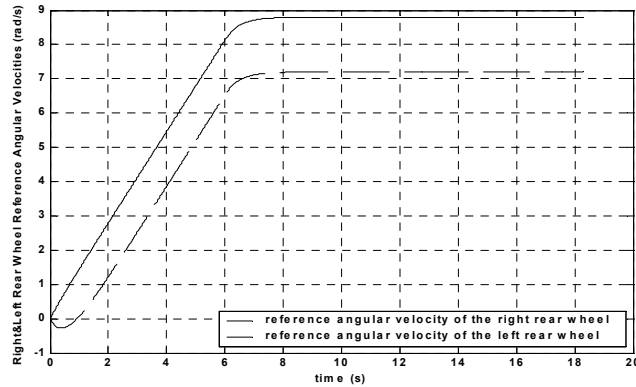


Figure 2.16. Reference Angular Velocities for Positive V_x and V_y

When V_x is increased from 0 V to maximum voltage of +5 V in six seconds and then remained constant, and V_y is given +3 V by the user, the result for such a case is shown in Figure 2.16. Since V_y is given a positive voltage the wheelchair will turn to the right, which means that the reference angular velocity of the left

rear wheel will be higher. Although +5 V is supplied by the user as a voltage in x direction, the angular velocity of the left rear wheel does not reach to its maximum value. Because, the speed is reduced due to the supplied positive voltage in y direction. If a higher voltage is given in y direction, the speed of the wheels are reduced more for a safer wheelchair steering process.

2.3.3. Velocity Control of the Wheelchair

The speed of the wheelchair is controlled by means of control of the angular velocities of the right and left rear wheels. Encoders can be used to measure the angular velocities. Once they are measured, the actual angular velocities are compared with the reference ones that are the outputs of the joystick. The errors are to be minimized by PI controllers.

With a proportional controller, the controller output is proportional to the error. The advantage of a proportional-only control is its simplicity

With a derivative action, the controller output is proportional to the amount of time rate of change of the error. Derivative action can compensate for a changing measurement. It provides extra damping to the system. A disadvantage of derivative control is that controller output is zero when the error signal is constant. Therefore, it is never used alone.

With integral action, the controller output is proportional to the amount of the accumulated error. The primary advantage of integral control is that it has a tendency to reduce the steady state error. Controllers have been developed that combine the use of proportional and integral control. The result is a proportional-integral (PI) controller, which is used in the simulation of the wheelchair system because of the immediate acting proportional control coupled with the corrective acting integral control. PI control is preferred over P control for smaller final error and over PID for smoother start-up.

Since the equations of motion of the wheelchair system are highly nonlinear, coupled equations; control gains for PI system are chosen by trial and error. The

speed and smoothness of the response, and system stability are examined by carrying out several simulations under varying road conditions; and suitable values for proportional and integral gain are selected accordingly.

The user decides the speed of the wheelchair by joystick movements in terms of voltage in x direction, and the controller takes care of the rest.

Control of the angular velocities of each of the rear wheels independently eliminates the effects of a downhill grade upon speed by a significant reduction of the excessive speed increase of the wheelchair. When the wheelchair is driven on a side slope, it tends to turn to a directly downhill course and speeds up. With PI control of the angular velocities the chair does not speed up as much. How the heading angle of the wheelchair is controlled for such a case is another question. This is analyzed in the next section.

2.3.4. Yaw Angle Control of the Wheelchair

The desired direction of the wheelchair is determined by the user in terms of the joystick input of voltage in y direction. The higher this voltage is the more sharp the wheelchair turns. Normally, the wheelchair driver will determine the heading angle of the wheelchair by means of controlled movements of the joystick. If the direction of the wheelchair is not proper according to his idea he will move the joystick more or less to the left or right. When the joystick is moved to the right a positive voltage in y direction is produced which causes the wheelchair to turn right, and a negative voltage is produced as the joystick is moved to the left that makes the wheelchair turn left.

The desired heading of the wheelchair determined by the user is defined by a 'Look-up Table' [20] in the simulations as can be seen in Figure 2.17. 'Look-up Table' is used to define the commands of the patient in terms of direction angle of the wheelchair mathematically. As an example, if the user wants to move forward for 10 seconds, then turn to left with a heading angle of 30^0 , such a

scenario is defined by a mathematical function using ‘Look-up Table’ so that the reference yaw angle in patient’s mind is modeled.

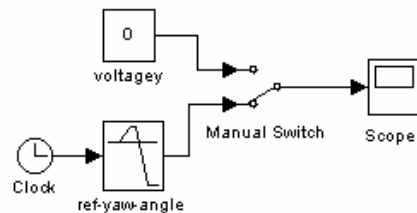


Figure 2.17. Reference Yaw Angle Block

Note that manual switch is used either to give a constant ‘voltage y’ of zero or changing values for reference yaw angle. Constant voltage of zero in y direction is given for the case when the wheelchair is driven on changing slope roads with no turn. The reference yaw angle of zero indicates that no voltage is supplied in y direction of the joystick. For the simulations carried out on constant slope roads, the steering effect is considered. Therefore, in such cases changing values of yaw angles are given as reference inputs.

Human control of the direction angle is modeled by a proportional (P) control in the simulations. Because, a human being can estimate the error and move the joystick proportional to this error, which will result in a suitable ‘Voltage y’ output accordingly. However, it is difficult for the user to take the integral of the error or to estimate the rate of change of the error. Therefore, proportional control is used to model the human mental control behavior for the heading angle of the wheelchair. A proper proportional gain is determined after several simulations are carried out. The controlled output is the ‘Voltage y’, which is the input to the joystick as can be seen in Figures 2.6 and 2.7.

Figure 2.18 shows the actual and reference yaw angles for a specific case. Note that actual angular velocity follows the desired path. The xy position of the wheelchair for this specific case is shown in Figure 2.19. The wheelchair moves forward for 10 seconds, then turns to left with a heading angle of 30° and keeps this direction for 5 seconds. Finally, wheelchair turns to right with a heading angle of 90° .

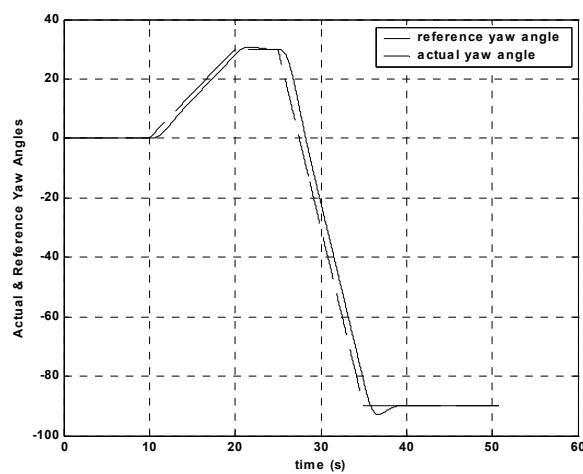


Figure 2.18. Actual and Reference Yaw Angle for a Specific Case

The output of the human controller is the voltage input of the joystick in y direction. For the case shown in Figure 2.19, the user wants to move forward in 10 seconds then turn to left, which results in negative ‘voltage y’ after 10 seconds as can be seen in Figure 2.20. Since the wheelchair is desired to turn 90° to the right at 25th second the value of ‘Voltage y’ becomes positive. Note that the voltage input to the joystick in y direction is zero when the user wants to move forward without turn or keep the direction constant after turn.

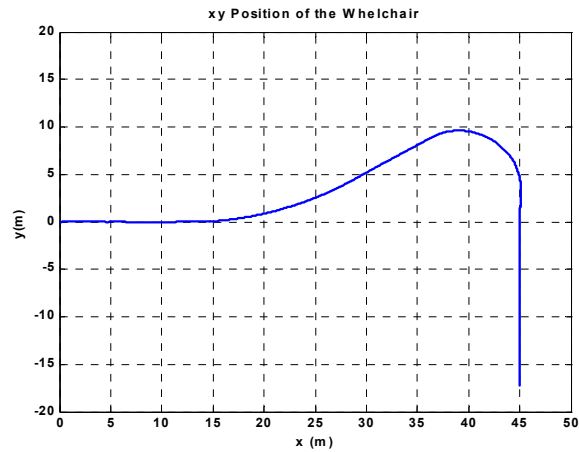


Figure 2.19. xy Position of the Wheelchair for a Specific Case

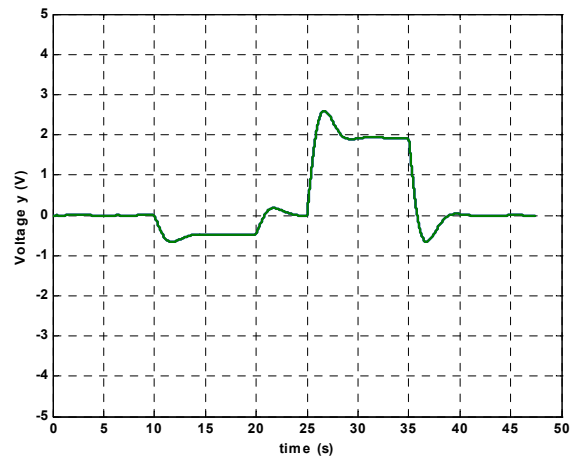


Figure 2.20. 'Voltage y' for the Specific Case

2.3.5. Methods of Stability Augmentation

One of the methods for stability augmentation is the speed reduction during steering as previously mentioned in Section 2.3.2. When the wheelchair driver wants to have a sharp turn at a high speed such a user command is modified by the joystick module. The desired path is followed but the velocity of the wheelchair is reduced for the purpose of stability. This method causes some time lag but improves the stability.

The patient may want to follow such a path as shown in Figure 2.21 at maximum velocity, where the wheelchair turns 90° to the left while moving straight, keeps its direction for some time, then turns around itself about 360° . This command is modified by the joystick module such that the angular velocities of the right and left rear wheels are reduced as the voltage applied in y direction of the joystick is increased, as shown in Figure 2.22.

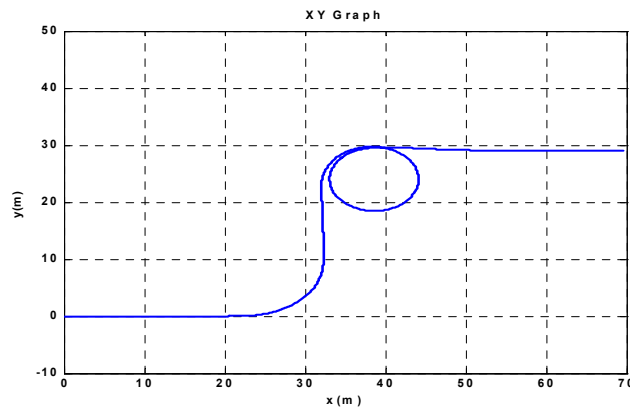


Figure 2.21. Sharp Turns of the Wheelchair at Maximum Speed

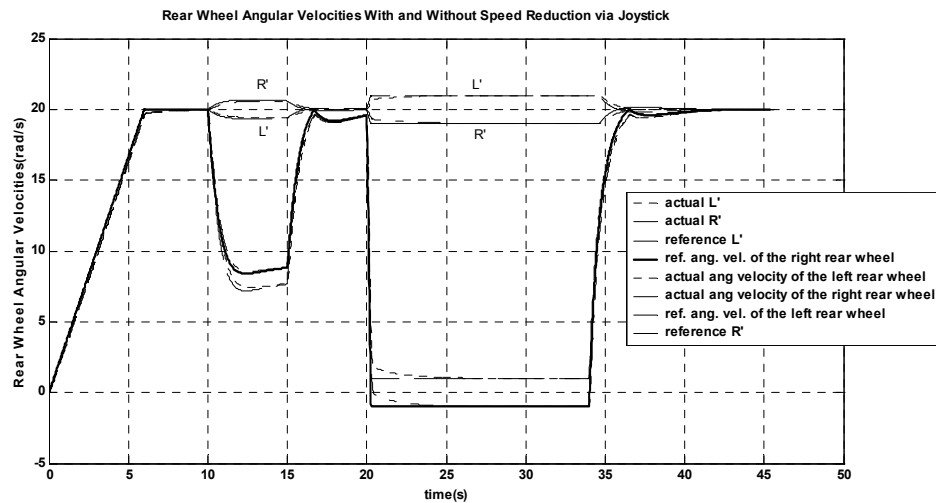


Figure 2.22. The Angular Velocities of the Right and Left Rear Wheels

In Figure 2.22, two cases for the angular velocities are shown, where in one case the angular velocities thus the speed of the wheelchair is reduced via joystick module, and in the other case the user's reference command is applied without any modification. As the user increases 'Voltage y' more, the speed of the wheelchair is reduced more for a safe steering. However, the increase or decrease of the 'Voltage y' is limited in the simulations by means of saturation blocks since the joystick can supply voltages in the range of -5 V and $+5\text{ V}$ only.

When the wheelchair turns to the left, the reaction forces at the outer wheels increase, which means that the total reaction force on the right wheels increases, whereas it decreases, as the wheelchair turns right. Figure 2.23 shows the total reaction force on the right wheels for the wheelchair that follows the path in Figure 2.21. Note that the decrease in the reaction force during right turn is not as much as in the case where the users' commands are not modified, which can prevent the tendency of the wheelchair system from toppling to the left side in more unreliable situations. Therefore, it can be said that such a reduction in speed improves the stability of the wheelchair during sharp turns.

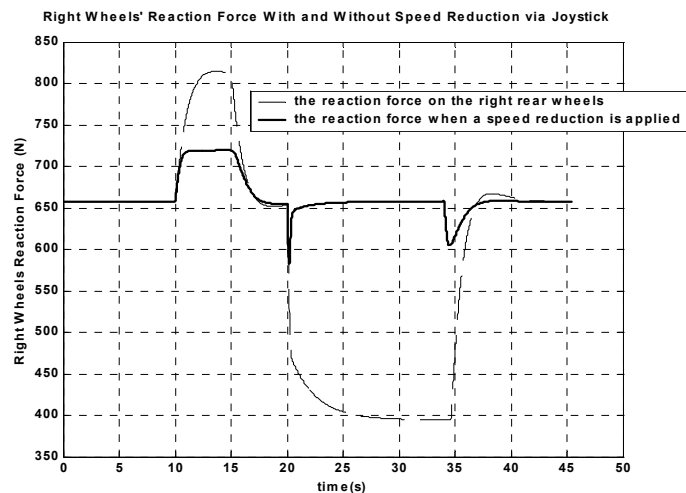


Figure 2.23. The Total Reaction Force on the Right Wheels

A sudden increase in the speed of the wheelchair may be caused by an inadequate user command. A sudden increase of the angular velocities will cause also a jump in the torques which may result in an unstable situation. As described previously, joystick module modifies the user's commands when the driver wants to have sharp turns with a high speed such that the speed is reduced as the 'voltage y' is increased. However, this reduction may also cause a sudden decrease of the angular velocities, which may not be preferred. Therefore, a shape filter is used to prevent this. This shape filter is formed by the following transfer function.

$$G(s) = \frac{a}{s+a} \quad (2.238)$$

If the value of 'a' decreases, the magnitude of the input signal at a high frequency is decreased more as shown in Figure 2.24, but the phase angle between the input and output signal is increased, which will cause a lag in the wheelchair system such that the user's commands will not be executed properly. According to the simulation results, the value of 'a' is selected to be 2.

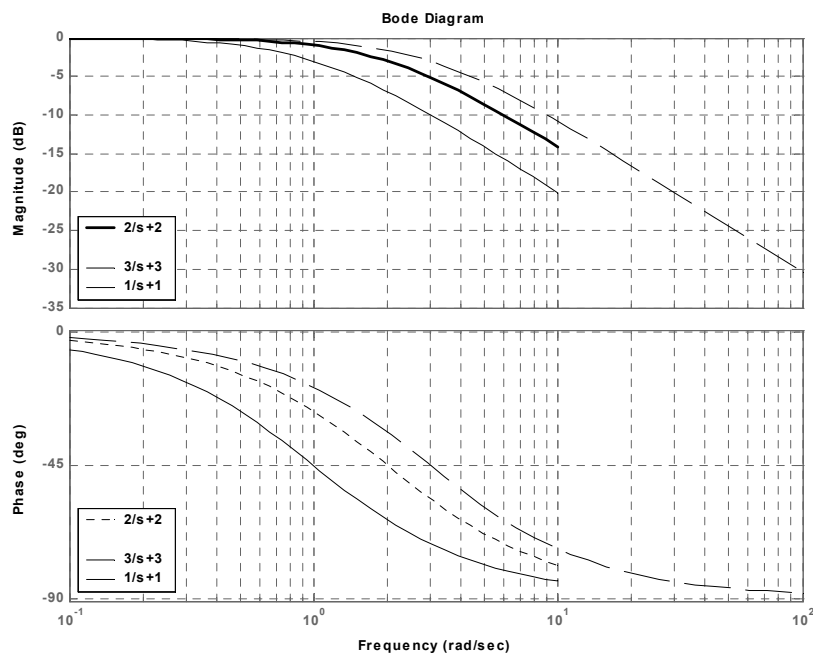


Figure 2.24. Bode Diagram for $a/(s+a)$

Let's give an example to a case where no shape filter is used. The wheelchair turns 180° to the left, keeps its direction, and then turns around itself as shown in Figure 2.25. The reference and actual yaw angles are also shown in the same figure. The user increases the voltage input in y direction of the joystick in order to have sharp turns. Therefore, the angular velocities are reduced by the joystick as can be seen in Figure 2.26.

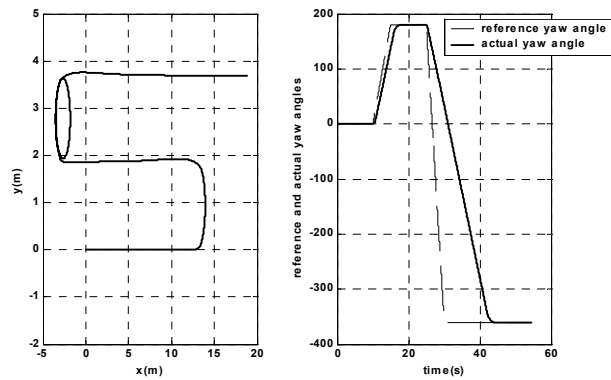


Figure 2.25. xy Position and Yaw Angle of the Wheelchair

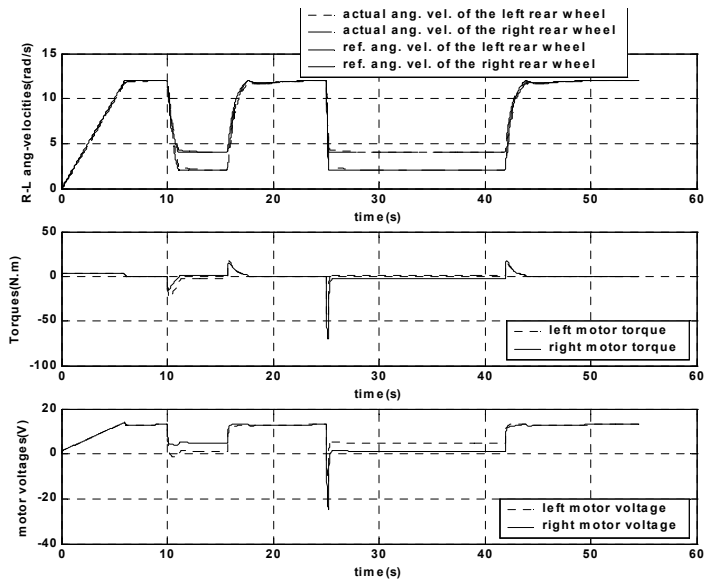


Figure 2.26. Angular Velocities, Torques and Motor Voltage

Note that the sudden reduction of the speed while the wheelchair turns about 360° causes a sudden drop in the motor torques, which results in a sudden decrease of the total reaction force on the rear wheels as can be seen in Figure 2.27. This may cause the wheelchair to topple about the front.

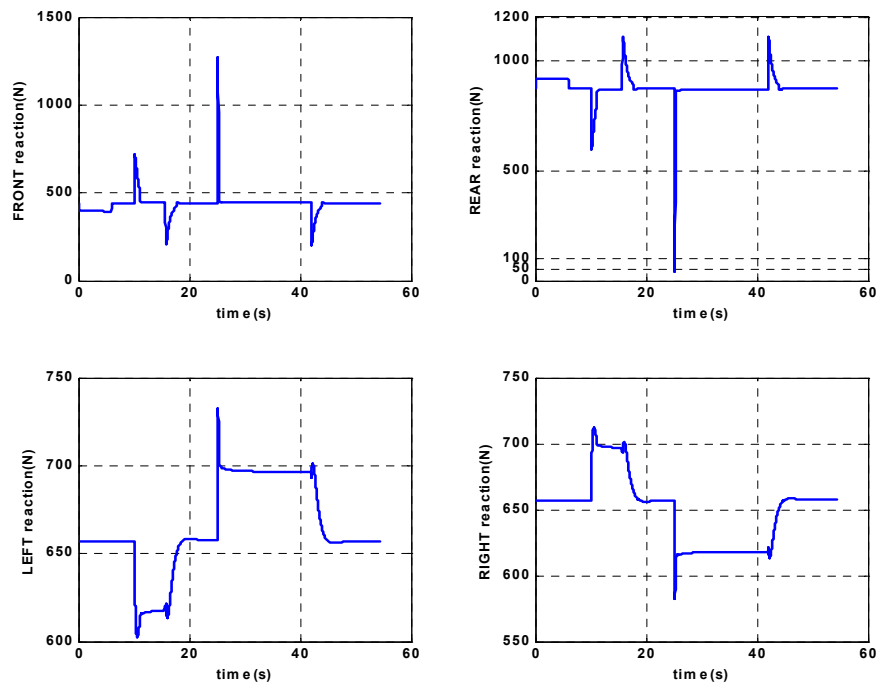


Figure 2.27. Reaction Forces

When a shape filter is used to reduce the magnitude of the angular velocities at high frequencies, the result obtained is shown in Figure 2.28 on the next page. Note that the reduction of the speed is more gradual, and does not cause a sudden critical decrease in the motor torques now. The stability of the wheelchair system is improved such that the tendency of the wheelchair to topple about the front is prevented. Note that the reaction force on the rear side of the wheelchair drops from 900 N to 50 N in the case where no filter is used. However when a shape

filter is used instead, the reaction on the rear wheels decreases to 600 N only, as shown in Figure 2.29.

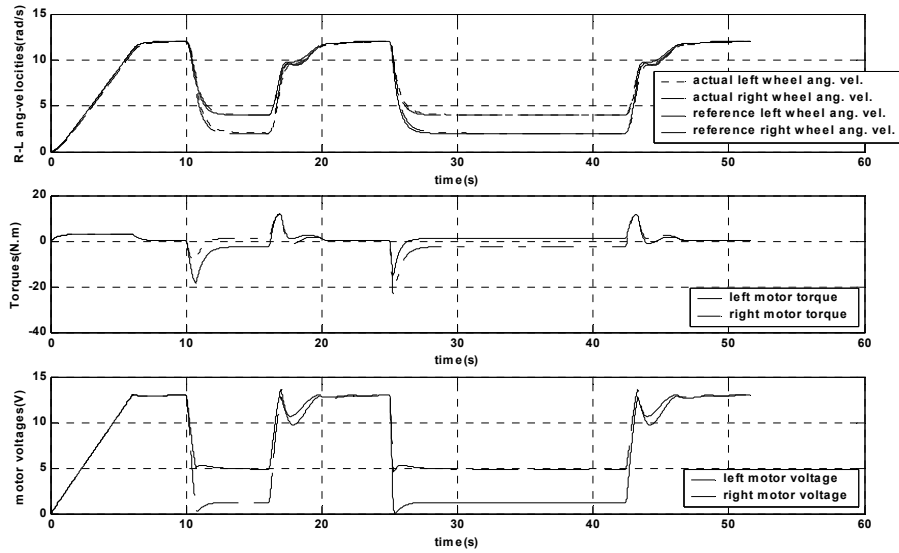


Figure 2.28. Angular Velocities, Torques and Motor Voltages When a Shape Filter is Used

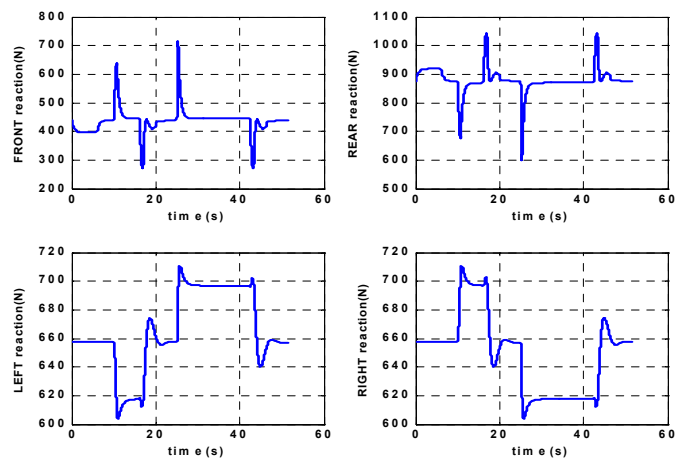


Figure 2.29. Reaction Forces When a Shape Filter is Used

When the total reaction force on one side of the wheelchair approaches zero, this means that the wheelchair will tend to fall over to the other side. In such a case, if the center of mass is shifted to that side this fall may be prevented. Therefore, as a third method of stability augmentation this technique is used.

It is assumed that the velocity and acceleration of the new center of mass G' with respect to wheelchair fixed frame $F_w \{G; \vec{u}_1^{(w)}, \vec{u}_2^{(w)}, \vec{u}_3^{(w)}\}$ are negligible. Moreover, the effect of center of mass shifting on the inertia of the wheelchair is neglected.

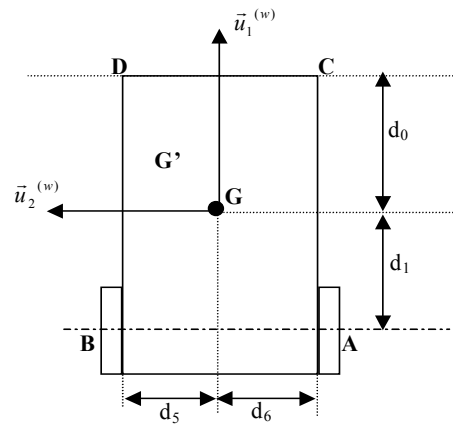


Figure 2.30. Top View of the Wheelchair

As the reaction force on the rear wheels decreases the value of 'd₀' is increased by shifting the mass center to the back, and if the reaction force on the right wheels decreases the value of 'd₆' is decreased by shifting the center of mass to the right side.

According to the geometry of the wheelchair as shown in Figure A.1 in Appendix A, the seat of the wheelchair can move maximum 10 cm to the back, 15 cm to the front and 10 cm to the sides, which means that the maximum shifts of the center of mass to the back, front, and the sides are about 7 cm, 10 cm, and 7 cm respectively.

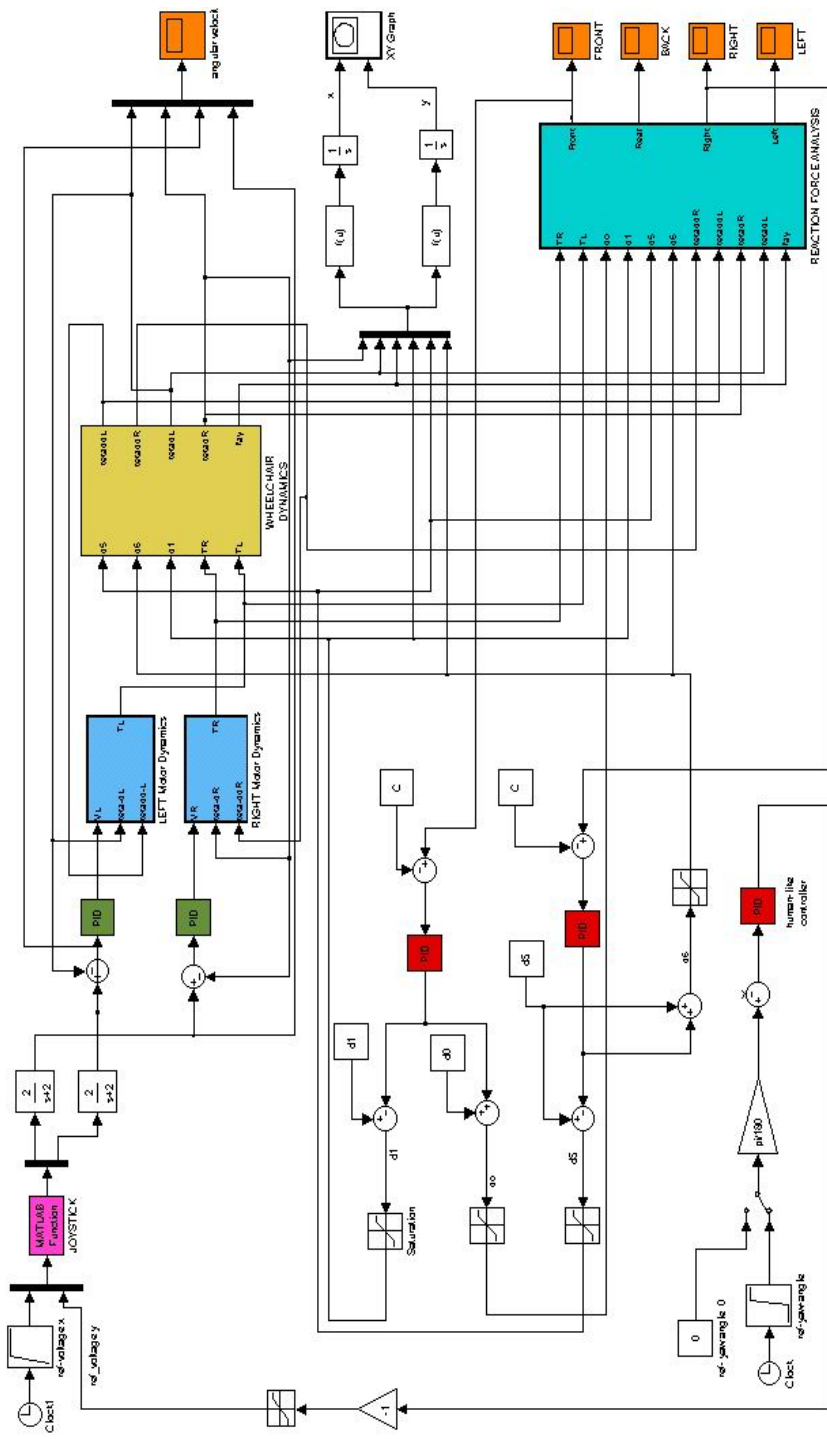


Figure 2.31. Simulink Model of the Wheelchair System on a Constant Slope Road, Including the Center of Mass Shifting

Figure 2.31 shows the Simulink Model, including the center of mass shifting for the wheelchair driven on a constant slope road. Note that the actual reaction forces on the front and left wheels are compared with the reference values that are to be measured by force transducers at the initial static state of the wheelchair system, and the outputs of the two independent PI controllers are used to get the new values for ' d_0 ', ' d_1 ', ' d_5 ', and ' d_6 '.

Figure 2.32 shows the new Simulink model including the center of mass shifting for the wheelchair driven on a changing slope road. The reaction force on the front wheels is compared with the reference value of the reaction force, and the output of the PI controller is used to get the new values for ' d_0 ', and ' d_1 '. Since the wheelchair steering effect is not considered in this simulation, the reaction force on the left and right wheels change only with changing values of slope along the path, but these changes are not critical. Therefore, center of mass is not shifted to the sides but only to the back and forth in this simulation.

To compare the results of center of mass shifting on the stability of the wheelchair, one should analyze the reaction forces. As an example, let's take the case where the wheelchair is driven on an uphill slope of 13° . The wheelchair follows a path as shown in Figure 2.33 on the next page. Note that the patient moves the joystick in x direction only for 10 seconds, then moves it to the left so that the wheelchair moves forward for 10 seconds, then turns to left with a heading angle of 90° . In other words, the voltage in y direction of the joystick is zero for 10 seconds, then gets negative values in order to turn left. The user wants to reach a heading angle of 90° in very few seconds, which indicates that the wheelchair is forced to have a steep turn by the patient.

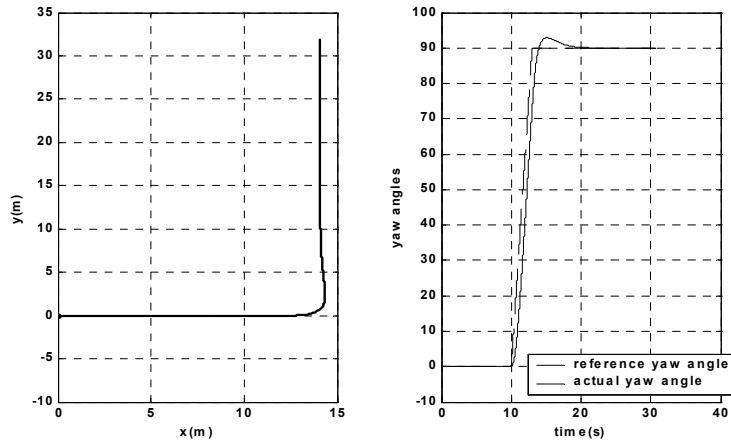


Figure 2.33. Position and Yaw Angle of the Wheelchair Steering on an Uphill Slope

The angular velocities of the right and left rear wheels are equal when the user does not move the joystick in y direction or wants to keep the direction of the wheelchair constant. The angular velocity of the right rear wheel becomes higher than the angular velocity of the left rear wheel during left turn as shown in Figure 2.34 on the next page. Right motor torque and voltage become higher with respect to left motor torque and voltage as the wheelchair starts turning left. When the wheelchair turns 90° to the left on an uphill slope it encounters with a side slope where the wheelchair will tend to turn left towards a downhill slope. In order to prevent this unintended motion of the wheelchair left motor supplies more torque than the right motor so as to keep the direction of the wheelchair constant after turn.

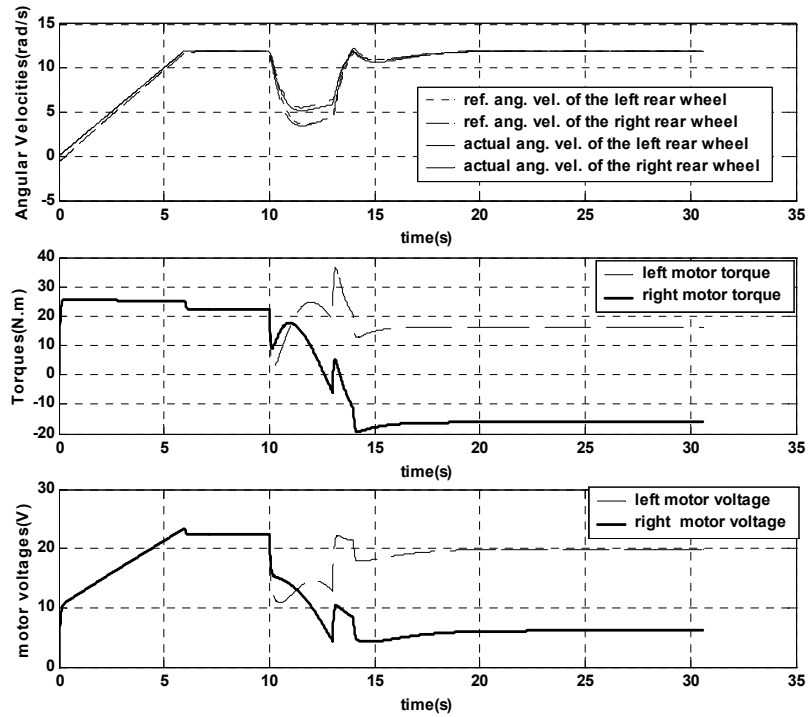


Figure 2.34. Angular Velocities of the Rear Wheels, Motor Torques and Motor Voltages for the Wheelchair Steering on an Uphill Slope

The changes in the reaction forces of the front and rear wheels are related with the changes in the motor torques. When the motor torques increase the reaction force on the rear wheels increases and the reaction force on the front wheels decreases as shown in Figure 2.35 on the next page. Note that as the wheelchair turns left on an uphill slope it encounters with a side slope, which results in the increase of the reaction force on the left wheels and decrease of the reaction force on the right wheels. The value of the reaction force on the right wheels does not get the value of zero so that the wheelchair does not topple to the left. However, this reaction force decreases from 650 N to 250 N.

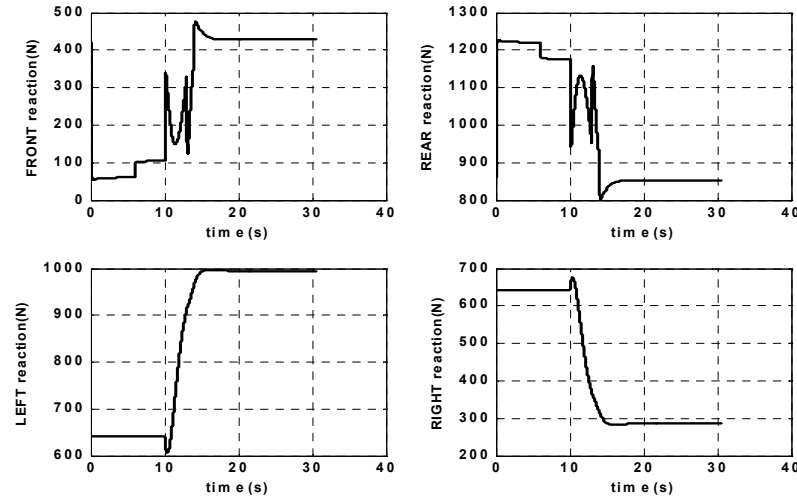


Figure 2.35. Reaction Forces for the Wheelchair Steering on an Uphill Slope

As the reaction force on the right wheels decreases, the center of mass is shifted to the right such that the distance of the center of mass of the wheelchair system to the right wheels decreases from 0.275 m to 0.205 m as shown in Figure 2.36, which causes a relative acceleration about 0.077 m/s^2 to the right with respect to the wheelchair base. However, the patient feels an absolute acceleration of about 0.723 m/s^2 to the left. This much acceleration is mainly caused by the steep steering action of the wheelchair on an uphill slope, since shifting of the center of mass to the right causes a relative acceleration of the wheelchair seat about 0.077 m/s^2 to the right with respect to the wheelchair base, which in fact does not contribute to the absolute acceleration felt by the user but even causes a little decrease in the value of the acceleration caused by the steering action. As the center of mass of the wheelchair system is shifted to the right, the reaction force on the right wheels decreases from 650 N to 450 N instead of 250 N, as shown in Figure 2.37, which can be considered as stability augmentation. The reaction force on the right wheels is increased compared to the right wheels' reaction force obtained in case where the center of mass is not shifted.

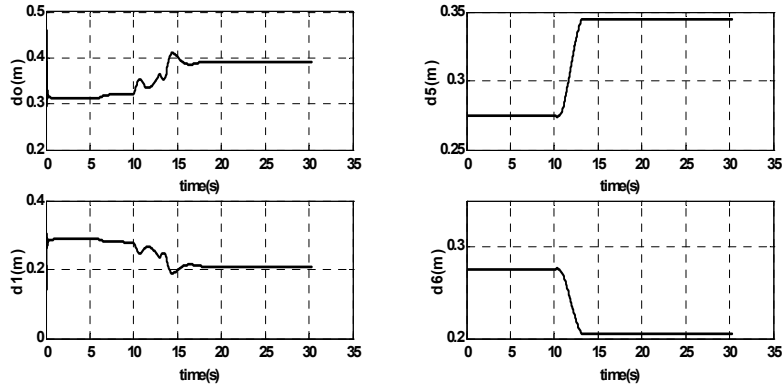


Figure 2.36. Position of the Shifted Center of Mass

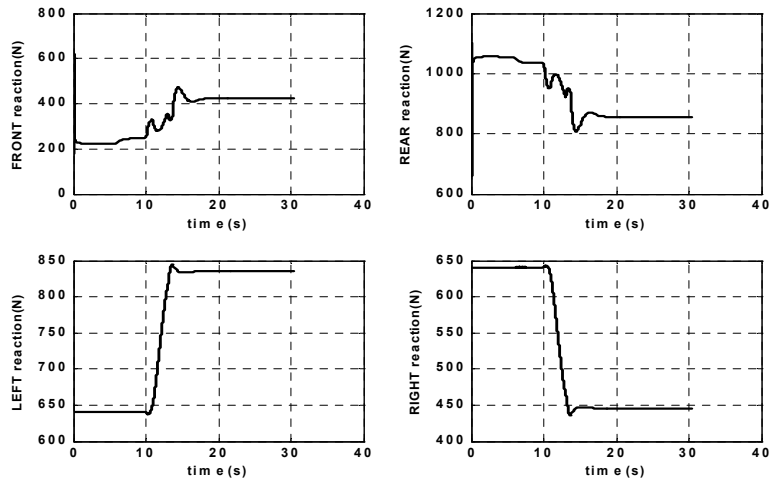


Figure 2.37. Reaction Forces After the Center of Mass is Shifted

If a movable plate is placed on the base of the wheelchair, and the seat is placed on this plate, the center of mass of the wheelchair system can be shifted by shifting the plate in back and forth direction and shifting the seat to the sides above the plate.

Detailed discussion for the reduction of several unstable cases by the method of center of mass shifting is performed in Section 3.3 of Chapter 3.

CHAPTER 3

CASE STUDIES

3.1. System Analysis for Reliable Situations

In this section, several case studies are performed for the wheelchair system traveling on different constant sloped, and changing sloped roads. In all the cases considered here, the wheelchair system remains stable.

3.1.1. Reliable Cases for Roads With Constant Slopes

3.1.1.1. Case 1: Wheelchair Traveling on a Level Road

When the patient wants to move forward without any steering action on a level ground, he moves the joystick in x direction only, which results in a positive ‘Voltage x’ and zero ‘Voltage y’. This means that the reference yaw angle is determined to be zero by the user as shown in Plot (1) of Figure 3.1.

The reference angular velocities of the right and left rear wheels are always equal during this motion since the wheelchair does not turn. The speed of the wheelchair increases for 15 seconds and then remains constant. The increase of the speed results in increase of the motor torques and motor voltages as shown in Plot (2) of Figure 3.1.

As the motor torques increase the reaction force on the rear wheels also increases whereas the total reaction force on the front wheels decreases as expected. Since the wheelchair does not have a steering action, the total reaction forces on the right and left rear wheels remain constant during motion as shown in Plot (3) of Figure 3.1.

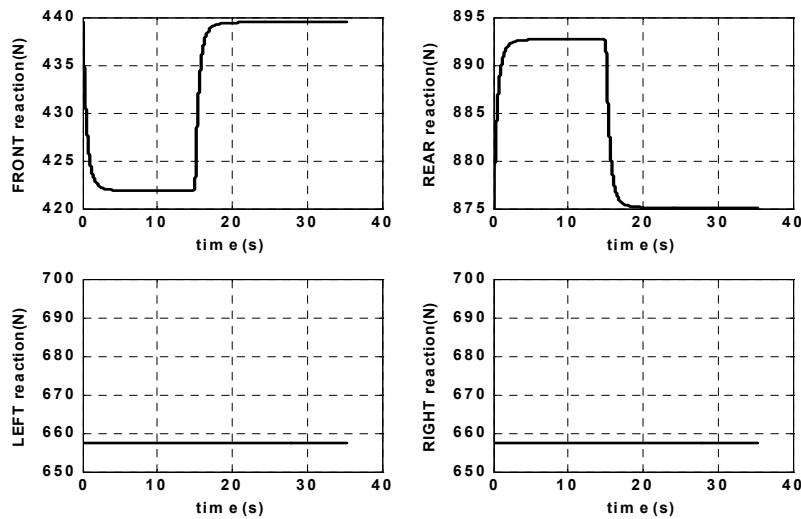
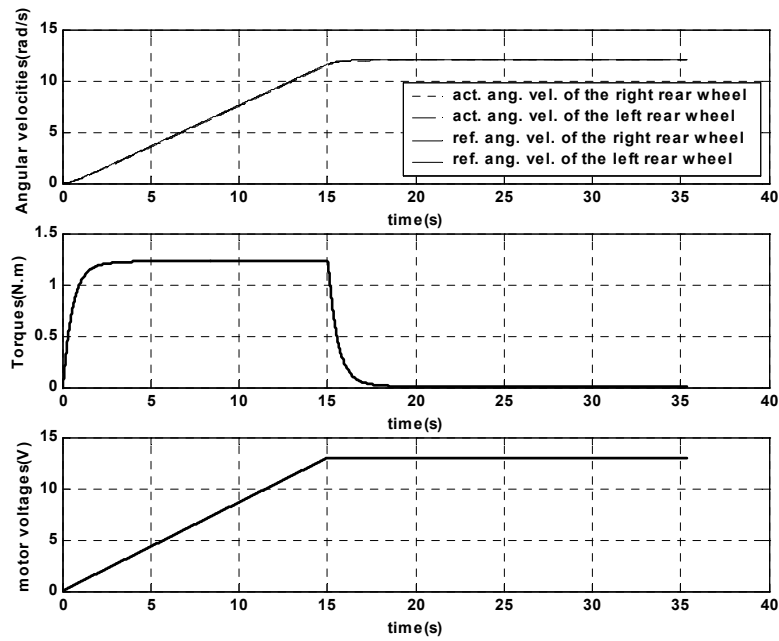
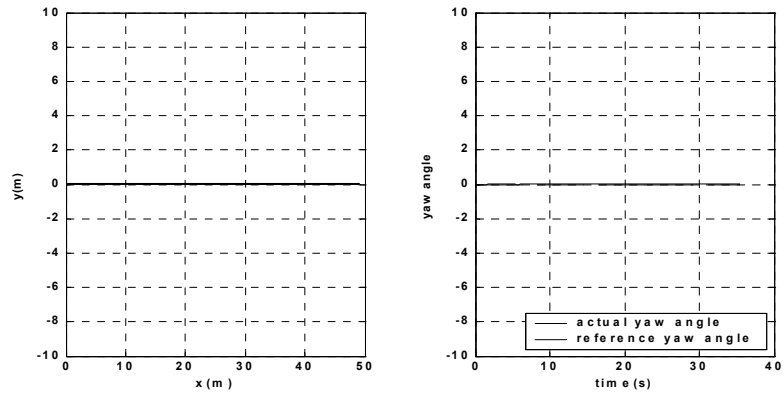


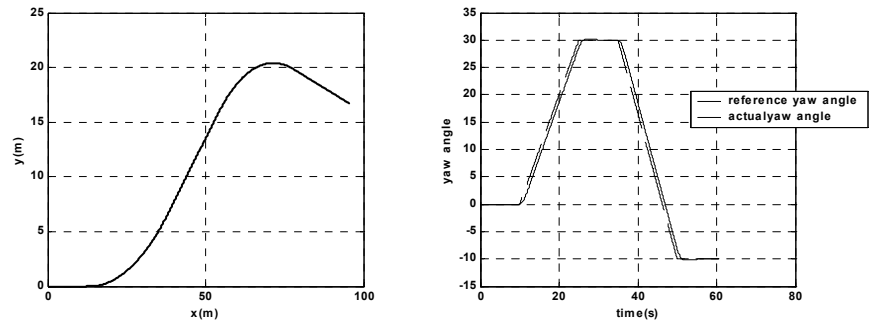
Figure 3.1. Response of the Wheelchair System for Case 1

3.1.1.2. Case 2: Wheelchair Steering on a Level Road

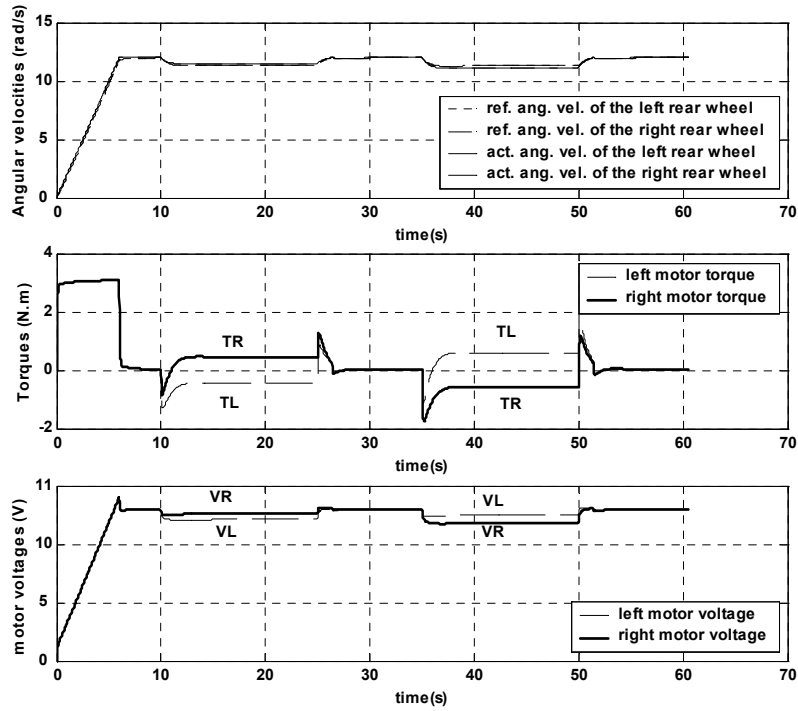
The wheelchair travels along a level ground as in Case 1, but it has a steering action now. It moves forward for 10 seconds, then turns to left with a heading angle of 30° , keeps its direction for 10 seconds, and finally turns to right with a heading angle of -10° as shown in Plot (1) of Figure 3.2. Note that the wheelchair does not have steep turns and the actual yaw angle follows the reference yaw angle.

In order to make the wheelchair turn left the user moves the joystick to the left so that a negative voltage is produced in y direction of the joystick. Therefore, the angular velocities of the right and left rear wheels are reduced as shown in Plot (2) of Figure 3.2. But the reduction in the speed of the wheelchair is not much since both of the turns are not steep. If the voltage in y direction of the joystick were increased more, this reduction would be higher. When the wheelchair turns left the angular velocity of the right rear wheel becomes higher than the angular velocity of the left rear wheel as expected. Therefore, right motor torque is higher than the left motor torque during left turn. As the wheelchair keeps its direction after the left turn, the angular velocities, motor torques and motor voltages become equal. Finally, when the wheelchair turns right the angular velocity of the left rear wheel, left motor torque and left motor voltage are increased with respect to the right rear wheel's angular velocity, right motor torque and voltage. Again, motor torques, angular velocities and motor voltages become equal since the wheelchair direction remains constant after the right turn.

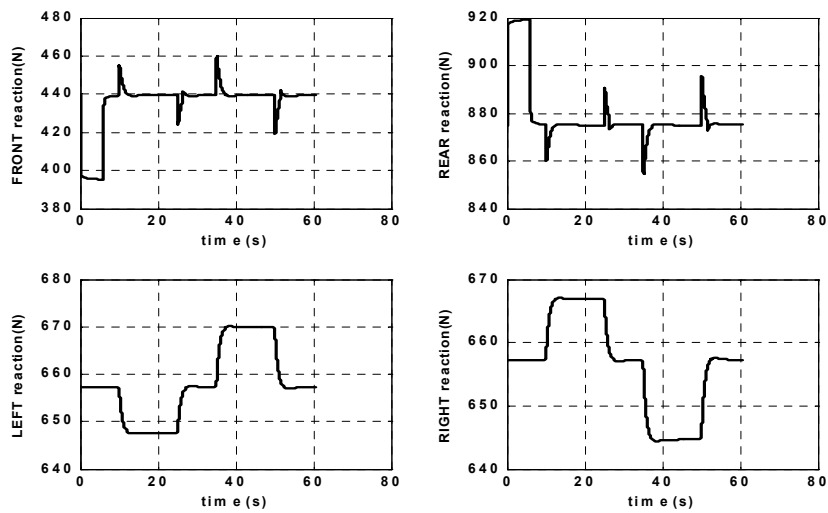
As the motor torques are increased the reaction force on the rear wheels increases, and the reaction force on the front casters decreases. When the wheelchair turns left, the reaction force on the outer wheels increases which means that the total reaction force on the right rear wheels increases, and the reaction force on the left rear wheels decreases as can be seen in Plot (3) of Figure 3.2. The reaction force on the left rear wheels increases whereas the reaction force on the right rear wheels decreases, as the wheelchair turns right.



(1)



(2)



(3)

Figure 3.2. Response of the Wheelchair System for Case 2

3.1.1.3. Case 3: Wheelchair Braking on a Downhill Slope

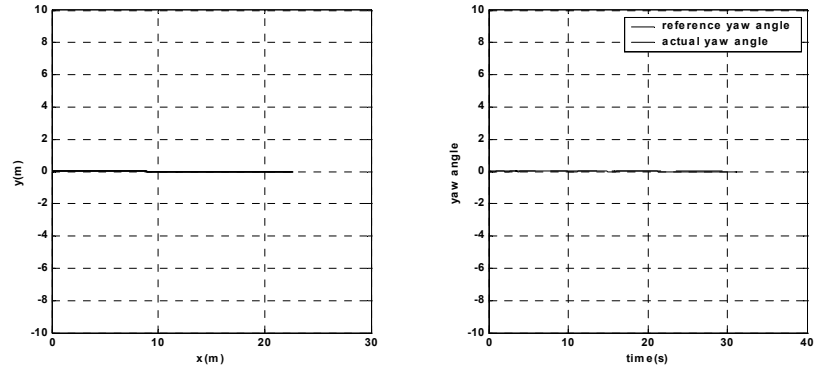
The wheelchair moves forward without any steering on a road with a constant downhill slope of 5° . The reference yaw angle remains at a constant value of zero since the wheelchair does not turn, as shown in Plot (1) of Figure 3.3.

The speed of the wheelchair increases for 10 seconds, and then remains constant for 5 seconds, and finally, the user wants to stop by reducing the value of speed to zero as shown in Plot (2) of Figure 3.3. The angular velocities of the right and left wheels are equal during motion since the heading angle of the wheelchair remains always zero. When the speed of the wheelchair is increased, right and left motor torques decrease and get negative values to maintain the desired speed of the wheelchair on a downhill slope. The negative values of torques decrease more when the user wants to brake. Control of the angular velocities of both rear wheels prevents an excessive increase in the wheelchair speed due to the downhill slope effects.

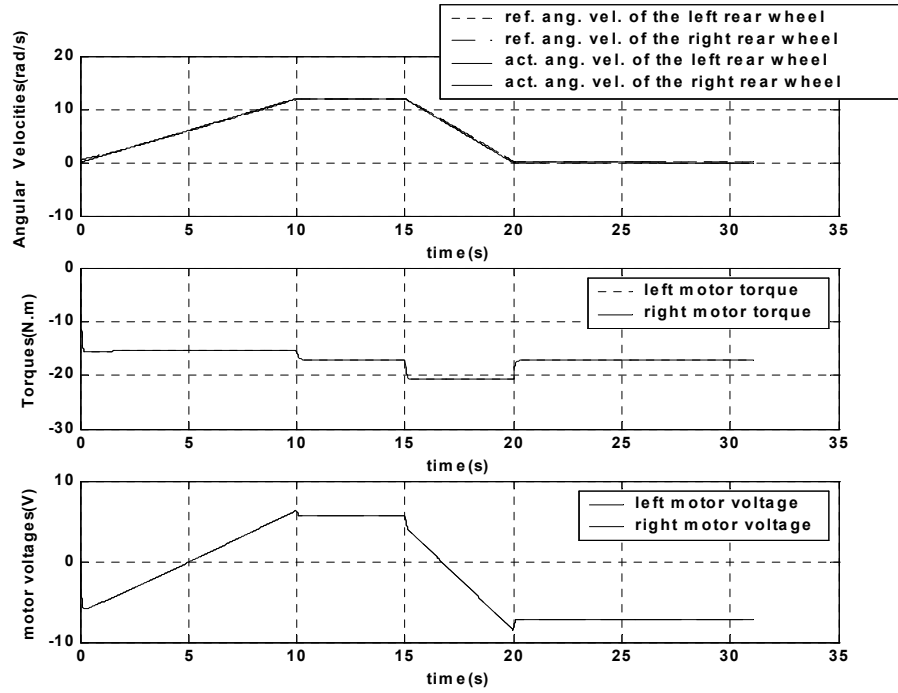
The reaction force on the front casters increases in few seconds initially due to a downhill slope, whereas the reaction force on the rear wheels decreases. As the right and left motor torques decrease the reaction force on the rear wheels also decrease as shown in Plot (3) of Figure 3.3. The reaction force on the front casters increases while motor torques decrease. The reaction forces on the left and right rear wheels remain always constant since there is no steering action of the wheelchair.

Note that the values of the reaction force on the left and right wheels are lower than the ones obtained in Case 1. Since the road has a downhill slope, the total weight of the wheelchair in $\bar{u}_3^{(w)}$ direction (perpendicular to the slope) is decreased due to the effect of the slope as shown in Equation 3.1 where α is the downhill slope of the road, m is the total mass of the wheelchair system and W is the total weight.

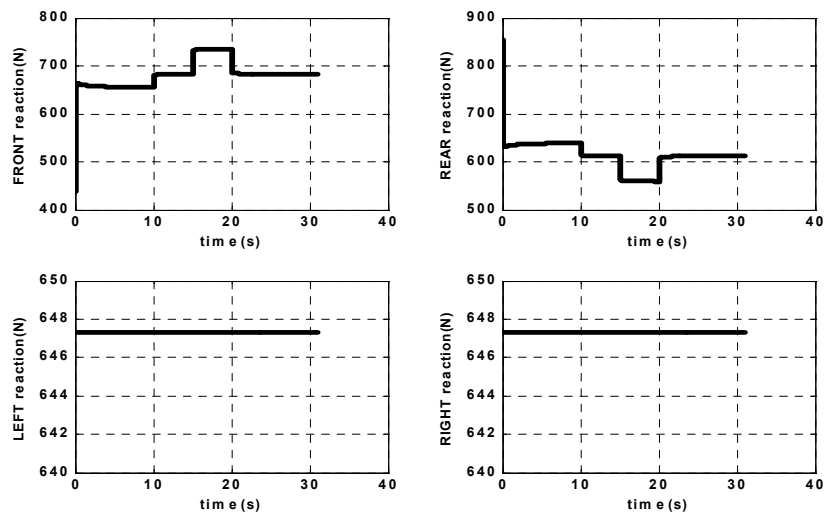
$$W = mg\cos(\alpha) \tag{3.1}$$



(1)



(2)



(3)

Figure 3.3. Response of the Wheelchair System for Case 3

3.1.1.4. Case 4: Wheelchair Braking on an Uphill Slope

The wheelchair moves forward without any steering on a road with a constant uphill slope of 5° . The reference yaw angle remains at a constant value of zero since the wheelchair does not turn, as shown in Plot (1) of Figure 3.4.

The speed of the wheelchair increases for 10 seconds, and then remains constant for 5 seconds, and finally the user brakes as shown in Plot (2) of Figure 3.4. The angular velocities of the right and left wheels are equal during motion since the heading angle of the wheelchair remains always zero. When the speed of the wheelchair is increased right and left motor torques also increase and get positive values to maintain the desired speed of the wheelchair on an uphill slope. Motor voltages increase as the user increases the speed of the wheelchair by means of movements of the joystick in x direction.

The reaction force on the front casters decreases in few seconds initially due to the effect of an uphill slope whereas the reaction force on the rear wheels increases. As the motor torques increase the reaction force on the rear wheels also increases as shown in Plot (3) of Figure 3.4. The front reaction increases while motor torques decrease. The reaction forces on the left and right rear wheels remain always constant and equal to each other since there is no steering action of the wheelchair.

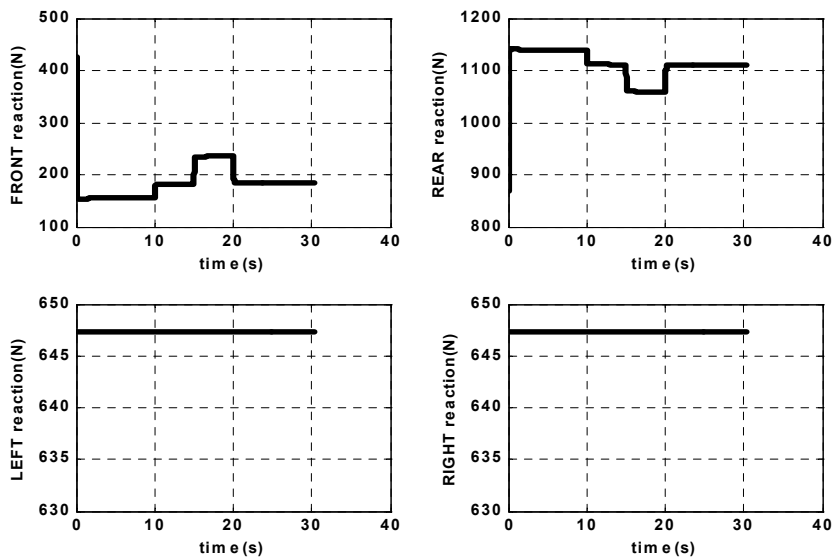
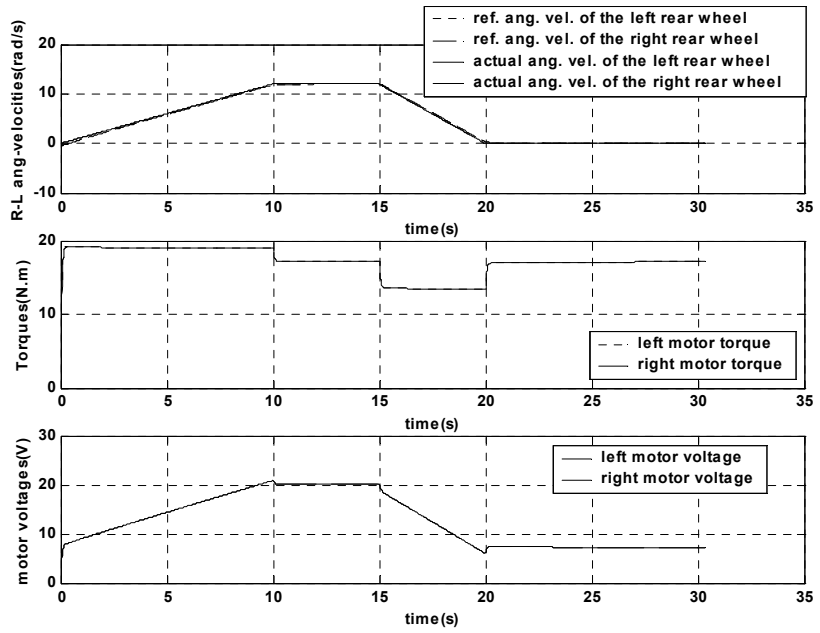
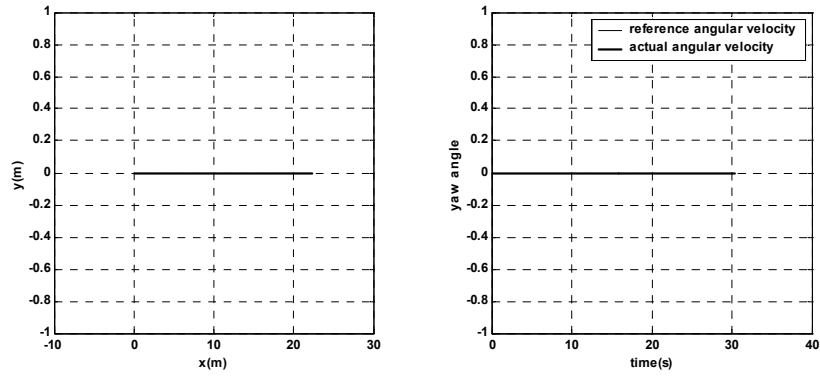


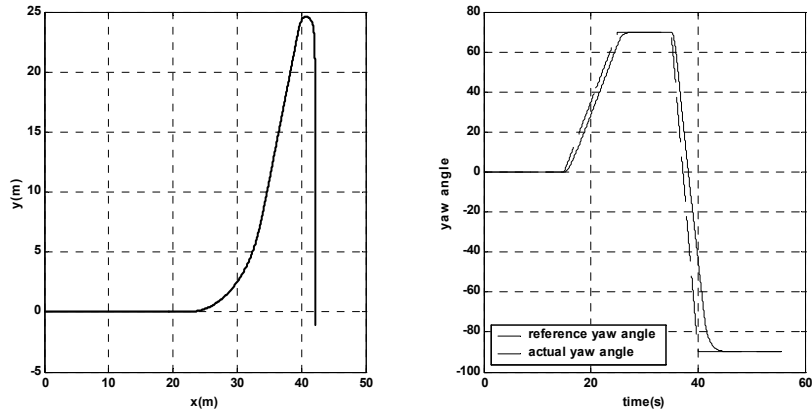
Figure 3.4. Response of the Wheelchair System for Case 4

3.1.1.5. Case 5: Wheelchair Steering on a Downhill Slope

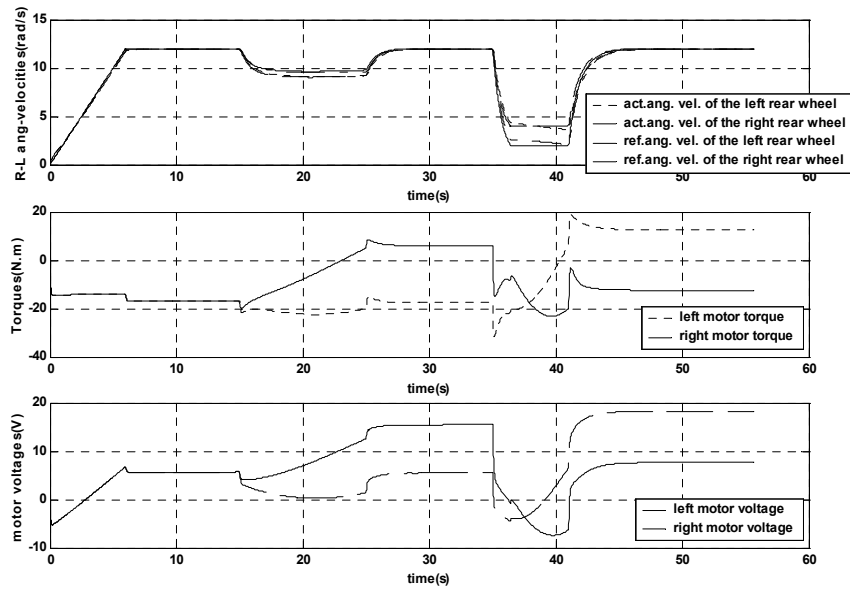
Wheelchair moves forward for 15 seconds, then turns to left with a heading angle of 70° , keeps its direction for 10 seconds, and finally turns 90° to the right. For such a movement of the wheelchair the reference yaw angle determined by the patient can be seen in Plot (1) of Figure 3.5.

When the wheelchair turns to left, the angular velocity of the right rear wheel becomes higher than the angular velocity of the left rear wheel as expected as shown in Plot (2) of Figure 3.5. Note that the speed is reduced more when the wheelchair turns to right since this turn is steeper than the left turn. Because, the wheelchair heading angle changes from 0° to 70° in 10 seconds whereas it changes from 70° to -90° in about 5 seconds. As the voltage in y direction of the joystick is increased more the speed of the wheelchair is reduced more. Note that as the user increases the value of voltage in y direction of the joystick, the difference between the angular velocities of the right and left rear wheels increases for a steep turn. After the wheelchair turns 90° to the right it keeps the heading angle constant so that it moves forward in that direction. Since the wheelchair always tends to move along the downhill slope left motor torque remains higher than the right motor torque to keep this direction. During left turn right motor torque and voltage become higher with respect to left motor torque and voltage as expected.

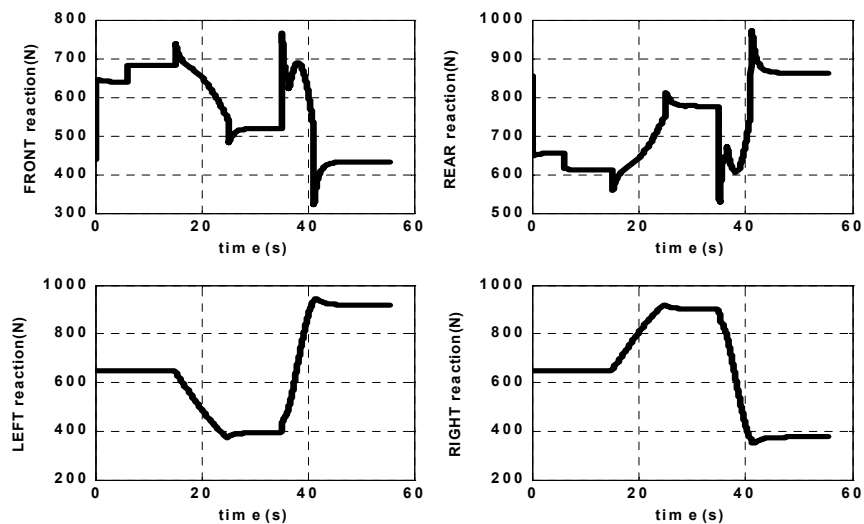
When the wheelchair turns left the reaction force on the left wheels decreases and the reaction force on the outer right wheels increases as expected, as shown in Plot (3) of Figure 3.5. The total reaction force on the right wheels decreases during right turn. The reaction force on the front wheels decreases with increasing motor torques.



(1)



(2)



(3)

Figure 3.5. Response of the Wheelchair System for Case 5

3.1.1.6. Case 6: Wheelchair Steering on a Side Slope

When the wheelchair is driven on a road with a positive side slope it has a tendency to turn right towards the downhill slope. In this case, the wheelchair is driven on a constant side slope of 5° . The patient wants to move forward for 15 seconds and then turn to left with a heading angle of 30° . The wheelchair follows the path as shown in Plot (1) of Figure 3.6 as a response to the command of the user. Note that the wheelchair tends to turn right at the beginning due to the effect of a side slope although the user wants to move forward. When the user notices this error he moves the joystick to the left to move in forward direction.

The speed of the wheelchair is increased in 6 seconds and then remained constant for a forward movement. When the wheelchair turns left the angular velocity of the right rear wheel becomes higher relative to the angular velocity of the left rear wheel. When the wheelchair user wants to keep its direction after the turn the angular velocities of the right and left rear wheels become equal again as shown in Plot (2) of Figure 3.6. Since the wheelchair has a tendency to turn right on a positive side slope, right motor supplies a higher torque than the left motor does during motion in order to prevent this unintended motion. Note that right motor voltage is always higher than left motor voltage similarly.

The reaction force on the rear wheels increases as shown in Plot (3) of Figure 3.6 whereas the reaction force on the front wheels decreases when the wheelchair turns left, since the wheelchair encounters an uphill slope during this turn. The reaction force on the left wheels decreases during left turn, and it increases when the turn is ended, and then remains constant while the wheelchair keeps its direction after this turn. Note that the total reaction force on the right rear wheels is higher than the total reaction force on the left rear wheels always during the motion due to the effect of a positive side slope.

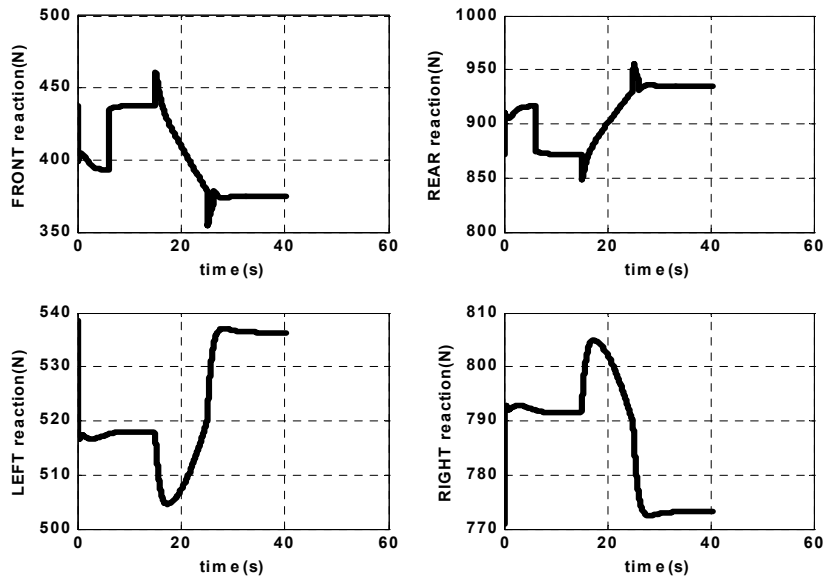
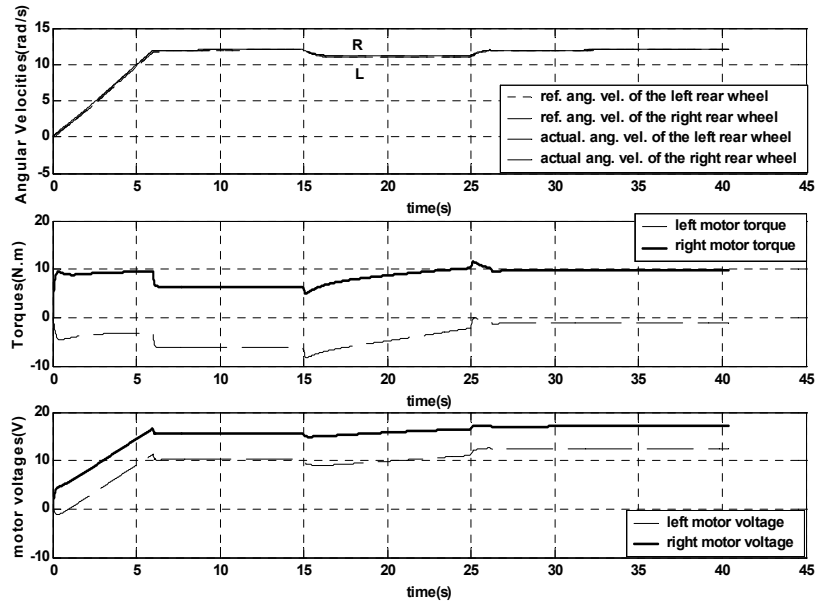
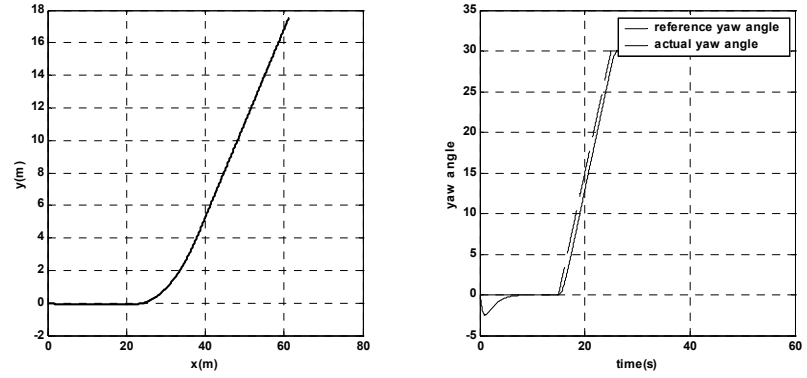


Figure 3.6. Response of the Wheelchair System for Case 6

3.1.1.7. Case 7: Wheelchair Steering on an Uphill Slope

The wheelchair is driven on a road with a constant uphill slope of 10° . The patient wants to move forward for 15 seconds, then turn to left with a heading angle of 10° , and keep its direction for 10 seconds, and finally turn to right with a heading angle of -60° . The wheelchair follows the path as shown in Plot (1) of Figure 3.7 as a response to such a command of the user.

When the wheelchair turns left the angular velocity of the right rear wheel becomes higher with respect to the angular velocity of the left rear wheel as shown in Plot (2) of Figure 3.7. The right motor torque becomes slightly higher than the left motor torque as the wheelchair turns left, but when the wheelchair keeps its direction after left turn left motor torque increases with respect to right motor torque in order to prevent the wheelchair moving towards the downhill slope. During right turn, the angular velocity of the left rear wheel is higher than the angular velocity of the right rear wheel, which results in a higher left motor torque. However, as the wheelchair moves forward after right turn, right motor torque becomes higher than the left motor torque to prevent the wheelchair moving towards the downhill slope. Note that when the wheelchair turns right the speed is reduced more with respect to the left turn since the right turn is steeper.

Due to the effect of an uphill slope, the reaction force on the front casters decrease in few seconds at the beginning of the motion as shown in Plot (3) of Figure 3.7. The changes in the front and rear reactions are related with the changes in the motor torques. As the wheelchair turns left the reaction force on the left wheels increases slightly due to the effect of increasing left motor torque whereas this reaction decreases during right turn due to the effect of decreasing left motor torque. At the beginning of the right turn the reaction force on left wheels increases slightly, but then decreases due to effect of a side slope encountered during right turn.

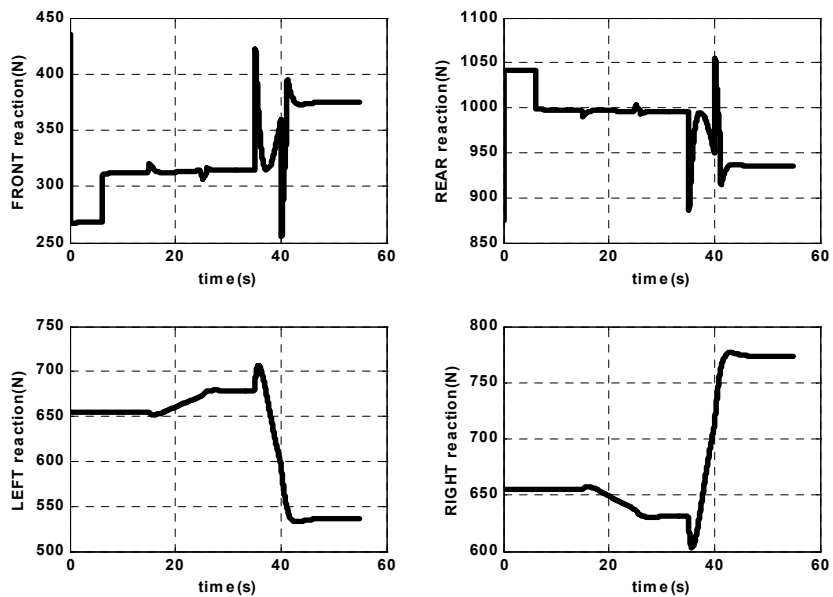
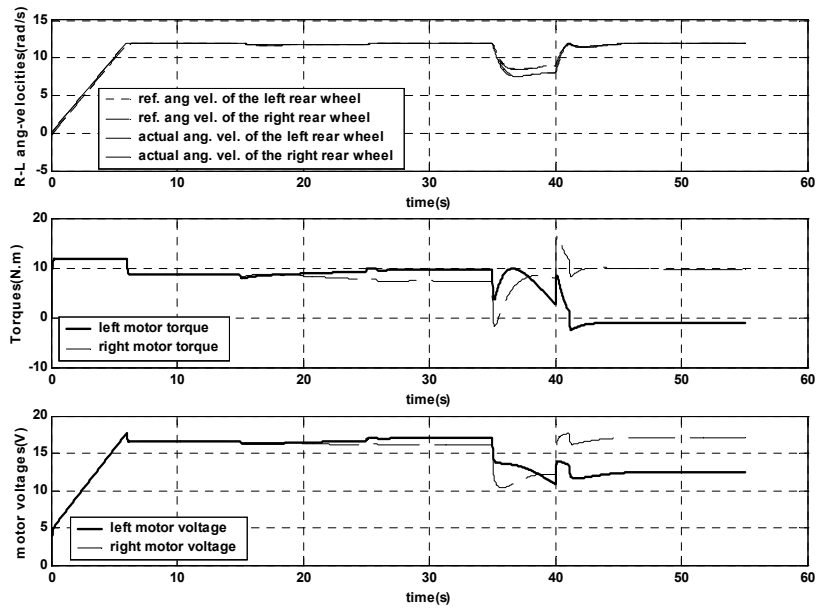
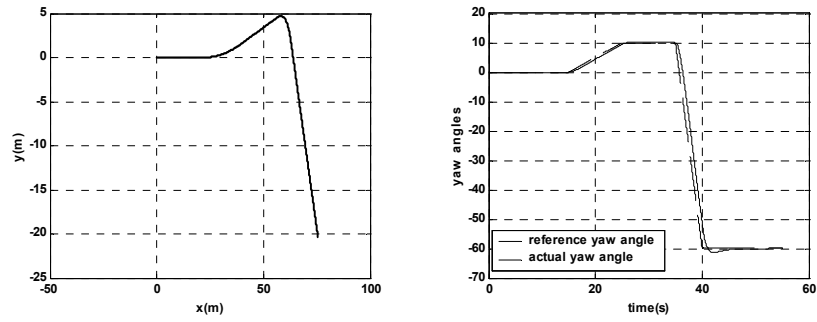


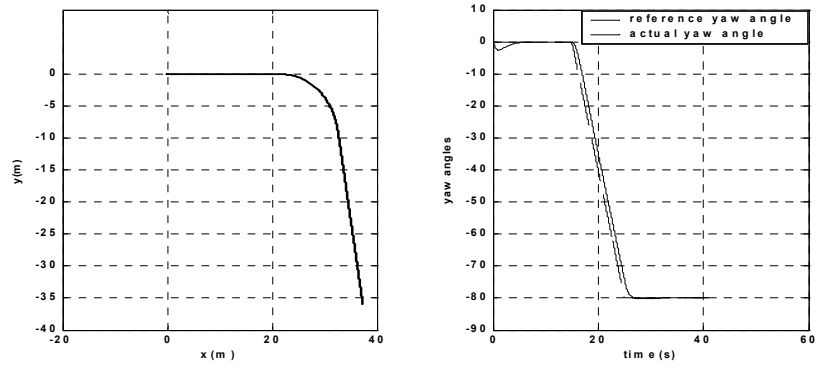
Figure 3.7. Response of the Wheelchair System for Case 7

3.1.1.8. Case 8: Wheelchair Steering on a Road With Both Uphill and Side Slopes

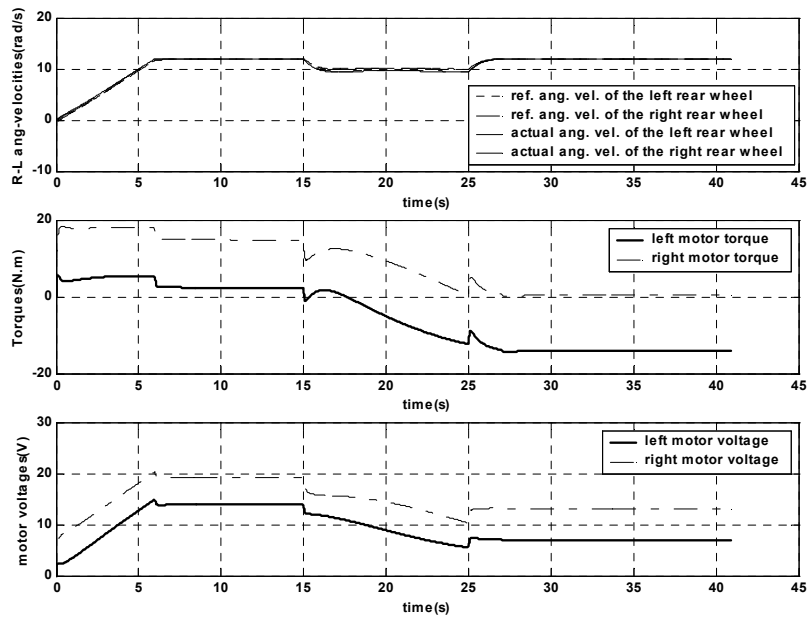
The wheelchair travels on a road with a constant side slope of 5° and upslope of 10° together. The user wants to drive the wheelchair forward for 15 seconds, turn to left with a heading angle of -80° , and then move forward in this direction. For such a user's command the path of the wheelchair can be seen in Plot (1) of Figure 3.8. Note that the wheelchair wants to turn right at the beginning due to the effect of a positive side slope. In order to prevent this, the wheelchair user moves the joystick to the left in order to make the wheelchair follow a straight path.

When the wheelchair turns right the angular velocity of the left rear wheel becomes slightly higher than the angular velocity of the right rear wheel. The difference between the angular velocities is not much since the wheelchair already has a tendency to turn right. The values of the right motor torque and voltage are always higher than the values of the left motor torque and voltage in order to prevent the wheelchair turning more to the right towards the downhill slope which is an unintended motion of the wheelchair in case of traveling on a road with a positive side slope.

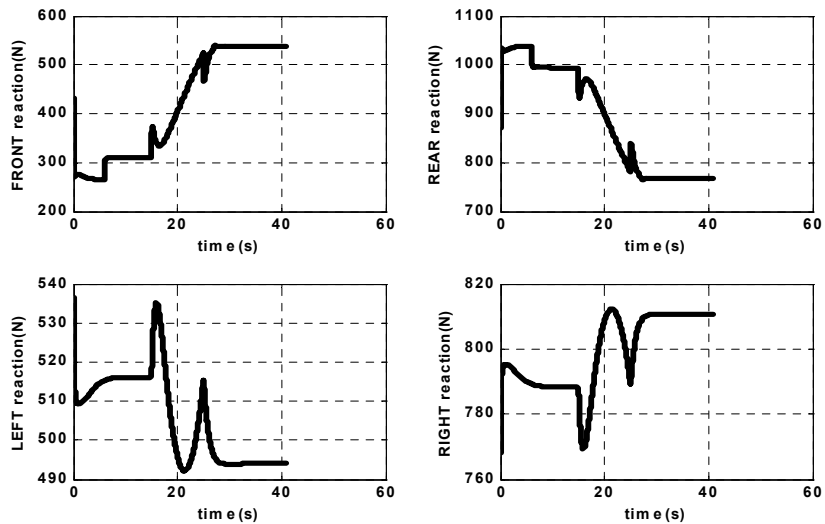
The total reaction force on the rear wheels increases in few seconds at the beginning of the motion due to the effect of an uphill slope, and the total reaction on the right wheels increases at the same time due to the effect of a positive side slope as shown in Plot (3) of Figure 3.8. When the wheelchair starts turning right the reaction force on the right wheels decreases and the reaction force on the left wheels increases initially since the left wheels are the outer wheels during turn. However, as the wheelchair turns right on an uphill slope the reaction force on the right wheels increases since the wheelchair encounters with a side slope during this turn.



(1)



(2)



(3)

Figure 3.8. Response of the Wheelchair System for Case 8

3.1.2. Reliable Cases for Roads With Changing Slopes

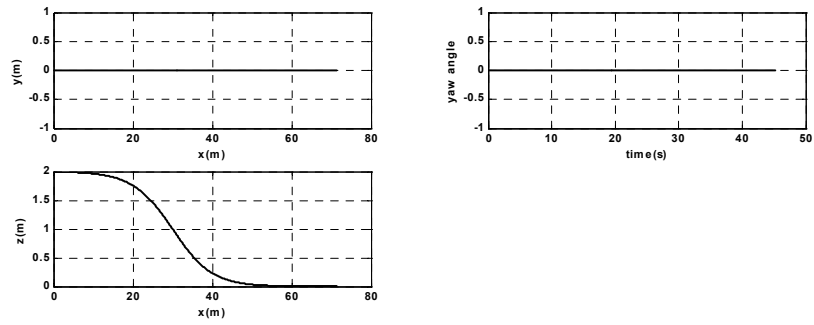
In this section, wheelchair motion is analyzed in different roads with different changing slopes by several cases, where in all cases the system is stable. Remember that the wheelchair does not have a steering action while it travels on such roads. The effects of sudden slope changes rather than steering effects on the system stability are investigated for the wheelchair traveling on changing sloping roads.

3.1.2.1. Case 9: Wheelchair on a Road With a Changing Downhill Slope

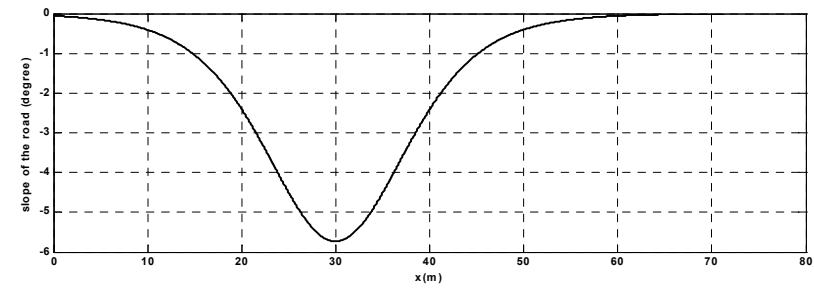
The patient wants to have a straight path in xy plane as shown in Plot (1) of Figure 3.9. The wheelchair moves forward on a road where the downhill slope of the road is changing in a continuous manner. The road profile and the slope changes of the road can be seen in Plot (1) and Plot (2) of Figure 3.9, respectively.

Note that the angular velocities of the right and left rear wheels are equal during motion since the wheelchair does not turn. The speed of the wheelchair is increased by means of joystick movements in x direction for 10 seconds and then remained constant as shown in Plot (3) of Figure 3.9. When the wheelchair encounters with a downhill slope the values of motor torques decrease and get negative values in order to maintain the desired speed of the wheelchair on a downhill slope as the PI controllers for the angular velocities prevent an excessive increase in the wheelchair speed.

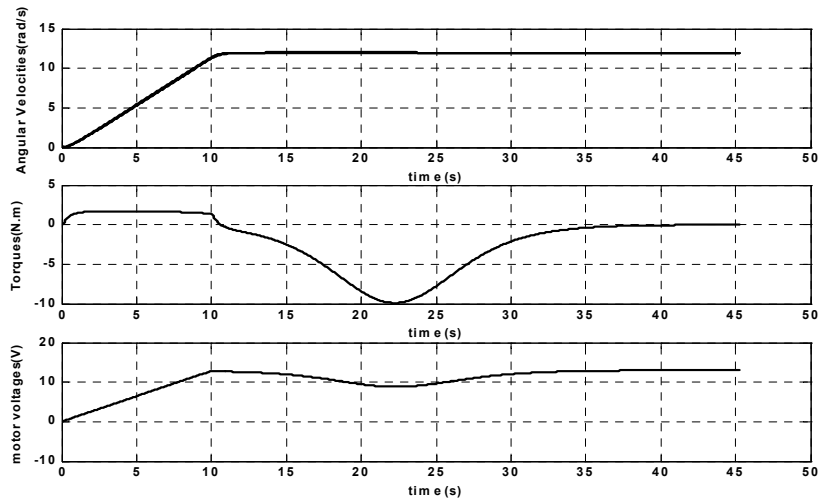
The reaction force on the front wheels increase and the reaction force on the rear wheels decrease as the downhill slope of the road increases, as shown in Plot (4) of Figure 3.9. Normally one expects no change in the right and left wheels' reaction forces since there is no steering action, but the changes in these forces are related with the slope changes along the path.



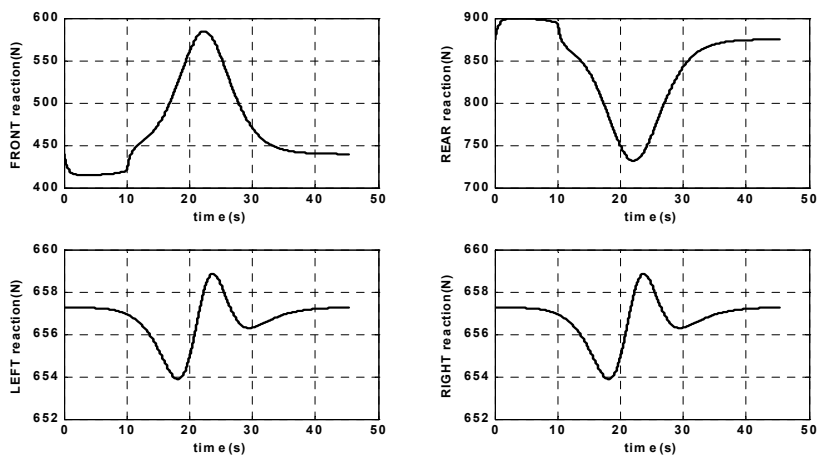
(1)



(2)



(3)



(4)

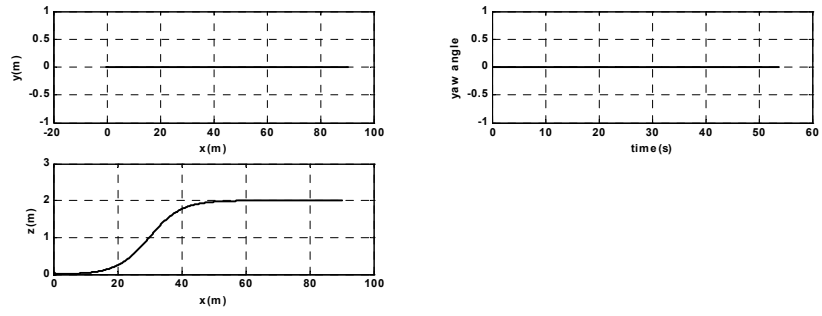
Figure 3.9. Response of the Wheelchair System for Case 9

3.1.2.2. Case 10: Wheelchair on a Road With a Changing Uphill Slope

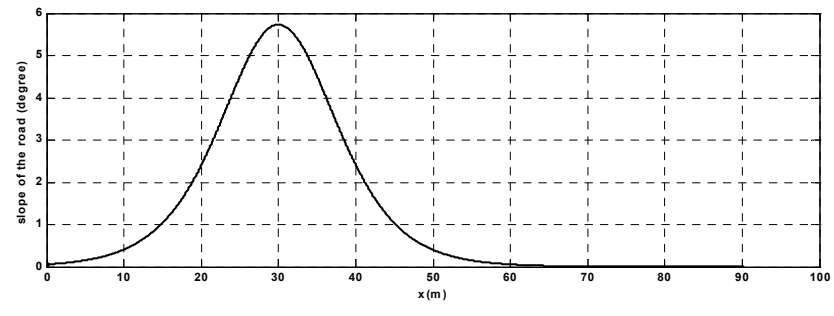
The wheelchair follows a straight path on a road with a changing uphill slope as can be seen in Plot (1) of Figure 3.10. The slope of the road starts with 0° and gradually increases to a value of about 6° as shown in Plot (2) of Figure 3.10. The patient applies no voltage in y direction of the joystick not to have a steering action, which means that he moves the joystick in x direction only but not to the left or right.

The angular velocities of the right and left rear wheels are equal during motion as shown in Plot (3) of Figure 3.10. The motor torques increase with increasing uphill slope of the road in order to maintain the desired speed of the wheelchair. Motor voltages also increase as the wheelchair speed and the slope of the road are increased.

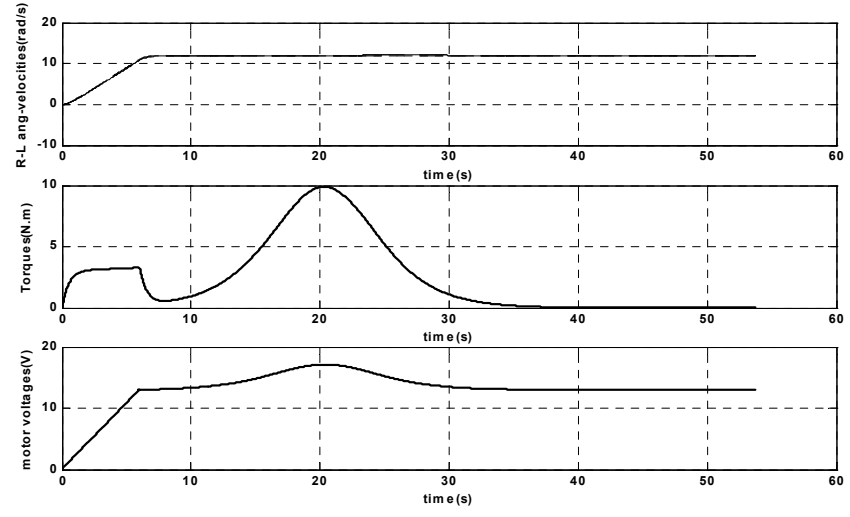
The reaction force on the front wheels decreases with increasing uphill slope of the road, and the reaction force on the rear wheels decreases as the uphill slope of the road decreases, which can be seen in Plot (4) of Figure 3.10. The changes in the left and right reaction forces are related with the changes in the slope of the road as in the previous case. The values of the reaction forces on the right and left rear wheels are always equal during motion since the wheelchair does not have a steering action.



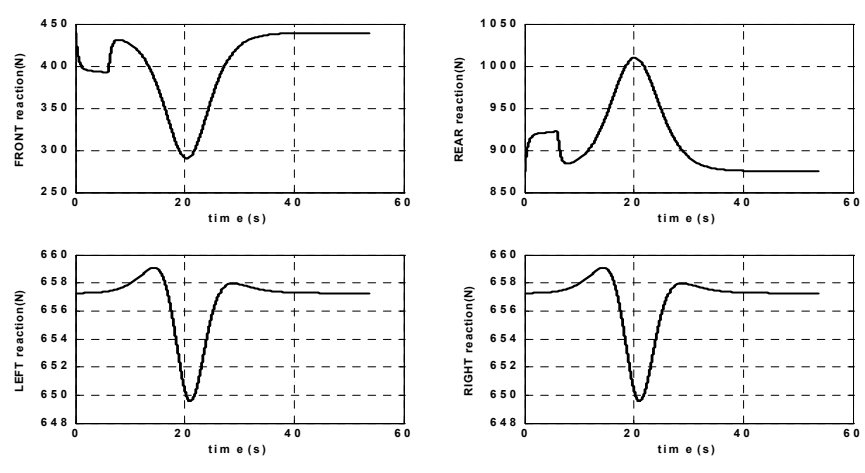
(1)



(2)



(3)



(4)

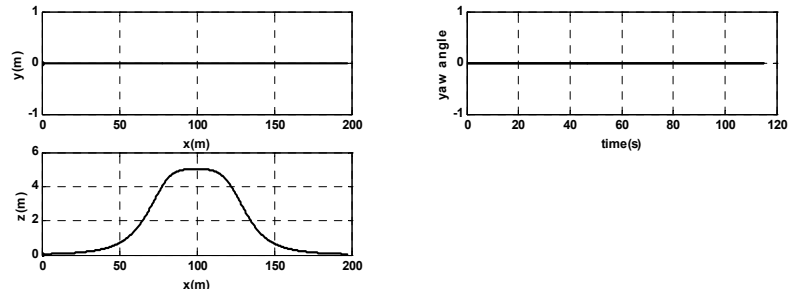
Figure 3.10. Response of the Wheelchair System for Case 10

3.1.2.3. Case 11: Wheelchair on a Road With Changing Uphill and Downhill Slopes

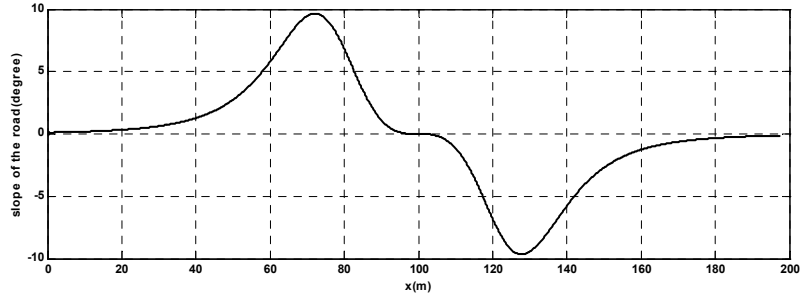
The wheelchair follows a straight path on a bumpy road which has both changing downhill and uphill slopes as can be seen in Plot (1) of Figure 3.11. The change of the slope of the road along the path is shown in Plot (2) of Figure 3.11. The user applies no voltage in y direction of the joystick not to have a steering action as in the previous cases for changing sloped roads.

The angular velocities of the right and left rear wheels are equal during motion as shown in Plot (3) of Figure 3.11. The motor torques increase with increasing uphill slope of the road and decrease with decreasing uphill slope of the road in order to maintain the desired speed of the wheelchair. Motor voltages also increase as the wheelchair speed and the uphill slope of the road are increased, and the downhill slope of the road is decreased.

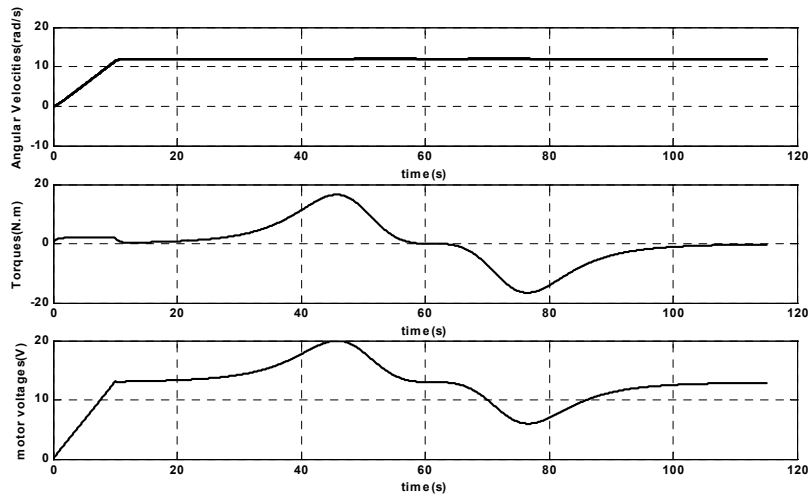
The reaction force on the front wheels decreases with increasing uphill slope of the road, and increases as the downhill slope of the road is increased. The reaction force on the rear wheels increases when the wheelchair encounters an uphill slope, and it decreases as the wheelchair travels on a downhill slope, which can be seen in Plot (4) of Figure 3.11. The changes in the left and right reaction forces are related with the changes in the slope of the road as in previous cases in this section. Note that the values of reaction forces on the right and left rear wheels are always equal during motion since the wheelchair does not turn..



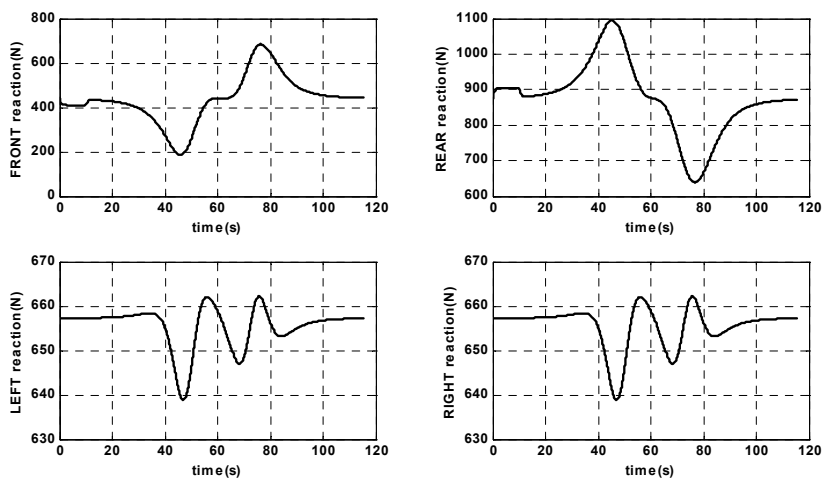
(1)



(2)



(3)



(4)

Figure 3.11. Response of the Wheelchair System for Case 11

3.2. System Analysis for Unreliable Situations

In this section the wheelchair motion is analyzed on roads with constant or changing slopes . In all cases, the wheelchair system is unstable.

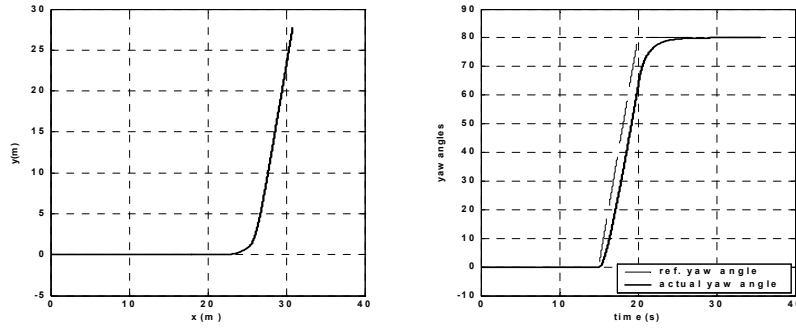
3.2.1. Unreliable Cases for Roads With Constant Slopes

3.2.1.1. Case 12: Wheelchair Toppling to the Right on a Downhill Slope

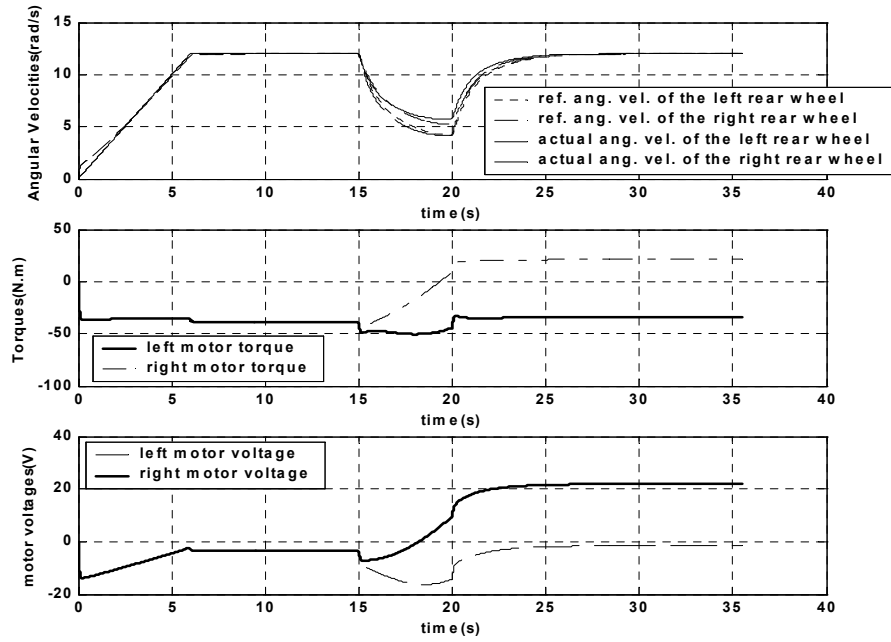
Wheelchair is driven on a constant downhill slope of 23° . The patient wants to move forward for 15 seconds, then turn to left with a heading angle of 80° as shown in Plot (1) of Figure 3.12. The user moves the joystick in x direction for a forward movement, then he moves it to the left in order to perform a left turn.

When the wheelchair moves forward with no turn the angular velocities of the right and left rear wheels remain equal as shown in Plot (2) of Figure 3.12. As the wheelchair starts turning left, the speed is reduced automatically and the angular velocity of the right rear wheel becomes higher with respect to the angular velocity of the left rear wheel, which is expected. During left turn, right motor torque and voltage are higher than left motor torque and voltage, and after turn this situation is still valid in order to prevent the wheelchair turning ahead to the downhill slope.

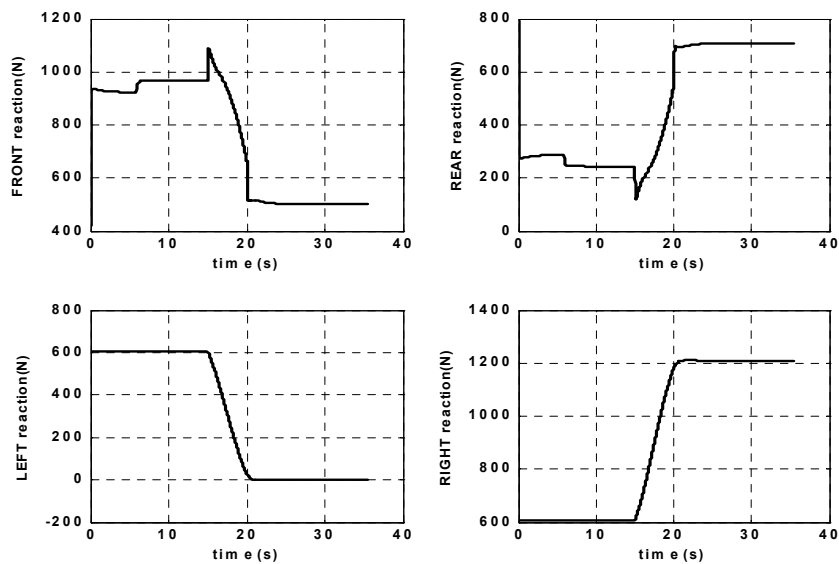
Note that the reaction force on the front wheels are higher with respect to the reaction force on the rear wheels initially due to the effect of a downhill slope as can be seen in Plot (3) of Figure 3.12. The reaction force on the front wheels decreases and the reaction force on the rear wheels increases as the motor torques increases. When the wheelchair turns left the reaction force on the outer wheels increases, which means that the reaction force on the left wheels decreases. Note that the reaction force on the left wheels takes a value of zero, which means that the wheels on the left side of the wheelchair lose contact with the ground. Therefore it can be said that the wheelchair topples to the right.



(1)



(2)



(3)

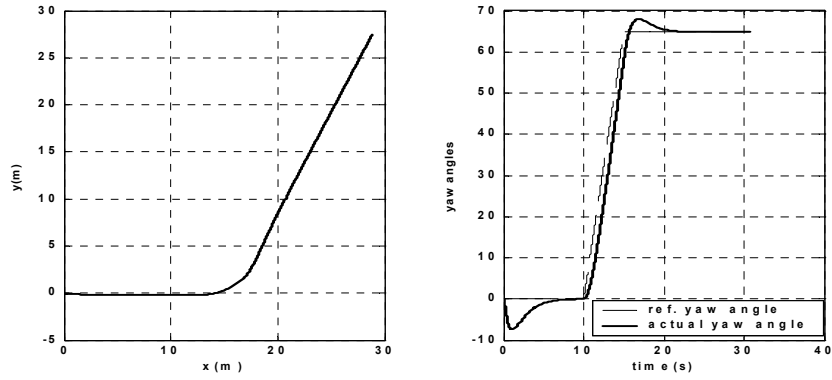
Figure 3.12. Response of the Wheelchair System for Case 12

3.2.1.2. Case 13: Wheelchair Toppling to the Back on a Side Slope

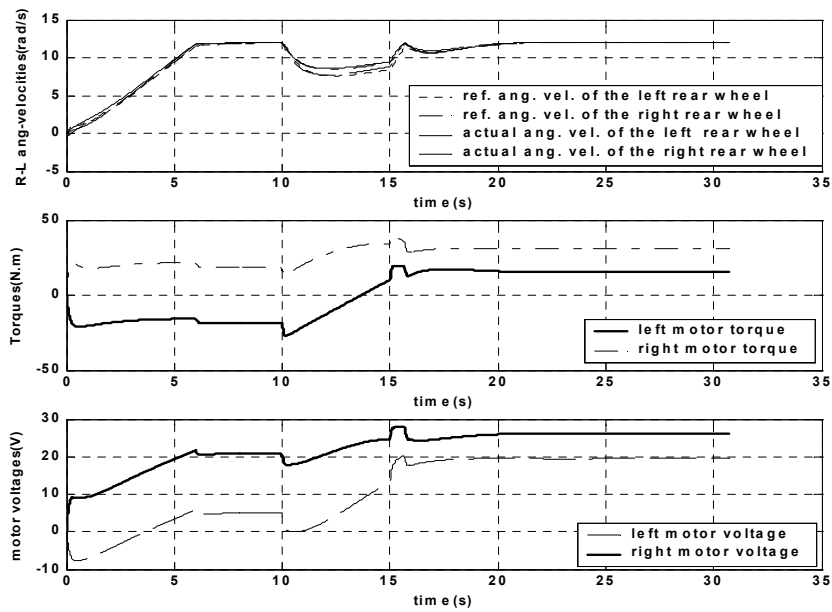
Wheelchair is driven on a road with a side slope of 15° . The patient moves the joystick in x direction only for 10 seconds then moves it to the left to turn left. As a result of such a user's command, the wheelchair moves forward for 10 seconds, and then turns to left with a heading angle of 65° as shown in Plot (1) of Figure 3.13.

The angular velocities of the left and right rear wheels remain equal for 10 seconds as shown in Plot (2) of Figure 3.13. Note that the speed of the wheelchair is increased in 6 seconds then remained constant until the left turn. When the wheelchair turns left the speed is reduced automatically for a safe steering. The angular velocity of the right rear wheel becomes higher than the angular velocity of the left rear wheel during left turn as expected. Note that the right motor torque and voltage remain always higher than the left motor torque and voltage during motion in order to prevent the wheelchair from turning right towards the downhill slope which is an unintentional behaviour of the wheelchair on a road with a positive side slope.

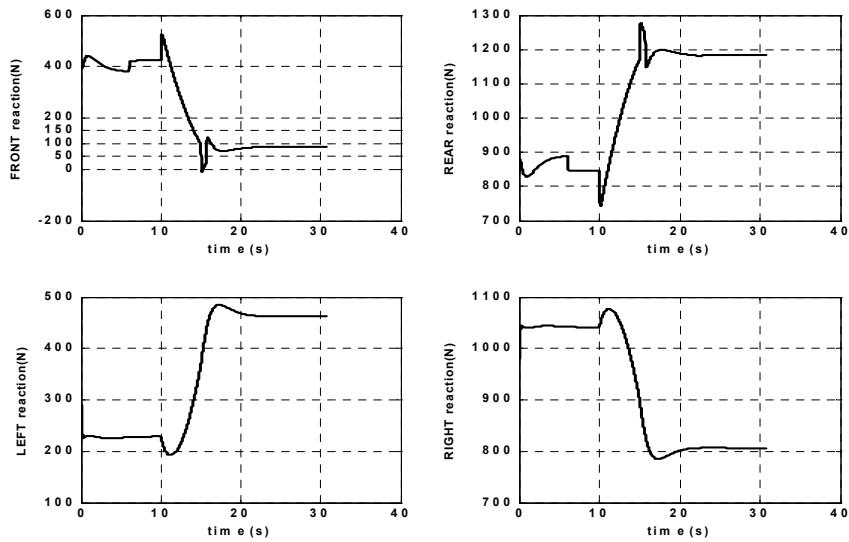
When the wheelchair turns to left it encounters with an uphill slope, which results in the increase of the reaction force on the rear wheels and decrease of the reaction force on the front casters. The reaction force on the front wheels gets a value of zero in this case as shown in Plot (3) of Figure 3.13, which means that the front casters lose contact with the ground. Therefore, the wheelchair topples to the back. During left turn, the increase in the reaction force on the right wheels is not much due to the effect of a side slope. Because, the right motor torque is already higher than the left motor torque during motion to prevent the wheelchair turning right towards the downhill slope. Note that after the wheelchair turns left the reaction force on the left wheels increases since the wheelchair keeps its heading angle constant after turn.



(1)



(2)



(3)

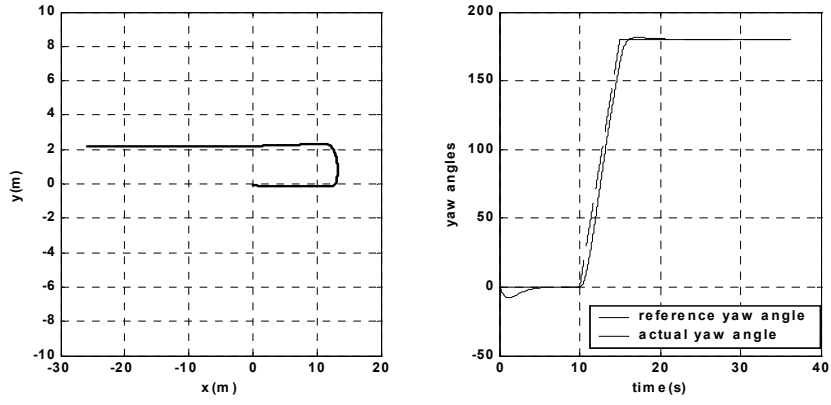
Figure 3.13. Response of the Wheelchair System for Case 13

3.2.1.3. Case 14: Wheelchair Toppling to the Back on a Road With a Constant Uphill and Side Slope

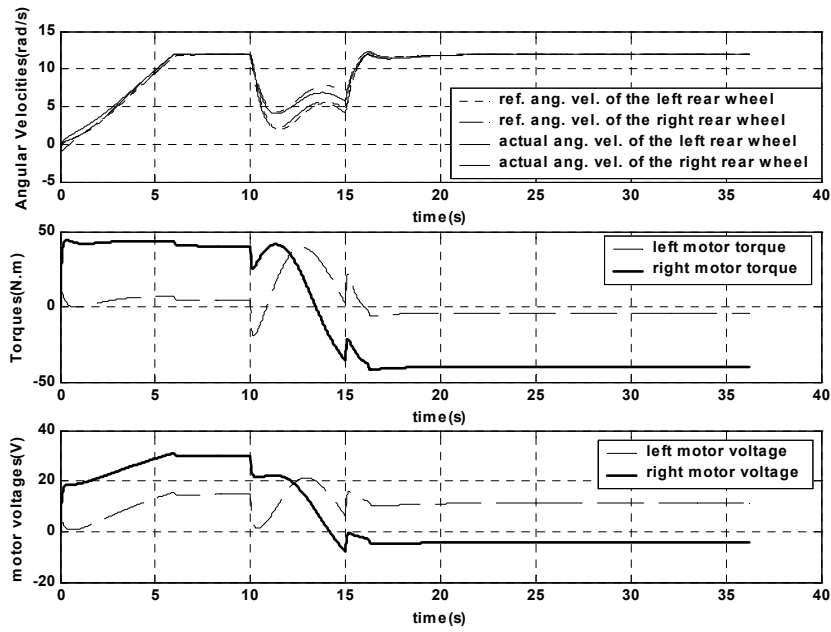
The wheelchair travels on a road that has a constant side slope of 15° and an uphill slope of 13° . The wheelchair user wants to move forward for 10 seconds, then turn to left with a heading angle of 180° and keep this direction afterwards, as shown in Plot (1) of Figure 3.14.

The angular velocities of the right and left rear wheels are equal when the wheelchair moves forward or keeps its direction angle constant after turn. When the wheelchair turns left the angular velocity of the right rear wheel becomes higher than the angular velocity of the left rear wheel as shown in Plot (2) of Figure 3.14. During left turn, right motor torque and voltage become higher with respect to left motor torque and voltage. Right motor torque is higher than left motor torque during straight movement of the wheelchair so as to prevent the wheelchair from turning right towards the downhill slope. After the wheelchair turns left, left motor torque becomes higher than right motor torque while the direction angle of the wheelchair remains constant. Because, the wheelchair tends to turn left towards the downhill slope as it keeps its direction after left turn.

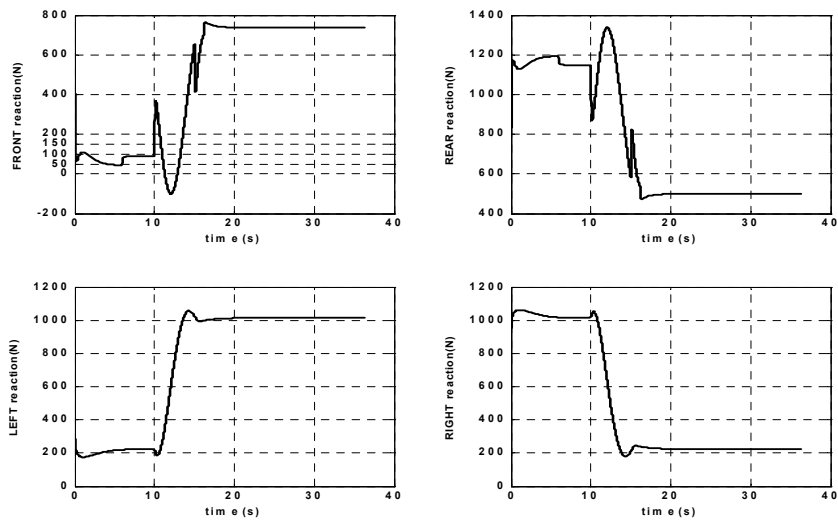
When the wheelchair turns left it encounters with an uphill slope. Therefore the reaction force on the rear wheels increases and the reaction force on the front wheels decreases at the beginning of the left turn as shown in Plot (3) of Figure 3.14. The reaction force on the front casters gets a value of zero which results in toppling of the wheelchair to the back. As the wheelchair turns left it encounters with a side slope also so that the reaction force on the left wheels increases and the reaction force on the right wheels decreases.



(1)



(2)



(3)

Figure 3.14. Response of the Wheelchair System for Case 14

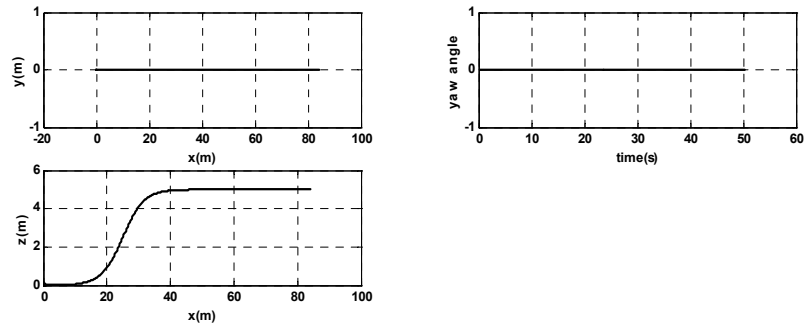
3.2.2. Unreliable Cases for Roads With Changing Slopes

3.2.2.1. Case 15: Wheelchair Toppling to the Back on a Road With a Changing Uphill Slope

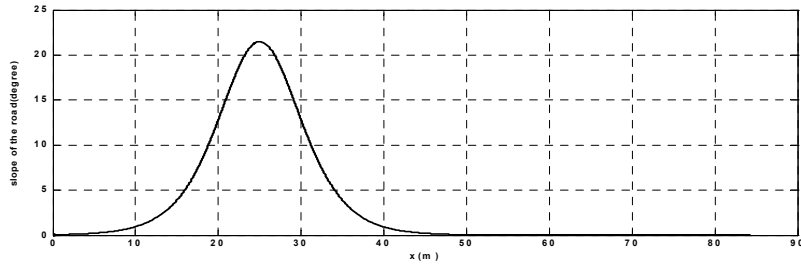
The wheelchair moves forward without any steering on a road profile as shown in Plot (1) of Figure 3.15. The changes of the slope along the path can be seen in Plot (2) of Figure 3.15. Since the wheelchair does not turn the patient supplies a voltage in x direction of the joystick only, resulting in a reference yaw angle of 0° .

The angular velocities of the right and left rear wheels are always equal during motion since there is no steering action of the wheelchair. The speed of the wheelchair is increased in 6 seconds by the user by means of joystick movements in x direction only, and then remained constant as shown in Plot (3) of Figure 3.15. The motor torques increase with increasing slope of the road in order to maintain the desired wheelchair speed. The motor voltages increase as the speed of the wheelchair is increased by the patient and the slope of the road is increased.

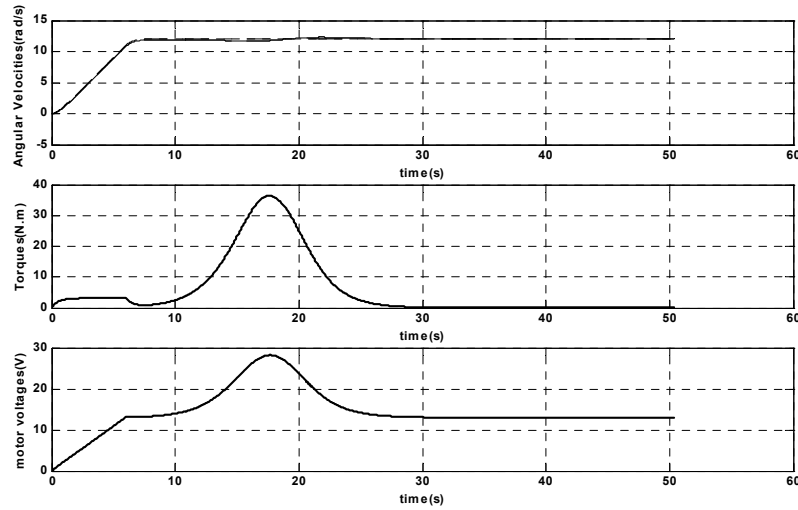
The reaction force on the rear wheels increase with increasing motor torques due to increasing slope of the road as shown in Plot (4) of Figure 3.15. As the uphill slope of the road is increased, the reaction force on the front casters decreases as expected. In this case, the reaction force on the front casters gets a value of zero even below zero, which means that the front casters lose contact with the ground resulting in toppling of the wheelchair to the back. The changes in the right and left wheels' reaction are related with the changes of the slope along the path. Note that they remains always equal since the wheelchair does not have any maneuverability.



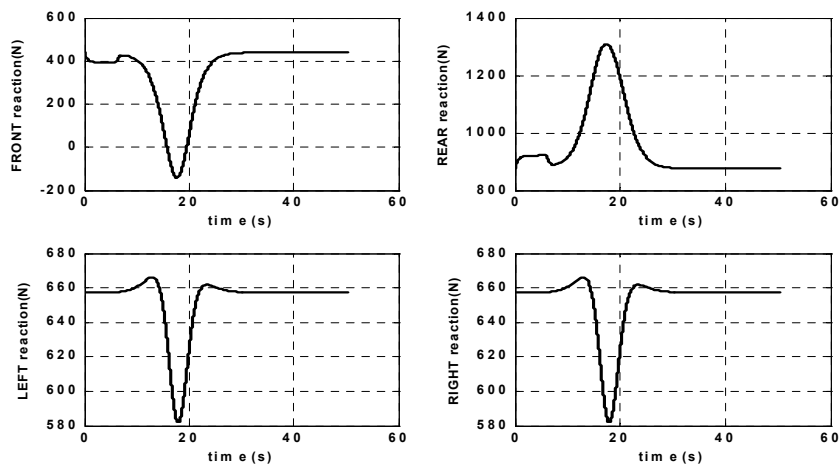
(1)



(2)



(3)



(4)

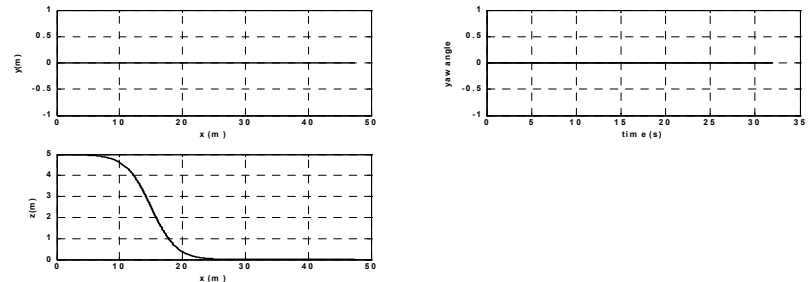
Figure 3.15. Response of the Wheelchair System for Case 15

3.2.2.2. Case 16: Wheelchair Toppling to the Front on a Road With a Changing Downhill Slope

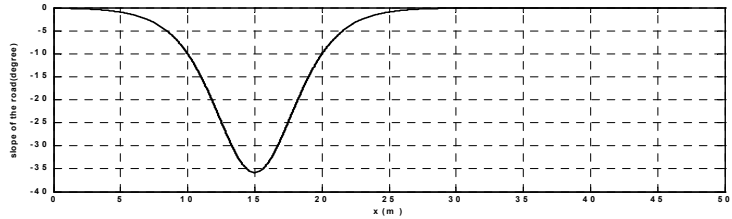
The wheelchair moves forward without any steering on a road with a changing downhill slope as shown in Plot (1) of Figure 3.16. The changes of the slope along the path can be seen in Plot (2) of Figure 3.16. Since the wheelchair does not turn the patient supplies no voltage in y direction but voltage in x direction of the joystick only, which results in a reference yaw angle of 0° as in the previous case.

The angular velocities of the right and left rear wheels are always equal during motion since there is no steering action of the wheelchair. The speed of the wheelchair is increased in 10 seconds by the user, and then remained constant as shown in Plot (3) of Figure 3.16. Note that the speed of the wheelchair increases slightly as the downhill slope of the road increases, and decreases slightly as the slope of the road starts to decrease again. This is the unintentional behaviour of the wheelchair due to the effect of a downhill slope, which is prevented by using PI controllers for the angular velocities of both of the rear wheels independently. As the downhill slope of the road is increased, the motor torques decrease and get negative values in order to maintain the desired speed on a downhill slope.

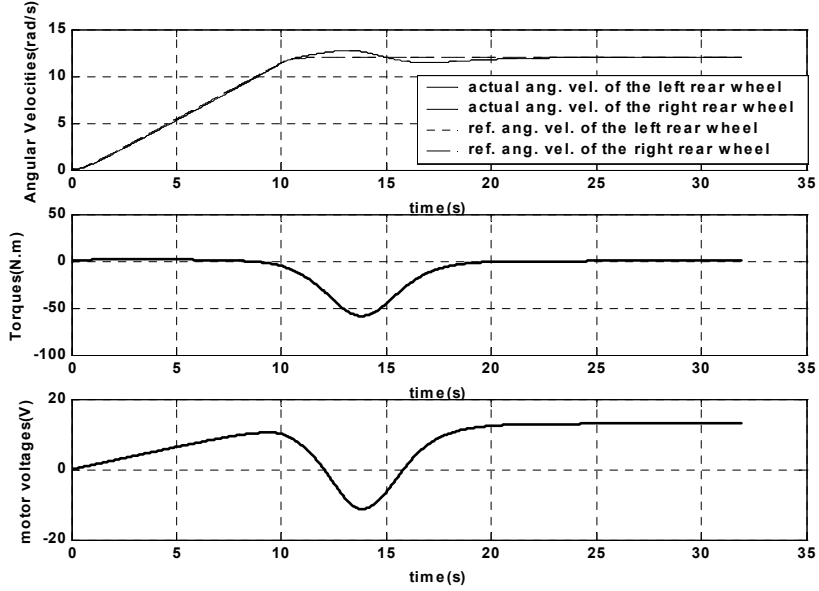
The reaction force on the rear wheels decrease with increasing downhill slope of the road as shown in Plot (4) of Figure 3.16. As the downhill slope of the road is increased, the reaction force on the front casters increases as expected. In this case, the reaction force on the rear wheels gets a value of zero which means that the rear wheels lose contact with the ground resulting in toppling of the wheelchair to the front. The changes in the right and left wheels' reaction are related with the changes of the slope along the path as in the previous case. Note that they remains always equal to each other since the wheelchair does not have any steering action.



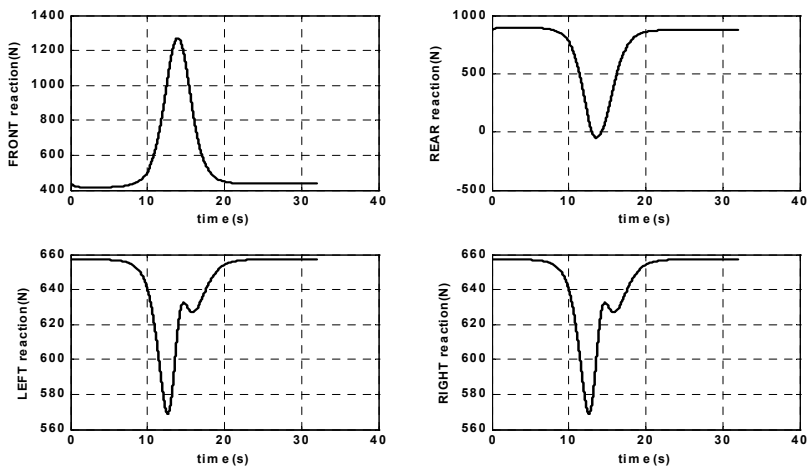
(1)



(2)



(3)



(4)

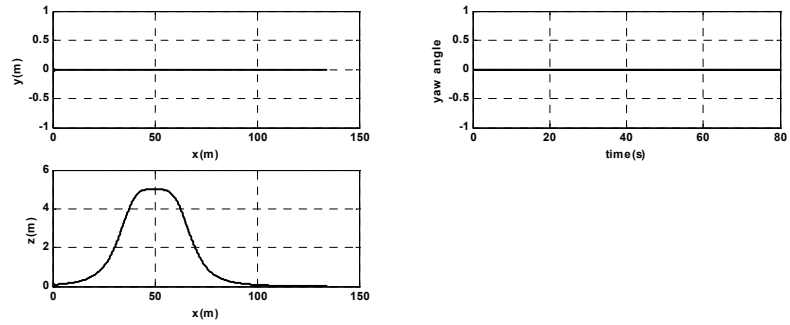
Figure 3.16. Response of the Wheelchair System for Case 16

3.2.2.3. Case 17: Wheelchair Toppling to the Back on a Road With Both Changing Downhill and Uphill Slopes

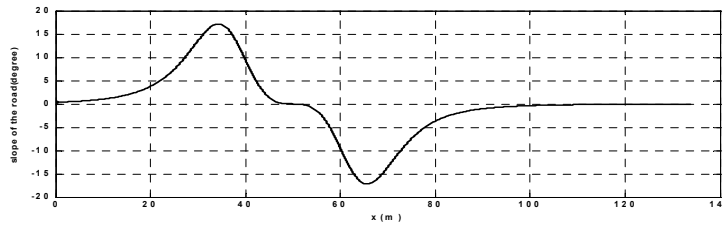
The wheelchair travels on a bumpy road on which has both changing uphill and downhill slopes as shown in Plot (1) of Figure 3.17. The reference heading angle supplied by the user is always zero during motion since no voltage is applied in y direction of the joystick. The slope changes along the path can be seen in Plot (2) of Figure 3.17.

The speed of the wheelchair is increased in 10 seconds, then remained constant as shown in Plot (3) of Figure 3.17. In other words, the user moves the joystick in x direction supplying a voltage of 3 V, then holds the joystick in the same position. Right motor torque and voltage are equal to left motor torque and voltage during motion since the user applies no voltage in y direction of the joystick. The motor torques and voltages increase with increasing uphill slope of the road and decreasing downhill slope of the road. Motor torques get negative values on a downhill slope in order to maintain the desired speed so that an excessive increase in the wheelchair speed is prevented on a downhill slope. However, motor torques get positive values on an uphill slope.

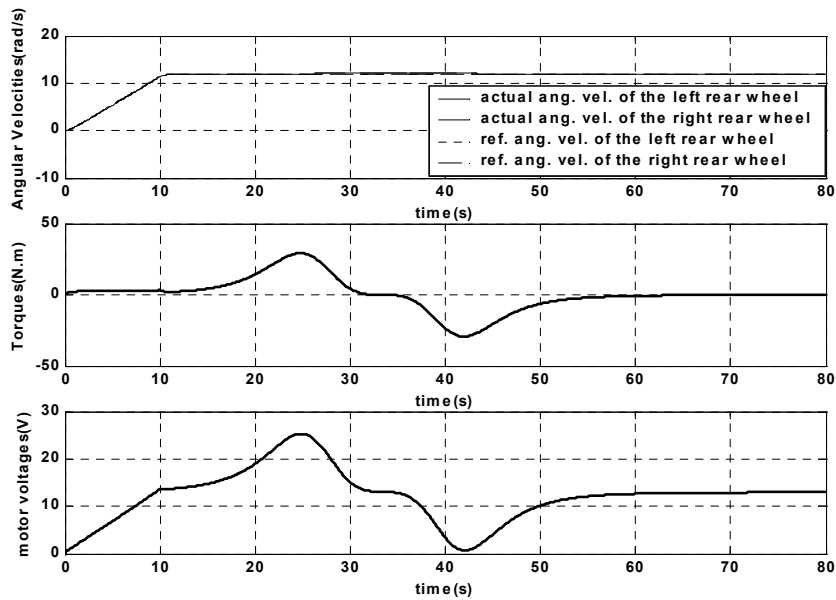
As the wheelchair moves on an uphill slope the reaction force on the front casters decreases as shown in Plot (4) of Figure 3.17. In this case, it gets a value of zero. Therefore, the wheelchair topples to the back. Note also that the reaction force on the rear wheels increases with increasing uphill slope of the road and decreases with increasing downhill slope of the road as expected. As in all previous cases for the roads with changing slopes, the reaction forces on the left and right wheels remain always equal to each other during motion since the wheelchair does not have a steering action. The changes in these reactions are related with the changes of the slope along the path.



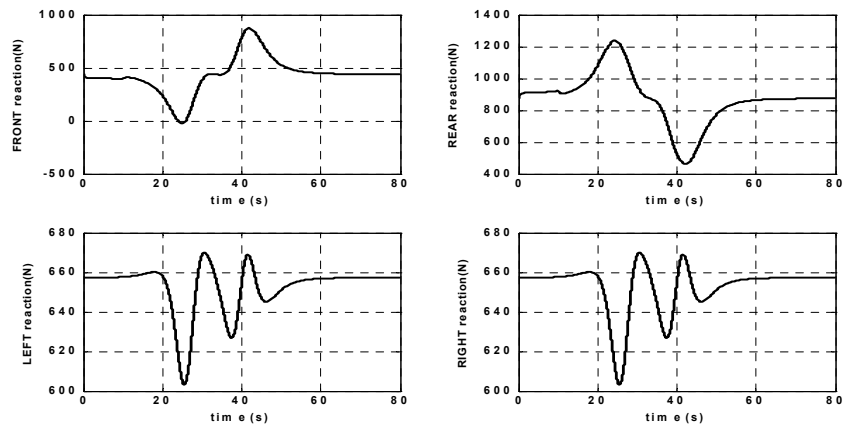
(1)



(2)



(3)



(4)

Figure 3.17. Response of the Wheelchair System for Case 17

3.3. Reduction of Unreliable Cases by the Methods of Stability Augmentation

Remember that speed reduction via joystick module during steering action, shape filter and shifting of center of mass are three methods used for stability augmentation. How the speed reduction and shape filter affect the stability was considered in Section 2.3.5 of Chapter 2. In this section, the effects of center of mass shifting on the stability are examined for the unreliable cases analyzed in Section 3.2.

3.3.1. Enhancement of Stability for Case 12

Remember Case 12 in Section 3.2.1.1 where the wheelchair driven on a constant downhill slope of 23° moves forward for 15 seconds, then turns to left with a heading angle of 80° and keeps its direction afterwards. The position of the wheelchair on the earth, and the reference-actual yaw angles are shown in Plot (1) of Figure 3.18. The angular velocities of the rear wheels, motor torques and motor voltages can be seen in Plot (2) of Figure 3.18.

Plot (3) of Figure 3.18 shows the new position of the center of mass. In this plot d_0 is the distance of the center of mass from front casters, d_1 is the distance of the center of mass from rear wheels, d_5 is the distance that locates the center of mass with respect to the left wheels, and d_6 is the distance of the center of mass from right wheels. As shown in this plot, the center of mass is shifted to the front about 0.07 m as the reaction force on the front casters decreases. The patient feels an absolute acceleration of about 0.086 m/s^2 to the back as the center of mass is shifted to the front, which should not disturb him. Speed reduction during left turn mainly contributes to the absolute acceleration felt by the patient in backwards direction whereas the relative acceleration caused by shifting of the center of mass to the front decreases the effect of acceleration that is resulted from speed reduction.

When the reaction force on the left wheels decreases the center of mass is shifted to the left about 7 cm so that the value of d_5 is decreased from 0.275 m to 0.205 m. The patient feels a relative acceleration of about 0.077 m/s^2 to the left with respect to wheelchair base as the center of mass is shifted to the left side. Note that the patient will also be affected by the acceleration of about 0.15 m/s^2 to the left caused by the steering action via left turn. Therefore, the absolute acceleration felt by the patient is about $0,227 \text{ m/s}^2$ to the left. Note that this much acceleration is mainly caused by the effect of steering since the relative acceleration felt by the patient due to the shifting of center of mass does not contribute much to the absolute acceleration felt by the user. Therefore, if the user already stands the acceleration caused by the steering action, he should also stand the acceleration caused by shifting of the center of mass. As the center of mass is shifted to the left the reaction force on the left wheels increases and the reaction force on the right wheels decreases. When the center of mass is shifted to the left, the stability is augmented compared to Case 12 where the center of mass is fixed such that the reaction force on the left wheels gets a value of 200 N but not zero during left turn, as shown in Plot (4) of Figure 3.18, which prevents the wheelchair from toppling to the right.

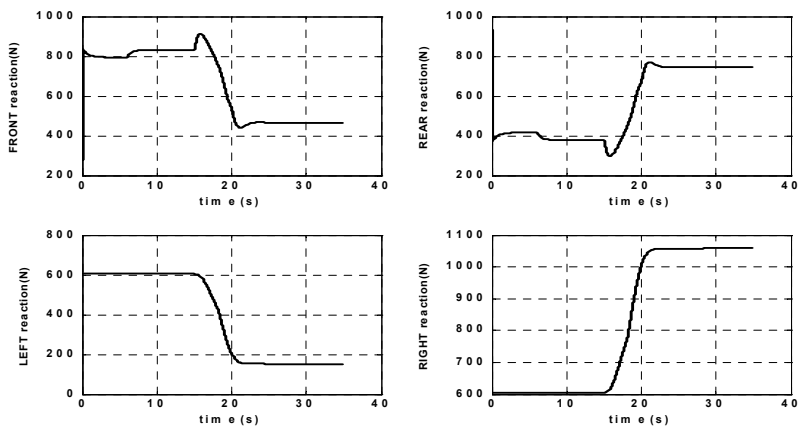
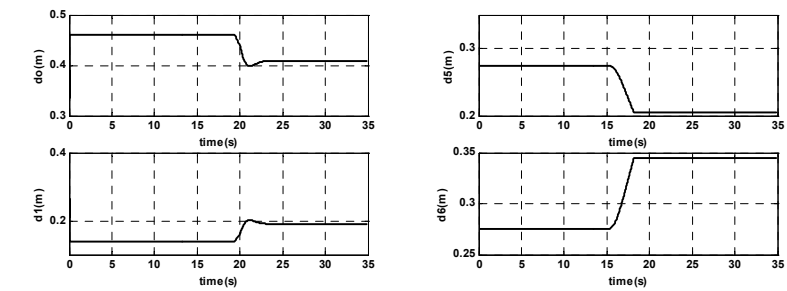
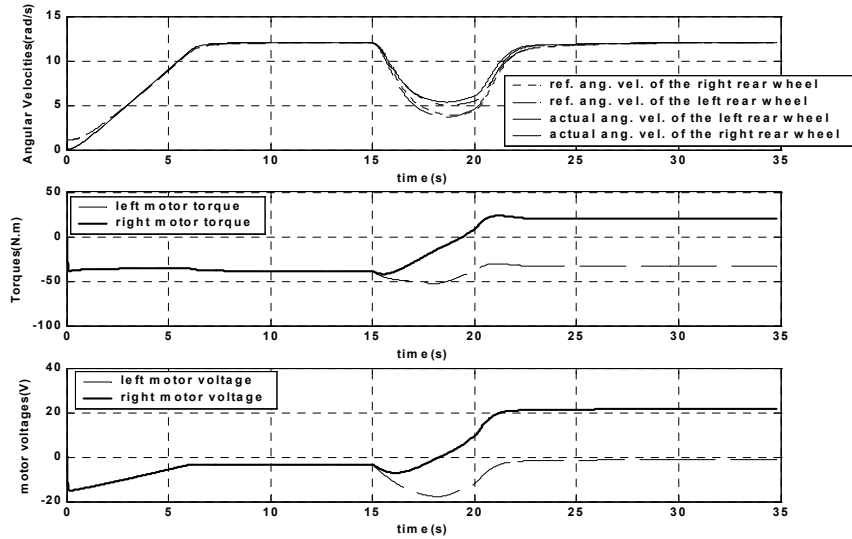
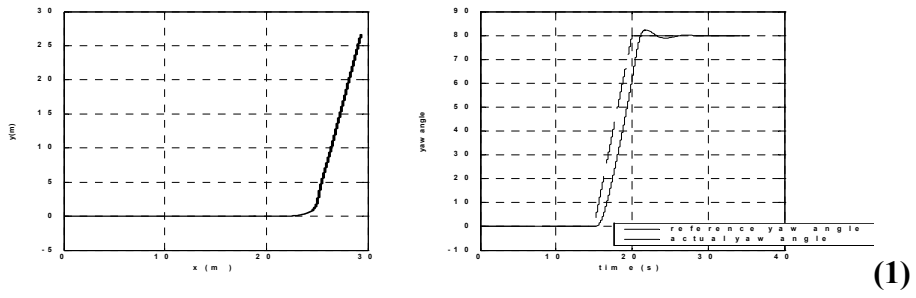


Figure 3.18. System Response With Enhanced Stability for Case 12

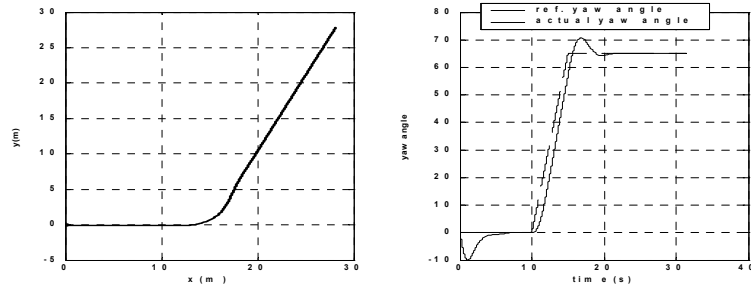
3.3.2. Enhancement of Stability for Case 13

Remember Case 13 in Section 3.2.1.2 where the wheelchair moves forward for 10 seconds, then turns to left with a heading angle of 65° on a road with a constant side slope of 15° , finally keeps its direction constant after turn as shown in Plot (1) of Figure 3.19. The angular velocities of the rear wheels, motor torques and motor voltages discussed previously in Section 3.2.1.2 are shown in Plot (2) of Figure 3.19.

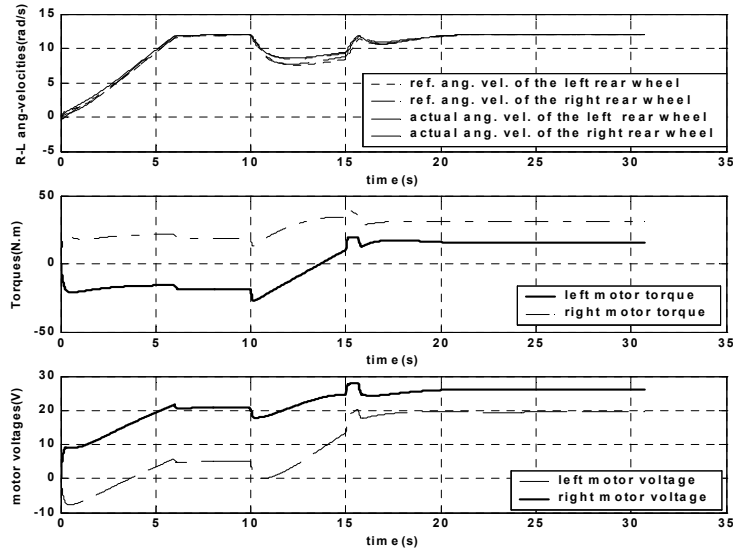
When the wheelchair turns to left on a positive side sloped road it encounters with an uphill slope, which results in the increase of the reaction force on the rear wheels and decrease of the reaction force on the front casters. Remember that the reaction force on the front casters gets a value of zero in Case 13, which means that the front casters lose contact with the ground. Therefore, the wheelchair topples to the back. In order to prevent this, the center of mass is shifted to the front so that the value of d_0 which is the distance of the center of mass to the front casters (d_0) is decreased from 0.4 m to 0.3 m as shown in Plot (3) of Figure 3.19. As a result, the reaction force on the front wheels is increased such that it decreases from 450 N to 200 N during left turn as shown in Plot (4) of Figure 3.19, whereas it decreased to a value of zero before shifting of the center of mass. Therefore the wheelchair is prevented from toppling to the back. As the center of mass is shifted to the front the patient feels an absolute acceleration of about 0.26 m/s^2 to the back. The acceleration caused by speed reduction during turn mainly contributes to the absolute acceleration felt by the user, since the patient feels a relative acceleration of only $0,04 \text{ m/s}^2$ to the front relative to the wheelchair base as the center of mass is shifted to the front. Note that the relative acceleration caused by shifting of the center of mass to the front slightly reduces the effect of the wheelchair acceleration to the back that is resulted from speed reduction during turn.

During left turn the increase in the reaction force on the right wheels is not much due to the effect of a side slope. Because the right motor torque is already higher than the left motor torque during motion to prevent the wheelchair turning right

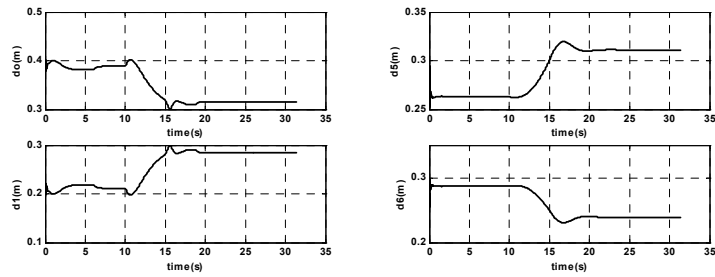
towards the downhill slope. Note that after the wheelchair turns left the reaction force on the left wheels increases since the wheelchair keeps its heading angle constant after turn. As the reaction force on the right wheels is decreased the center of mass is shifted to the right such that the distance d_6 is decreased from 0.275 m to 0.22 m as shown in Plot (3) of Figure 3.19, which causes a relative acceleration of about 0.034 m/s^2 to the right on the patient with respect to wheelchair base. The acceleration caused by steering action on a side slope is about $0,3 \text{ m/s}^2$ to the left. Therefore, the absolute acceleration felt by the user is about $0,266 \text{ m/s}^2$ to the left, which means that shifting of the center of mass resulted in a little decrease of absolute acceleration felt by the user during left turn on a side slope.



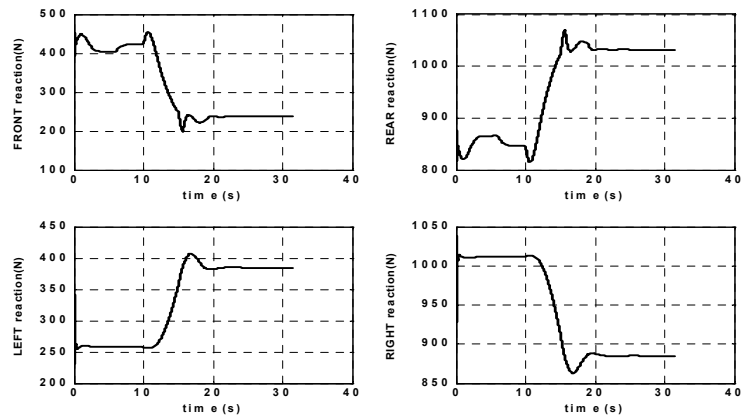
(1)



(2)



(3)



(4)

Figure 3.19. System Response With Enhanced Stability for Case 13

3.3.3. Enhancement of Stability for Case 14

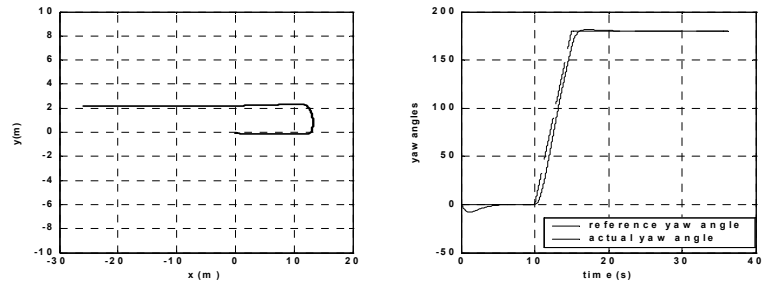
Remember Case 14 in Section 3.2.1.3 where the wheelchair moves forward for 10 seconds, then turns to left with a heading angle of 180° , and keep its heading angle constant after turn as shown in Plot (1) of Figure 3.20. The wheelchair is driven on a road which has both a constant side slope of 15° and uphill slope of 13° . The angular velocities of the rear wheels, motor torques and motor voltages discussed before can be seen in Plot (2) of Figure 3.20.

When the wheelchair turns left it encounters with an uphill slope. Therefore, the reaction force on the rear wheels increases and the reaction force on the front wheels decreases. The reaction force on the front wheels gets a value of zero during turn as shown in Plot (3) of Figure 3.14, which results in toppling of the wheelchair to the back. In order to prevent the wheelchair from falling to the back the center of mass is shifted to the front such that the distance of the center of mass from the front casters is decreased from 0.34 m to 0.29 m as shown in Plot (3) of Figure 3.20, which results in a relative acceleration of the wheelchair seat with respect to the wheelchair base of about 0.125 m/s^2 to the front. However, the patient feels an absolute acceleration of 0.575 m/s^2 to the back. Here, acceleration caused by shifting of center of mass to the front does not contribute much to the absolute acceleration felt by the user, even it causes a little decrease. The reaction force on the front casters decreases to a minimum value of 180 N but not zero as shown in Plot (4) of Figure 3.20 so that the wheelchair is prevented from toppling to the back.

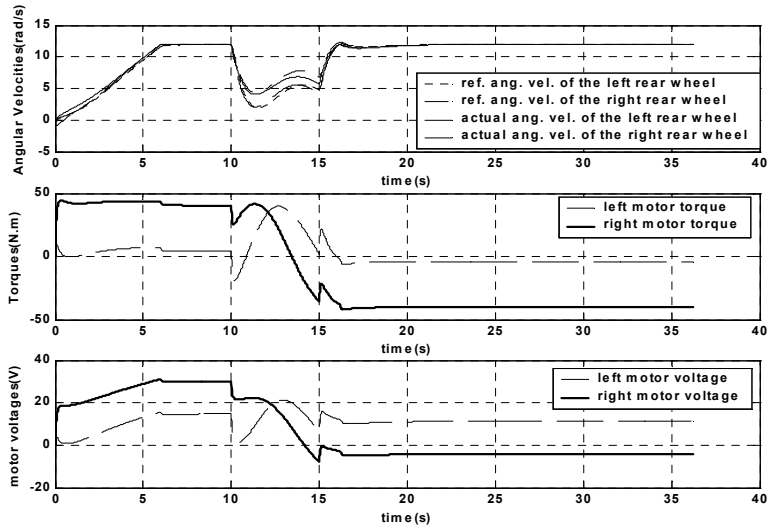
As the reaction force on the front wheels decreases the center of mass is shifted to the front, and the center of mass is shifted to the left while the reaction force on the left wheels decreases.

As the wheelchair turns left it also encounters with a side slope so that the reaction force on the left wheels increases and the reaction force on the right wheels decreases. In such a case, the center of mass is shifted to the right such that the distance of the center of mass from left wheels is increased from 0.275 m

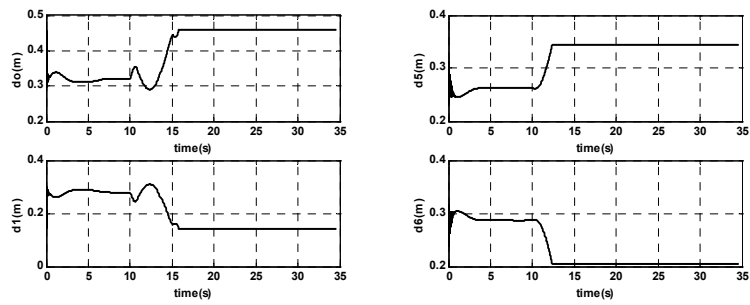
to 0.345 m as shown in Plot (3) of Figure 3.20. The relative acceleration felt by the patient during shifting of center of mass is about $0,077 \text{ m/s}^2$ to the right with respect to wheelchair base. Steep steering action of the wheelchair causes an acceleration of about $0,2 \text{ m/s}^2$ to the left. Therefore, the patient feels an absolute acceleration of $0,123 \text{ m/s}^2$ to the left, so one can say that shifting of center of mass caused a little reduction in the absolute acceleration felt by the user. The reaction force on the right wheels gets a value of 400 N after left turn as shown in Plot (4) of Figure 3.20 whereas this value was 200 N in Case 14 where the center of mass is not shifted.



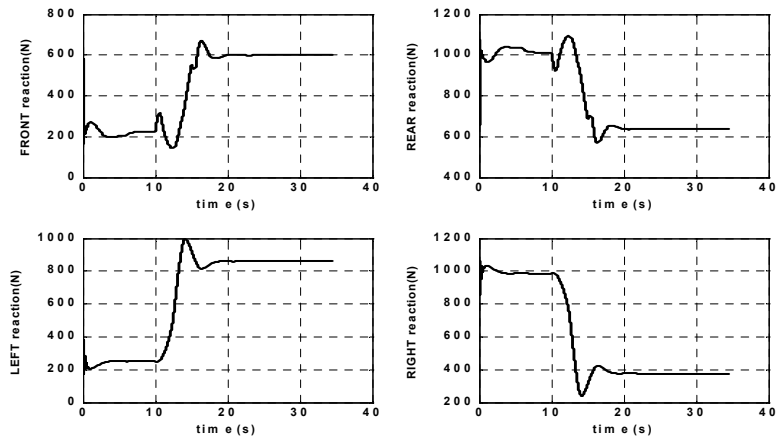
(1)



(2)



(3)



(4)

Figure 3.20. System Response With Enhanced Stability for Case 14

3.3.4. Enhancement of Stability for Case 15

Remember Case 15 in Section 3.2.2.1 where the wheelchair moves forward without any steering on a road with a changing uphill slope. The path of the wheelchair on the earth and the yaw angle are shown in Plot (1) of Figure 3.21. One can see the change of the uphill slope along the path in Plot (2) of Figure 3.21. The angular velocities of the right and left rear wheels are equal during motion since the wheelchair does not turn to the left or right, as shown in Plot (3) of Figure 3.21. As mentioned previously in Section 3.2.2.1, the motor torques and motor voltages increase with increasing uphill slope of the road.

Remember that the reaction force on the rear wheels increases as the uphill slope of the road increases, and the reaction force on the front casters decreases with increasing slope of the road. The reaction force on the front casters gets a value of zero even below, which means that the wheelchair topples to the back side. In order to prevent this, the center of mass is shifted to the front such that the distance of the center of mass from front casters is decreased from 0.38 m to 0.29 m as shown in Plot (4) of Figure 3.21, which causes a relative acceleration of the wheelchair seat about 0.014 m/s^2 to the front with respect to wheelchair base. However, the patient feels an absolute acceleration of about $0,002 \text{ m/s}^2$ to the front, which should not disturb him. As a result, the reaction force on the front casters is increased from -150 N to 50 N with respect to the reaction force obtained in Case 15 so that the wheelchair is prevented from toppling to the back. Similarly, as the center of mass is shifted to the front the distance of the center of mass from the rear wheels increases, which causes an increase in the reaction force of the rear wheels when compared with the same reaction force in Case 15, as shown in Plot (5) of Figure 3.21.

Since the wheelchair has no steering action the reaction force on the left and right wheels remain always equal to each other, and the system has no danger of toppling to the sides. Therefore the center of mass moves only in back and forth direction but not to the left or right.

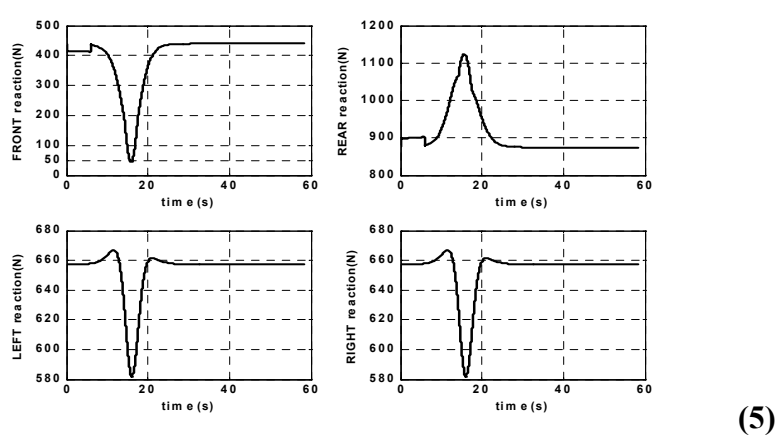
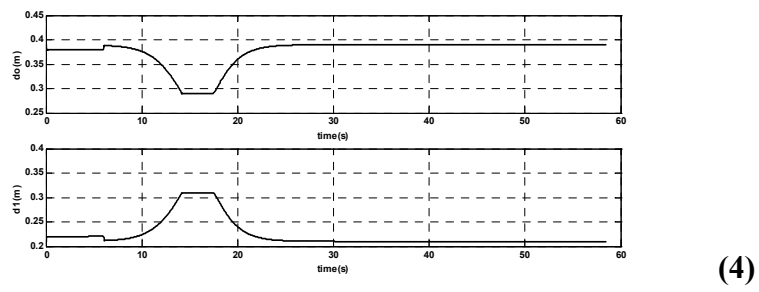
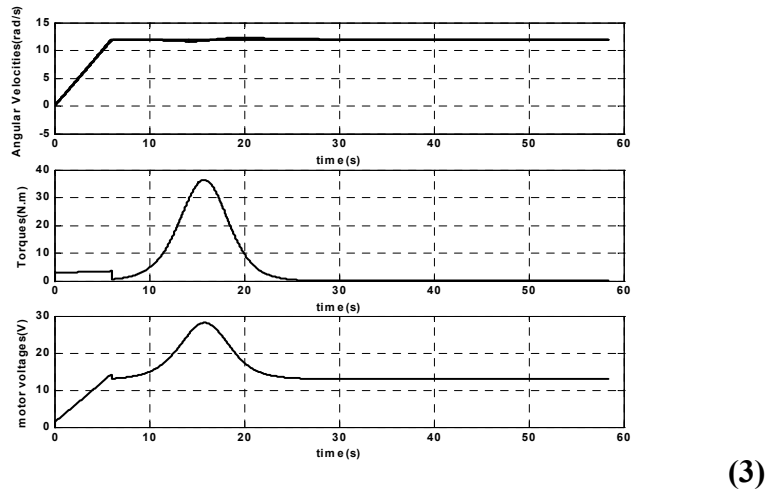
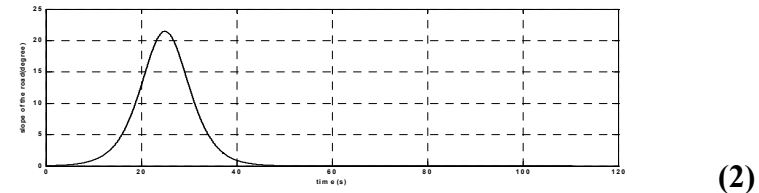
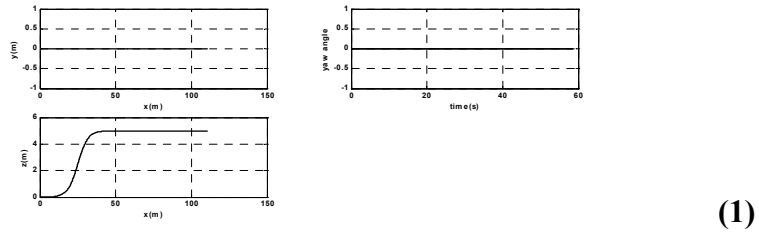


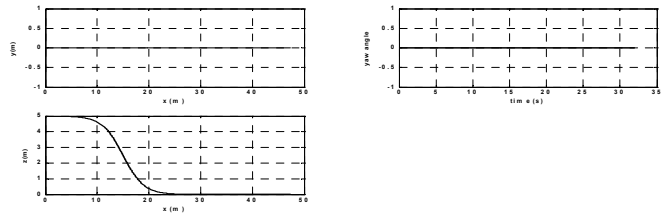
Figure 3.21. System Response With Enhanced Stability for Case 15

3.3.5. Enhancement of Stability for Case 16

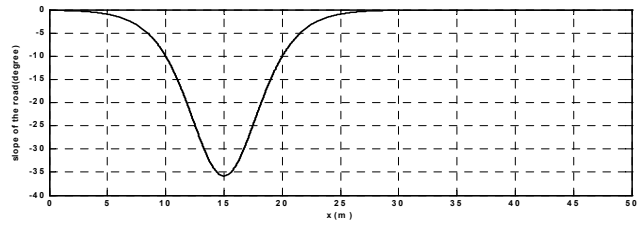
Remember Case 16 in Section 3.2.2.2 where the wheelchair is driven on a road with a changing downhill slope. There is no steering action of the wheelchair so that the patient does not supply any voltage in y direction of the joystick, which results in a reference yaw angle of zero as shown in Plot (1) of Figure 3.22. Change of the slope along the path is shown in Plot (2) of Figure 3.22. The angular velocities of the right and left rear wheels are equal during motion, and the motor torques and voltages decrease with increasing downhill slope of the road as shown in Plot (3) of Figure 3.22.

As the wheelchair moves forward on a downhill slope, the reaction force on the front casters increases, and the reaction force on the rear wheels decreases with the increasing downhill slope of the road. Remember that the reaction force on the rear wheels gets a value of zero in Case 16 so that the wheelchair topples to the front. In order to improve the stability in this case, the center of mass is shifted to the back such that the distance of the center of mass from rear wheels is decreased from 0.22 m to 0.14 m as shown in Plot (4) of Figure 3.22, causing a relative acceleration of about 0.077 m/s^2 to the back with respect to wheelchair fixed frame. The patient feels an absolute acceleration of about $0,037 \text{ m/s}^2$ to the front, which is mainly caused by increase in the wheelchair speed with increasing downhill slope. Note that, shifting of center of mass to the back reduced the value of absolute acceleration felt by the user. Referring to Plot (5) of Figure 3.22, one can see that the reaction force on the rear wheels is decreased from 900 N to 100 N but not to a value of zero so that the wheelchair is prevented from toppling to the front. As the center of mass is shifted to the back the reaction force on the front casters decreases compared to the case where the center of mass is fixed.

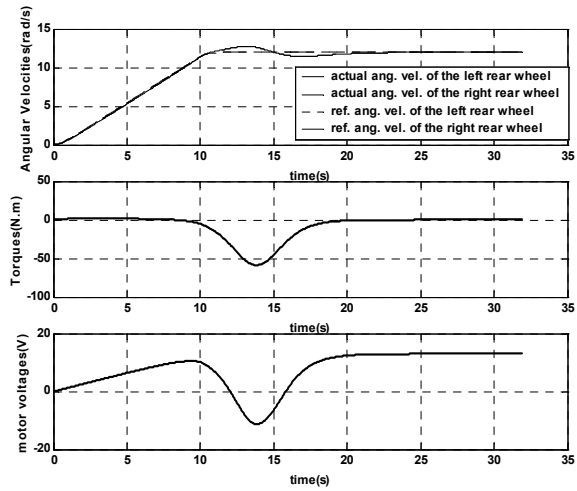
The center of mass is not shifted to the right or left side since the wheelchair does not have any danger to topple to the sides while it moves forward without steering.



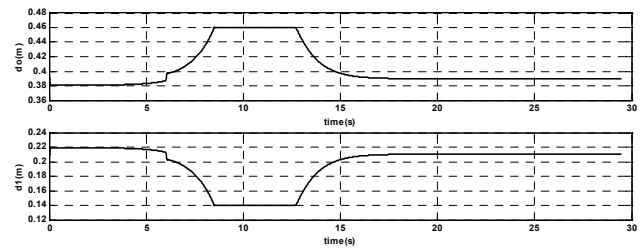
(1)



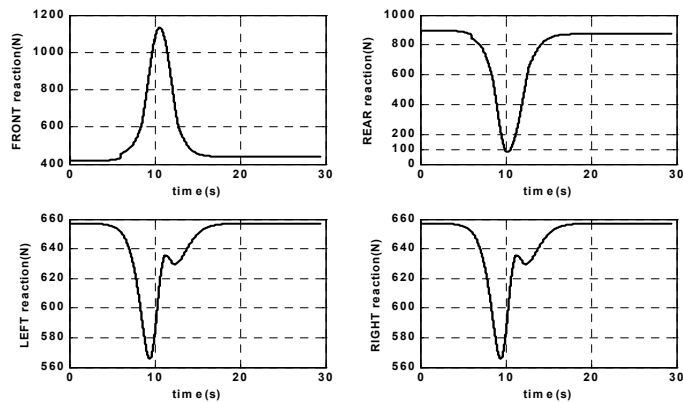
(2)



(3)



(4)



(5)

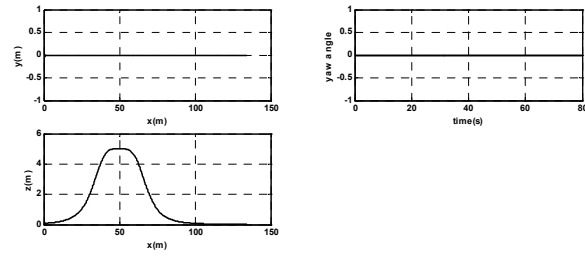
Figure 3.22. System Response With Enhanced Stability for Case 16

3.3.6. Enhancement of Stability for Case 17

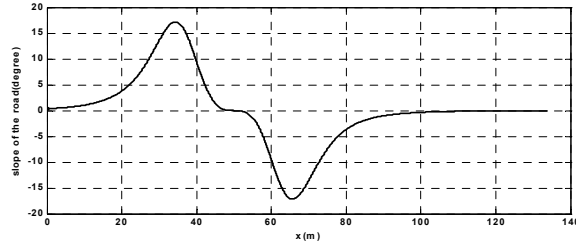
Referring to Case 17 in Section 3.2.2.3, the wheelchair moves forward on a bumpy road where the road has both changing uphill and downhill slopes as shown in Plot (1) of Figure 3.23. One can see the change of slope of the road along the path in Plot (2) of Figure 3.23. The reference yaw angle determined by the user is always zero during motion since he does not supply any voltage in y direction of the joystick not to have a steering action. The angular velocities of right and left rear wheels, motor torques and motor voltages are equal during motion as shown in Plot (3) of Figure 3.23, since the wheelchair does not turn. Note that the motor torques increase as the uphill slope of the road increases and downhill slope of the road decreases.

As the wheelchair moves along the uphill slope, the reaction force on the rear wheels increases and the reaction force on the front casters decreases. Remember that the wheelchair topples to the back in Case 17 when the reaction force on the front casters takes a value of zero. However, as the center of mass is shifted to the front this force takes the value of 200 N but not zero as shown in Plot (5) of Figure 3.23. The center of mass is shifted to the front about 0,1 m as shown in Plot (4) of Figure 3.23, which causes a relative acceleration of about 0.01 m/s^2 to the front with respect to wheelchair base. This much of relative acceleration combined with the acceleration of about $0,05 \text{ m/s}^2$ of the wheelchair to the back results in an absolute acceleration, felt by the patient, of $0,04 \text{ m/s}^2$ to the back. Note that the reaction force on the rear wheels decreases with a shift of the center of mass to the front as compared with the rear wheels' reaction force obtained in Case 17 where the center of mass is fixed relative to the wheelchair.

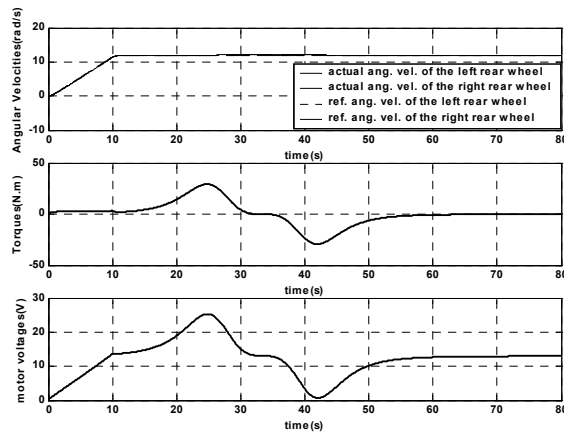
The reaction forces on the right and left rear wheels are same with the ones obtained in Case 17, since the center of mass is not shifted to the sides.



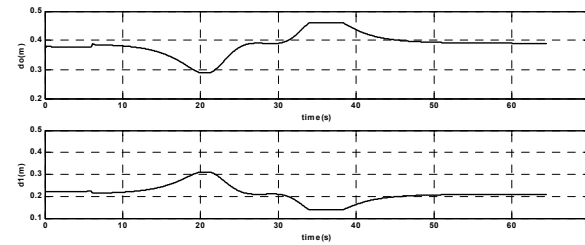
(1)



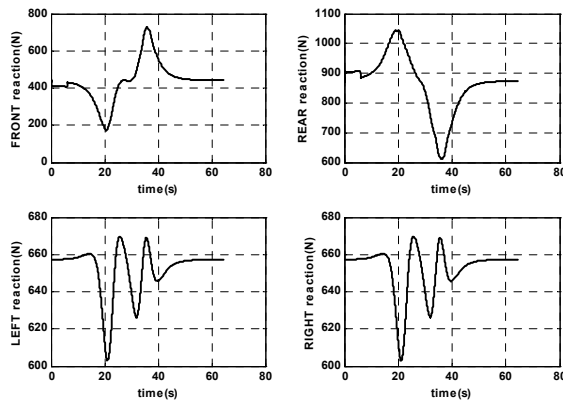
(2)



(3)



(4)



(5)

Figure 3.23. System Response With Enhanced Stability for Case 17

CHAPTER 4

CONCLUSIONS

4.1. Discussion

Stability augmentation of a semi-autonomous wheelchair has been considered within the scope of this thesis study. The system stability is examined by the analysis of reaction forces acting on the wheels by the ground. When the wheelchair tends to topple to the one side the total reaction forces on the other side of the wheelchair becomes zero or even below. In such a case, the wheels on that side of the wheelchair lose contact with the ground, which results in instability of the wheelchair-human system. Therefore, instead of analysis of each of the reaction forces on four wheels, which is not possible due to the static indeterminacy, it is sufficient to consider the total reaction force on two of the wheels that are in the same side of the wheelchair.

At the beginning of the study, detailed mathematical models of the system are obtained both for the wheelchair steering on roads with constant slopes, and the wheelchair moving forward on roads with changing slopes. Therefore, the effects of sudden slope changes along the path and the effects of steep steering actions on the system stability are concerned in two different models since the system dynamics becomes very complex to be handled when considering both of the effects at the same time. The equations of motion obtained for the wheelchair system traveling on roads with constant slopes are two, second order differential equations composed of coupled nonlinear terms. The system model obtained for the wheelchair traveling on roads with changing slopes consists of one nonlinear differential equation since the degree of freedom of the system is one in this case due to the fact that wheelchair moves only forward without any steering action.

As a next step in the study, control structure of the system is organized. Note that both speed and direction of the wheelchair is determined by the patient in terms

of joystick movements. These movements of the joystick define voltages in x and y direction of the joystick. The actual angular velocities of the rear wheels to be measured by encoders are compared with the reference values and the errors are minimized by PI controllers, which can be considered as a low-level speed control of the wheelchair system. On the other hand, the patient moves the joystick more to the left or right until the desired wheelchair direction angle is obtained. In order to model the control action of the user for the wheelchair direction angle as a high-level control, a proportional controller is used since the user can estimate the error but cannot take the derivative or integral of it. Control gains used in the simulations are selected by trial and error according to the speed of response, smoothness and stability of the system for several cases analyzed.

After the mathematical models and control structure of the system are constructed, simulations are carried out in Matlab Simulink environment to determine whether the system behavior is as expected under several specified driving and road conditions. As an example; as the patient supplies a voltage in x direction of the joystick only, the angular velocities of the rear wheels remain always equal during motion so that the wheelchair follows a straight path as expected; or the angular velocity of the right rear wheel becomes higher than the angular velocity of the left rear wheel during left turn when the user moves the joystick to the left supplying a negative voltage in y direction of the joystick. As the system response in several cases matched with the expected results, it is concluded that it is worthwhile to carry out the study and go on with the stability analysis.

In the third step of this thesis study, the stability of the wheelchair-human system is examined by means of analysis of reaction forces of the wheels by several simulations carried out for different driving and road conditions. And it is seen that the system becomes unstable in some of the cases due to the effects of steep steering actions on a slope and sudden slope changes along the path.

In the final step of the study, how the stability of the wheelchair may be improved was the question in hand. Three different methods are used to solve this problem. One is the speed reduction via joystick module during steep turns. The patient

may increase the speed of the wheelchair during steep turns on a slope, which may result in instability of the system. In such cases, the speed of the wheelchair is reduced for a safe steering, but the wheelchair follows the desired course. In other words, as the user wants to have steeper turns by supplying more voltage in y direction of the joystick, the speed of the wheelchair is reduced more. However, the reduction of the speed should not be jerky since a sudden increase or decrease in the wheelchair speed may also cause instability. Such instability may also be caused by a sudden movement of the joystick in x direction due to mental restrictions of the user or uncontrolled reflexes. In order to prevent this, a second method is considered for stability augmentation, which is the use of a shape filter in order to obtain a less jerky response for the speed. It is clear that the position of the patient in a powered wheelchair can have a large effect on the wheelchair stability. Therefore, as a final method for the improvement of stability, the center of mass of the wheelchair-human system is shifted gently in a controlled manner to the side where the value of the reaction force is zero or even below, so that toppling of the wheelchair is prevented for selected situations that are unstable when the center of mass is fixed. Such a shifting of center of mass is possible when the seat with the patient is shifted to the sides on a plate that can also be shifted on the base of the wheelchair to the back and forth. The relative acceleration felt by the patient with respect to the wheelchair base during shifting process is an important parameter since it can disturb the user. However, the patient always feels the absolute acceleration that is the combination of the relative acceleration of the wheelchair seat with respect to wheelchair base and the acceleration caused by the steering action or speed changes of the wheelchair. As a result of the simulations carried out, it is concluded that the relative acceleration caused by shifting of the center of mass does not contribute much to the absolute acceleration felt by the patient. The patient who can already stand the accelerations caused by steep steering action or speed changes can also easily stand the accelerations resulted from center of mass shifting. Even in some cases, the relative acceleration of the wheelchair seat with respect to wheelchair base caused by center of mass shifting cause a little reduction in the value of the absolute acceleration felt by the patient.

4.2. Conclusions and Recommendations for Future Work

The main objective in this thesis study is to increase the limit of independency for wheelchair users. These limitations are in fact related with the physical abilities and mental burdens of the patient as well as the characteristics of the riding surface and dynamic parameters of the wheelchair-human system. This study is performed to improve the stability of the wheelchair system under varying road conditions so as to enhance the life quality of many physically disabled people.

Although it is shown that the wheelchair-human system can be made more stable by the use of three methods proposed for the stability augmentation, the main disadvantage is, the application of these methods especially the method of active shifting of center of mass require the use of extra sensors and actuating mechanisms, which increases the cost and complexity of the whole system.

The wheelchair-human models obtained in this study provide reasonably accurate dynamic simulations of a semi-autonomous powered wheelchair driven on roads with constant and changing slopes. The proposed control strategies with the methods applied for the stability augmentation will be hopefully useful in the development of improved wheelchairs with improved independent motion and safety.

The most important development over the recent study would be a hardware implementation; evaluation and field-testing of the proposed control schemes as a future work.

In this study it is assumed that the patient does not move relative to the wheelchair fixed frame, which may be the case when the user is paralyzed or a seat belt is used. However, the dynamics of human body may be included while obtaining the mathematical model of the wheelchair-human system, and the effects of human postural movements on the system stability may be studied since these movements should change the position of the center of mass of the whole system.

The current model of the system does not include the effects of suspension dynamics also. Including the suspension dynamics would permit the simulation of the wheelchair system over uneven ground.

The Simulink models are developed in a modular manner so that if desired any part of the model like the control system or the mathematical model can be replaced by another one. This brings to researchers the advantage of testing the performance of their own control schemes or models. Therefore; a future research on the wheelchair-human system may be the development of different control strategies to be applied on the existing mathematical models of the wheelchair-human system obtained in this thesis study. An alternative method can be the use of fuzzy logic controllers.

REFERENCES

1. J.B. Shung, G. Stout, M. Tomizuka and D.M. Auslander, "Dynamic Modeling of a Wheelchair on a Slope"; *Journal of Dynamic Systems, Measurement and Control*; June 1983, Vol. 105, pp. 101-106.
2. J.B. Shung, G. Stout, M. Tomizuka and D.M. Auslander, "Feedback Control and Simulation of a Wheelchair"; *Journal of Dynamic Systems, Measurement and Control*; June 1983, Vol. 105, pp.96-100.
3. H. Ohnabe and F. Mizuguchi, "Turning Characteristics and Stability of Manual Wheelchairs on a Slope", 2001 Proceedings of the 23rd Annual International Conference, Istanbul, Turkey, October 2001, pp.1408-1411.
4. G. Boiadzjiev and D. Stefanov, "Powered Wheelchair Control Based on the Dynamical Criteria of Stability", *Mecathronics* 12 (2002), March 2001, pp. 543-562.
5. R.A. Cooper, MacLeish, Michael, "Racing Wheelchair Roll Stability While Turning: A Simple Model", *Journal of Rehabilitation Research & Development*, Spring 1992, Vol. 29, Issue 2, p. 23.
6. D.G. Kamper, T.C. Adams, S.I. Reger, M. Parnianpour, K. Barin and M. Linden, "A Low-Cost, Portable System for the Assessment of the Postural Response of Wheelchair Users to Perturbations", *IEEE Transactions on Rehabilitation Engineering*, December 1999, Vol. 7, No. 4, pp. 435-441.
7. <http://www.ensc.sfu.ca/research/erl/med>, 02.01.2003.
8. "Wheelchair- Part 2: Determination of Dynamic Stability of Electric Wheelchairs", Stockholm: International Organization for Standardization, 1986, ISO 7176-2.
9. "Wheelchair- Part 1: Determination of Static Stability", Stockholm: International Organization for Standardization, 1986, ISO 7176-1.

10. Antonis Argyros, Pantelis Georgiadis, Panos Trahanias and Dimitris Tsakiris, "Semi-Autonomous Navigation of a Robotic Wheelchair", *Journal of Intelligent and Robotic Systems*, 2002, Vol. 34, pp. 315-329.
11. H.R Rockland and S. Reisman, "Voice Activated Wheelchair Controller", *IEEE Transactions on Rehabilitation Engineering*, 1998, pp. 128-129.
12. T. Gomi and A. Griffith, "Developing Intelligent Wheelchairs for the Handicapped", *Assistive Technology and AI; LNAI 1458*, pp. 150-178.
13. M. Goodwin, D. Sanders, G. A. Poland and I.J. Scott, "Navigational Assistance for Disabled Wheelchair Users", *Journal of System Architecture*, 1997, pp. 73-79.
14. K. Ozgoren, "Lecture Notes on Advanced Dynamics", Mechanical Engineering Department; METU, 2003.
15. R. Ellis and D. Gulick, "Calculus with Analytic Geometry"; Fifth Edition, Saunders College Publishing, 1994, p. 387.
16. R. Ellis and D. Gulick, "Calculus with Analytic Geometry"; Fifth Edition, Saunders College Publishing, 1994, p. 269.
17. C.W. De Silva, "Control Sensors and Actuators"; Prentice Hall Inc., 1989, pp. 323-365.
18. <http://www.daysmedical.com/product.php?id=235>, 17.02.2003.
19. http://www.dynamic-controls.co.nz/mobility-products/cat_list.asp?cat=Dynamic+Wheelchair+Motors, 12.02.2003.
20. The Mathworks Inc., "Matlab Simulink User's Guide", The Mathworks Inc., 1999, p.162.
21. <http://www.personal.usyd.edu.au/~mslee/ESSwww/lee/zygal/glossary/anthropometry/winter.html>, 02.03.2003.
22. http://www.mech.utah.edu/ergo/educate/safety_modules/ctd-anthropometry/, access date: 02.03.2003.

23. L.G. Kraige and J.L. Meriam, "Engineering Mechanics: Vol. 2 Dynamics", John Wiley & Sons, 1993, pp. 675-680.

APPENDIX A

CALCULATION OF CENTER OF MASS FOR THE WHEELCHAIR-HUMAN SYSTEM

The geometries of components of human body are simplified such that human head is a sphere, trunk is a rectangular prism, arms and limbs of the human body are modeled as cylinders. The mass and dimensions of each component of the human body are taken from ‘Anthropometric Data’ [21] and ‘Relative Dimensions of the Average Human Body’ [22] as shown in Table C.1 and Figure C.1 of Appendix C. In this section, the position of the center of mass (G) of the wheelchair-human system is to be determined with respect to the point K which is on the middle of the back side of the base as shown in Figure A.1.

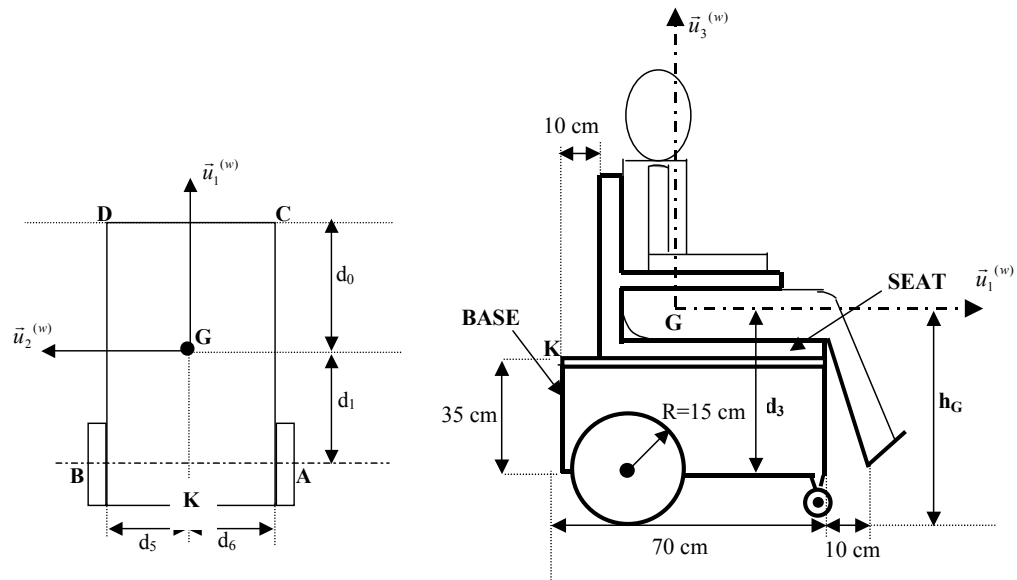


Figure A.1. Top and Side View of the Wheelchair-Human System

The total mass of the patient is taken to be 75 kg. The position of the center of mass of the each component of the wheelchair-human system obtained with respect to point K after some manipulations are shown in Table A.1 on the next page.

Table A.1. Center of Mass Calculation of the System Components

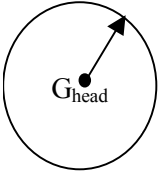
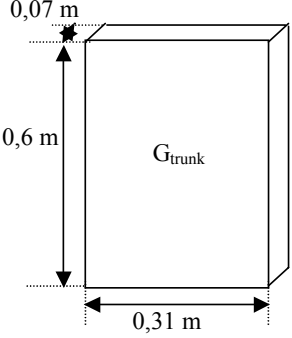
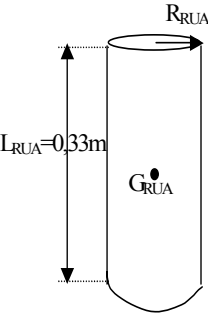
Component	Mass	x (m)	y(m)	z(m)
 <p style="text-align: center;">Head</p>	m _{Head} =5,67 kg	0,24 m	0 m	0,76 m
 <p style="text-align: center;">Trunk</p>	m _{Trunk} =34,7 kg	0,165 m	0 m	0,35 m
 <p style="text-align: center;">Right Upper Arm, Left Upper Arm</p>	m _{RUA} =1,96 kg m _{LUA} =1,96 kg	0,185 m	-0,21 m	0,48 m

Table A.1 (Continued)

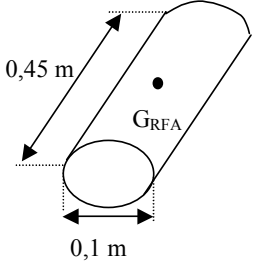
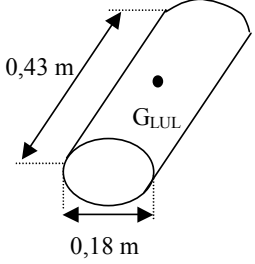
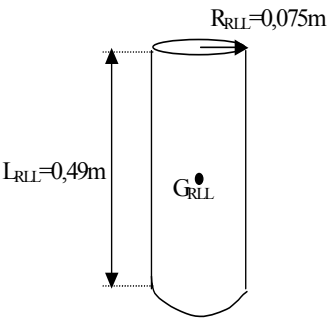
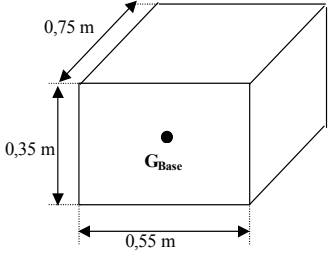
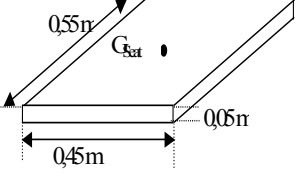
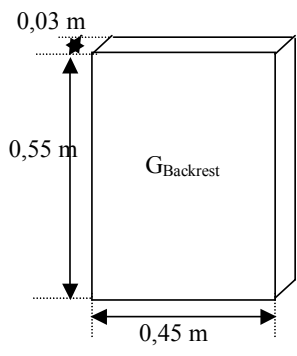
Component	Mass	x (m)	y(m)	z(m)
 <p style="text-align: center;">Right Forearm, Left Forearm</p>	$m_{RFA}=1,54 \text{ kg}$ $m_{LFA}=1,54 \text{ kg}$	$0,46 \text{ m}$ $0,46 \text{ m}$	$-0,2 \text{ m}$ $0,2 \text{ m}$	$0,37 \text{ m}$ $0,37 \text{ m}$
 <p style="text-align: center;">Right Upper Limb, Left Upper Limb</p>	$m_{RUL}=3,5 \text{ kg}$ $m_{LUL}=3,5 \text{ kg}$	$0,414 \text{ m}$ $0,414 \text{ m}$	$-0,062 \text{ m}$ $0,062 \text{ m}$	$0,14 \text{ m}$ $0,14 \text{ m}$
 <p style="text-align: center;">Right Lowerlimb, Left Lowerlimb</p>	$m_{RLL}=11,27 \text{ kg}$ $m_{LLL}=11,27 \text{ kg}$	$0,675 \text{ m}$ $0,675 \text{ m}$	$-0,077 \text{ m}$ $0,077 \text{ m}$	$-0,25 \text{ m}$ $-0,25 \text{ m}$

Table A.1 (Continued)

Component	Mass	x (m)	y(m)	z(m)
 <p style="text-align: center;">Base</p>	$m_{\text{Base}}=50 \text{ kg}$	$0,375 \text{ m}$	0 m	$-0,175 \text{ m}$
 <p style="text-align: center;">Seat</p>	$m_{\text{Seat}}=5 \text{ kg}$	$0,375 \text{ m}$	0 m	$0,025 \text{ m}$
 <p style="text-align: center;">Backrest</p>	$m_{\text{Backrest}}=3 \text{ kg}$	$0,015 \text{ m}$	0 m	$0,275 \text{ m}$

After the center of mass of each component is obtained, the center of mass of the wheelchair-human system can be derived as in Equation A.1 where m_{total} is the

total mass of the wheelchair-human system, m_i and \vec{r}_i are the mass and position vectors of the center of mass of each component, respectively.

$$\vec{r}_G = \sum_i \frac{m_i \vec{r}_i}{m_{total}} \quad (\text{A.1})$$

The total mass of the wheelchair human system is taken as follows.

$$m_{total} = 128kg \quad (\text{A.2})$$

After some manipulations are made on Equation A.1, the center of mass of the wheelchair-human system is obtained. Equations A.3, A.4, and A.5 define the position of the center of mass with respect to point K.

$$\vec{x}_{G/K} = 0,36m\vec{i} \quad (\text{A.3})$$

$$\vec{y}_{G/K} = 0m\vec{j} \quad (\text{A.4})$$

$$\vec{z}_{G/K} = 0,03m\vec{k} \quad (\text{A.5})$$

Referring Figure A.1, the parameters related to the geometry of the wheelchair are obtained as follows.

$$d_1 = 0,36 - R = 0,36 - 0,15 = 0,21m \quad (\text{A.6})$$

$$d_0 = 0,70 - R - d_1 = 0,75 - 0,15 - 0,21 = 0,39m$$

$$d_2 = \frac{d_5 + d_6}{2} = \frac{0,55}{2} = 0,275m \quad (\text{A.7})$$

$$h_G = 0,35 + 0,15 + 0,03 = 0,53m \quad (\text{A.8})$$

$$d_3 = h_G - R = 0,529m \quad (\text{A.9})$$

APPENDIX B

CALCULATION OF MASS MOMENT OF INERTIA FOR THE WHEELCHAIR-HUMAN SYSTEM

Mass moment of inertia of the components of wheelchair-human system which has a plane of symmetry about plane $\{\bar{u}_1^{(w)}, \bar{u}_3^{(w)}\}$, are calculated based on [23]. Table B.1 on the next page shows the calculations of mass moments of inertia of the each component.

Table B.1. Inertia Calculation of the System Components

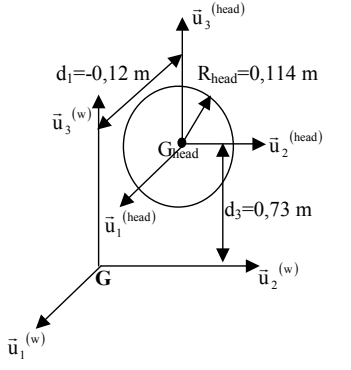
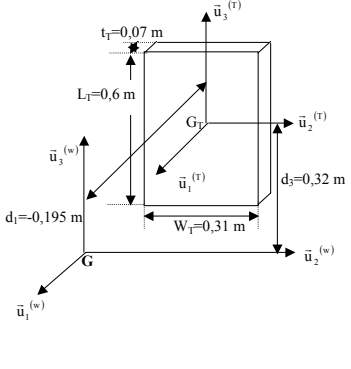
Component	Mass Moments of Inertia
 <p style="text-align: center;">Head</p>	$J_{11H} = \frac{2}{3} m_H R_H^2 + m_H d_3^2 = 3,0707 \text{kgm}^2$ $J_{22H} = \frac{2}{3} m_H R_H^2 + m_H (d_1^2 + d_3^2) = 3,1523 \text{kgm}^2$ $J_{33H} = \frac{2}{3} m_H R_H^2 + m_H d_1^2 = 0,1308 \text{kgm}^2$ $J_{13H} = m_H d_1 d_3 = -0,4967 \text{kgm}^2$
 <p style="text-align: center;">Trunk</p>	$J_{11T} = \frac{1}{12} m_T (L_T^2 + W_T^2) + m_T d_3^2 = 4,8848 \text{kgm}^2$ $J_{22T} = \frac{1}{12} m_T (L_T^2 + t_T^2) + m_T (d_1^2 + d_3^2) = 5,9433 \text{kgm}^2$ $J_{33T} = \frac{1}{12} m_T (W_T^2 + t_T^2) + m_T d_1^2 = 1,6157 \text{kgm}^2$ $J_{13T} = m_T d_1 d_3 = -2,171 \text{kgm}^2$

Table B.1 (Continued)

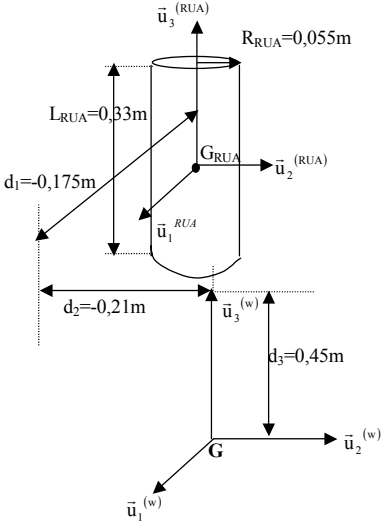
Component	Mass Moments of Inertia
 <p style="text-align: center;">Right Upper Arm, Left Upper Arm</p>	$J_{11RUA} = J_{11LUA} = \frac{1}{4} m_{RUA} R_{RUA}^2 + \frac{1}{12} m_{RUA} L_{RUA}^2 + m_{RUA} (d_2^2 + d_3^2) = 0,5026 \text{kgm}^2$ $J_{22RUA} = J_{22LUA} = \frac{1}{4} m_{RUA} R_{RUA}^2 + \frac{1}{12} m_{RUA} L_{RUA}^2 + m_{RUA} (d_1^2 + d_3^2) = 0,4762 \text{kgm}^2$ $J_{33RUA} = J_{33LUA} = \frac{1}{2} m_{RUA} R_{RUA}^2 + m_{RUA} (d_1^2 + d_2^2) = 0,1494 \text{kgm}^2$ $J_{12RUA} = m_{RUA} d_1 d_2 = +0,072 \text{kgm}^2$ $J_{12LUA} = m_{LUA} d_1 d_2 = -0,072 \text{kgm}^2$ $J_{13RUA} = J_{13LUA} = m_{RUA} d_1 d_3 = -0,1543 \text{kgm}^2$ $J_{23RUA} = m_{RUA} d_2 d_3 = -0,1852 \text{kgm}^2$ $J_{23LUA} = m_{LUA} d_2 d_3 = 0,1852 \text{kgm}^2$

Table B.1 (Continued)

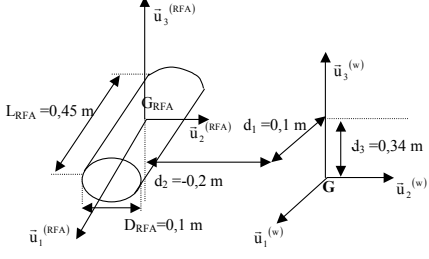
Component	Mass Moments of Inertia
 <p style="text-align: center;">Right Forearm, Left Forearm</p>	$J_{11 RFA} = J_{11 LFA} = \frac{1}{2} m_{RFA} R_{RFA}^2 + m_{RFA} (d_2^2 + d_3^2) = 0,2416 \text{kgm}^2$ $J_{22 RFA} = J_{22 LFA} = \frac{1}{4} m_{RFA} R_{RFA}^2 + \frac{1}{12} m_{RFA} L_{RFA}^2 + m_{RFA} (d_1^2 + d_3^2) = 0,2204 \text{kgm}^2$ $J_{33 RFA} = J_{33 LFA} = \frac{1}{4} m_{RFA} R_{RFA}^2 + \frac{1}{12} m_{RFA} L_{RFA}^2 + m_{RFA} (d_1^2 + d_2^2) = 0,104 \text{kgm}^2$ $J_{12 RFA} = m_{RFA} d_1 d_2 = -0,031 \text{kgm}^2$ $J_{12 LFA} = m_{LFA} d_1 d_2 = 0,031 \text{kgm}^2$ $J_{13 RFA} = J_{13 LFA} = m_{RFA} d_1 d_3 = +0,05236 \text{kgm}^2$ $J_{23 RFA} = m_{RFA} d_2 d_3 = -0,1047 \text{kgm}^2$ $J_{23 LFA} = m_{LFA} d_2 d_3 = 0,1047 \text{kgm}^2$

Table B.1 (Continued)

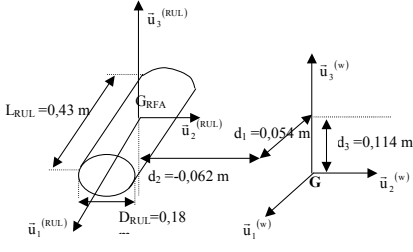
Component	Mass Moments of Inertia
 <p style="text-align: center;">Right Upperlimb, Left Upperlimb</p>	$J_{11RUL} = J_{11LUL} = \frac{1}{2} m_{RUL} R_{RUL}^2 + m_{RUL} (d_2^2 + d_3^2) = 0,07311 \text{kgm}^2$ $J_{22RUL} = J_{22LUL} = \frac{1}{4} m_{RUL} R_{RUL}^2 + \frac{1}{12} m_{RUL} L_{RUL}^2 + m_{RUL} (d_1^2 + d_3^2) = 0,1167 \text{kgm}^2$ $J_{33RUL} = J_{33LUL} = \frac{1}{4} m_{RUL} R_{RUL}^2 + \frac{1}{12} m_{RUL} L_{RUL}^2 + m_{RUL} (d_1^2 + d_2^2) = 0,08468 \text{kgm}^2$ $J_{12RUL} = m_{RUL} d_1 d_2 = -0,0117 \text{kgm}^2$ $J_{12LUL} = m_{LUL} d_1 d_2 = +0,0117 \text{kgm}^2$ $J_{13RUL} = J_{13LUL} = m_{RUL} d_1 d_3 = +0,0215 \text{kgm}^2$ $J_{23RUL} = m_{RUL} d_2 d_3 = -0,02474 \text{kgm}^2$ $J_{23LUL} = m_{LUL} d_2 d_3 = +0,02474 \text{kgm}^2$

Table B.1 (Continued)

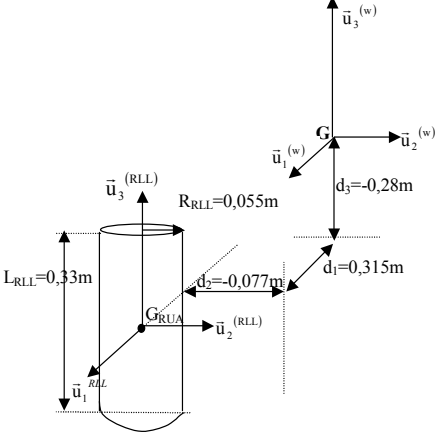
 <p style="text-align: center;">Right Lowerlimb, Left Lowerlimb</p>	$J_{11 RLL} = J_{11 LLL} = \frac{1}{4} m_{RLL} R_{RLL}^2 + \frac{1}{12} m_{RLL} L_{RLL}^2 + m_{RLL} (d_2^2 + d_3^2) = 1,1917 \text{kgm}^2$ $J_{22 RLL} = J_{22 LLL} = \frac{1}{4} m_{RLL} R_{RLL}^2 + \frac{1}{12} m_{RLL} L_{RLL}^2 + m_{RLL} (d_1^2 + d_3^2) = 2,2432 \text{kgm}^2$ $J_{33 RLL} = J_{33 LLL} = \frac{1}{2} m_{RLL} R_{RLL}^2 + m_{RLL} (d_1^2 + d_2^2) = 1,2168 \text{kgm}^2$ $J_{12 RLL} = m_{RLL} d_1 d_2 = -0,2734 \text{kgm}^2$ $J_{12 LLL} = m_{LLL} d_1 d_2 = +0,2734 \text{kgm}^2$ $J_{13 RLL} = J_{13 LLL} = m_{RLL} d_1 d_3 = -0,994 \text{kgm}^2$ $J_{23 RLL} = m_{RLL} d_2 d_3 = +0,243 \text{kgm}^2$ $J_{23 LLL} = m_{LLL} d_2 d_3 = -0,243 \text{kgm}^2$
--	---

Table B.1 (Continued)

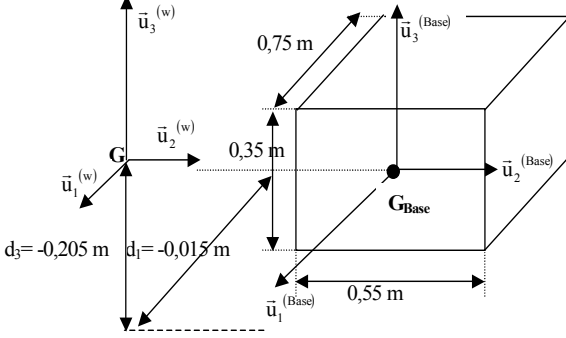
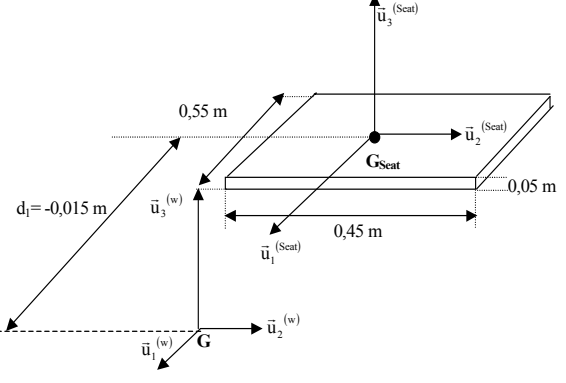
Component	Mass Moments of Inertia
 <p style="text-align: center;">Base</p>	$J_{11\text{Base}} = \frac{1}{12} m_{\text{Base}} (0,55^2 + 0,35^2) + m_{\text{Base}} d_3^2 = 3,8721\text{kgm}^2$ $J_{22\text{Base}} = \frac{1}{12} m_{\text{Base}} (0,35^2 + 0,75^2) + m_{\text{Base}} (d_1^2 + d_3^2) = 4,6583\text{kgm}^2$ $J_{33\text{Base}} = \frac{1}{12} m_{\text{Base}} (0,55^2 + 0,75^2) + m_{\text{Base}} d_1^2 = 3,3071\text{kgm}^2$ $J_{13\text{Base}} = m_{\text{Base}} d_1 d_3 = -0,9106\text{kgm}^2$
 <p style="text-align: center;">Seat</p>	$J_{11\text{Seat}} = \frac{1}{12} m_{\text{Seat}} (0,45^2 + 0,05^2) + m_{\text{Seat}} d_3^2 = 0,0854\text{kgm}^2$ $J_{22\text{Seat}} = \frac{1}{12} m_{\text{Seat}} (0,05^2 + 0,5^2) + m_{\text{Seat}} (d_1^2 + d_3^2) = 0,1057\text{kgm}^2$ $J_{33\text{Seat}} = \frac{1}{12} m_{\text{Seat}} (0,45^2 + 0,5^2) + m_{\text{Seat}} d_1^2 = 0,189\text{kgm}^2$ $J_{13\text{Seat}} = m_{\text{Seat}} d_1 d_3 = 0\text{kgm}^2$

Table B.1 (Continued)

<p style="text-align: center;">Backrest</p>	$J_{11BR} = \frac{1}{12} m_{BR} (0,45^2 + 0,55^2)$ $+ m_{BR} d_3^2 = 0,1057 \text{kgm}^2$ $J_{22BR} = \frac{1}{12} m_{BR} (0,55^2 + 0,03^2)$ $+ m_{BR} (d_1^2 + d_3^2) = 0,3384 \text{kgm}^2$ $J_{33BR} = \frac{1}{12} m_{BR} (0,45^2 + 0,03^2)$ $+ m_{BR} d_1^2 = 0,6 \text{kgm}^2$ $J_{13BR} = m_{BR} d_1 d_3 = -0,2536 \text{kgm}^2$
--	---

The total mass moment of inertia of the wheelchair-human system can be obtained by the following equation.

$$J_w = \sum_i J_i \quad (\text{B.1})$$

Using Equation B.1, one can get the components of the inertia of the wheelchair-human system as shown by the following four equations.

$$J_{11w} = 16,037 \text{kgm}^2 \quad (\text{B.2})$$

$$J_{22w} = 20,311 \text{kgm}^2 \quad (\text{B.3})$$

$$J_{33w} = 8,9524 \text{kgm}^2 \quad (\text{B.4})$$

$$J_{13w} = 3,9743 \text{kgm}^2 \quad (\text{B.5})$$

Remember that the inertia dyadic [15] of the wheelchair-human system is

$$\begin{aligned} \check{J}_{WG} = & J_{11} \bar{u}_1^{(w)} \bar{u}_1^{(w)} + J_{22} \bar{u}_2^{(w)} \bar{u}_2^{(w)} + J_{33} \bar{u}_3^{(w)} \bar{u}_3^{(w)} \\ & + J_{31} [\bar{u}_3^{(w)} \bar{u}_1^{(w)} + \bar{u}_1^{(w)} \bar{u}_3^{(w)}] \end{aligned} \quad (B.6)$$

Substitution of Equations B.2, B.3, B.4 and B.5 into the above equation, one can get the inertia dyadic of the wheelchair-human system.

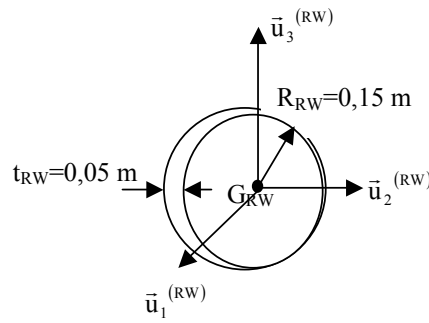


Figure B.1. Right Rear Wheel

In Figure B.1; R_{RW} , t_{RW} are the radius and thickness of the right rear wheel, G_{RW} is the center of mass of the right rear wheel, and $F_{RW} \{G_{RW}; \bar{u}_1^{(RW)}, \bar{u}_2^{(RW)}, \bar{u}_3^{(RW)}\}$ is the reference frame fixed on the right rear wheel, which is formed by the rotation of wheelchair fixed frame about axis $\bar{u}_2^{(w)}$ with a rotation angle of θ .

The inertia dyadics of the left, and right rear wheel shown in can be defined by Equation B.7

$$\check{J}_{RA} = \check{J}_{LB} = J_s \bar{u}_2^{(w)} \bar{u}_2^{(w)} + J_n [\bar{u}_3^{(w)} \bar{u}_3^{(w)} + \bar{u}_1^{(w)} \bar{u}_1^{(w)}] \quad (B.7)$$

where J_n and J_s are the lateral and polar inertia components of the rear wheels.

Lateral and polar inertia components of the right and left rear wheels are obtained by means of the following equation.

$$J_{nRW} = J_{nLW} = \frac{1}{4} m_{RW} R_{RW}^2 + \frac{1}{12} m_{RW} t_{RW}^2 = 0,0175 \text{kgm}^2$$

and,

$$J_{sRW} = J_{sLW} = \frac{1}{2} m_{RW} R_{RW}^2 = 0,03375 \text{kgm}^2$$

In these equations, m_{RW} is the mass of the right rear wheel.

$$m_{RW} = m_{LW} = 3 \text{kg}$$

APPENDIX C

ANTHROPOMETRIC DATA AND DIMENSIONS OF HUMAN BODY SEGMENTS

Table C.1. Anthropometric Data

Segment	Definition	Segment Wt/ Total Body Wt	Centre of Mass	Centre of Mass	Radius of Gyration	Radius of Gyration	Radius of Gyration
			Proximal	Distal	C of G	Proximal	Distal
Hand [see also]	wrist/knuckle II digit 3	.006	.506	.494	.297	.587	.577
Forearm	elbow/ulnar styloid	.016	.430	.570	.303	.526	.647
Upper arm	G.H jt/elbow	.028	.436	.564	.322	.542	.645
Forearm+hand	elbow/ulnar styloid	.022	.682	.318	.468	.827	.565
Upper limb	G.H jt/ ulnar styloid	.050	.530	.470	.368	.645	.596
Foot	Lat. mall/hd. MT2	.0145	.50	.50	.475	.690	.690
Shank	Fem cond./med. mall	.0465	.433	.567	.302	.528	.643
Thigh	Gr.troch/fem. cond.	.100	.433	.567	.323	.540	.653
Foot+shank	fem. cond./med. mall.	.061	.606	.394	.416	.735	.572
Lower Limb	Gr.troch/med. mall.	.161	.447	.553	.326	.560	.650
Head, neck, trunk	Gr troch/G.H joint	.578	.66	.34	.503	.830	.607
Head, neck, arms, trunk	Gr troch/G.H joint	.678	.626	.374	.496	.798	.621
Head and neck	[C7-T1 and 1st rib]/ear canal	.081	1.000*	.000*	0.495	1.116	-

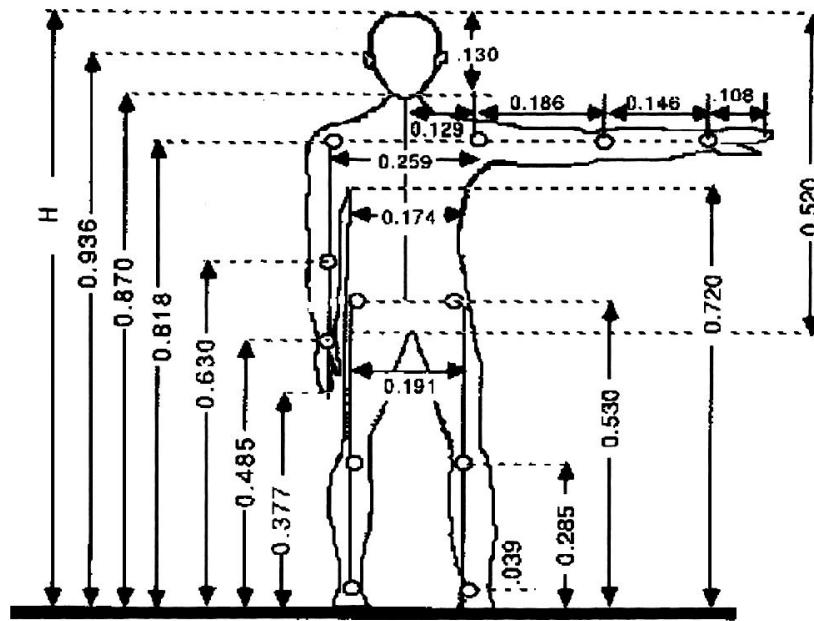


Figure C.1. Relative Dimensions of the Average Human Body